PRAJÑĀ प्रज्ञा

JOURNAL OF PURE & APPLIED SCIENCES

Published by
SARDAR PATEL UNIVERSITY
VOL.14, September 2006

* CONTENTS *

Sardar Patel University Press, Vallabh Vidyanagar

PRAJÑĀ
प्रज्ञा

EXCELLENCE MATTERS

JOURNAL OF PURE & APPLIED SCIENCES

VOLUME 14
SEPTEMBER 2006

PUBLISHED BY
SARDAR PATEL UNIVERSITY
Vallabh Vidyanagar

'Prajna' - Jounal of Pure & Applied Sciences, 14 (2006) 1-16

SYNTHESIS, THERMAL PROPERTIES AND MICROBIAL PROPERTIES OF POLYETHERKETONES PREPARED FROM PHENETOLE

Shveta Trivedi and Rajni M. Patel
Department of Chemistry, Sardar Patel University, Vallabh Vidyanagar – 388120.

Key Words

Polyetherketones, friedel-crafts reaction, thermal properties, microbial properties.

Abstract

Low molecular weight polyetherketones have been synthesized by friedel-crafts acylation reaction using phenetole, 1,4-phenelynedioxydiacetyl chloride, chloroacetyl chloride, 1,2-dichloroethane and dichloromethane in the presence of anhydrous aluminum chloride and carbon disulfide. Chlorine content was determined by Carius method. The resins were characterized by FT-IR spectroscopy. Thermogravimetric Analysis (TGA) and Differential Scanning Calorimetry (DSC) have been used for the determination of the thermal properties. All the polyetherketone resins were tested against bacteria, yeast and fungi for their microbial properties.

Introduction

The polyetherketones, obtained by Friedel-Crafts reaction are desirable class of polymers, which are drawing increasing interest at the present time. Polyetherketones are stiff and tough, and resist wear, abrasion, fatigue. They possess low flammability and, when burning, give low levels of smoke and toxic gas. They are solvent resistant and resistant to radiation. The key application areas are aerospace, electrical, oil industry, fluid handling, bearing film, monofilament, coatings, automotive, nuclear and ultra filtration membranes. Detailed property data and applications are available in review articles, papers and trade literature referred to therein [1-7].

The $AlCl_3$ catalyzed process has been extensively used [8-10] to produce research quantities of usually, low molecular weight polymers. The crystalline poly(etherketone)s are insoluble in the commonly used Friedel-Crafts reaction solvents such as dichloromethane, 1,2-dichloroethane, nitrobenzene etc., and this insolubility prevents attainment of high molecular weight.

High molecular weight polyketones by Friedel-Crafts reaction of tricyclic fused compound containing six membered heterocycle with diacid chloride in polyphospharic acid in the presence of $AlCl_3$ were prepared by Niume and Co-Workers [11].

Linear hyperbranched PEK was prepared by Jong-Beom Baek and Loon-Seng Tan [12-14] by using AB_2 monomers like; 3, 5-bis (4-fluorobenzoyl) phenol and 2,3-bis(4-phenyloxy phenyl)-6-quinoxaline carboxylic acid. Polymers were studied by WAXS which shows the same crystalline structure as that of the linear homopolymer, which was correlated well with DSC and TGA result. It was concluded that material properties could be controlled by controlling degrees of branching.

The use of polymer blends is becoming an important factor in satisfying the need of specific sectors of polymer industry. Nandan [15] studied miscibility behaviour of PEEK/PEK blends and thermal- morphological studies were carried out. DSC was used to determine Tg and Tm of the blends. Withold Brostow et. al. [16] studied on blending of fluorinated PAEK and epoxy resin.

Prosthetic device has a PAEK component [17] whose surface has been sulfonated to enhance its wettability, so that tissue growth on the surface is facilitated. Surgical instruments parts were made up of laminated PEK/C fiber sheets [18]. The sheets are autoclavable, x-ray transparent, biocompatible, and antimagnetic and chemical resistance. Mechanical properties of sheet are specified.

It is possible to synthesize low molecular weight resins containing various functional groups that are gaining prominanace because of their various microbial and pharmacological properties. [19-20]. In the present investigation, polyetherketones prepared from phenetole, 1,4-phenelynedioxydiacetyl chloride, chloroacetyl chloride, 1,2-dichloroethane and dichloromethane by Friedel Crafts reaction and were tested for their microbial properties using *Escherichia coli, Bacillus subtilis, Staphylococcus citreus, Pseudomonas fluorescens, Protecus vulgaris, Candida utilis, Sacharomyces cerevisiae, Pichia stipitis, Rhodotorula minuta, Aspergillus niger, Sporotichum pulverulentum, Trichoderma lignorum, Penicillium chrysogenum* and *Rhizopus stolonifer* **.**

Experimental:

Materials:

phenetole, chloroacetylchloride (CAC), 1,2-dichloroethane (DCE), dichloromethane (DCM), carbon disulfide (CS_2) and anhydrous aluminum chloride ($AlCl_3$) were of analytical grade.

Synthesis of 1,4-phenelynedioxydiacetyl chloride:

1,4-phenelynedioxydiacetyl chloride (1,4-PDC) was synthesized from 1,4-phenelyne dioxydiacetic acid (1,4-PDA). The product obtained was recrystallized from dry methylene chloride-hexane mixture (80:20) to obtain pure white crystalline needles of 1,4-PDC having melting point of 84 ^{0}C [21].

Synthesis of Polyetherketones

To the mixture of 1,4-PDC, carbon disulfide and anhydrous $AlCl_3$; phenetole and CAC/DCE/DCM were added and kept at 0 ^{0}C for 1 hour. The reaction mixture was heated at 60 ^{0}C for 6 hours using reflux condenser. The reaction mixture was then poured into 200 ml H_2O: HCl (1:1) mixture with constant stirring. The slight sticky product separated out. It was subjected to heat in water bath to remove carbon disulfide. The dark brown colored solid thus obtained was dried and powdered. The resins obtained were further purified using acetone as solvent and distilled water as non-solvent. Brown color is the characteristic of Friedel Crafts products obtained from aromatic compounds [22]. Conditions for the preparation of the polyetherketones have been mentioned in the Table-1 and the respective reaction scheme is shown in the Figures-1 and 2.

Characterization

FT-IR spectra of the resins were scanned on Perkin-Elmer-983 spectrophotometer. The percentage chlorine content of the resins was determined by Carius method [23]. The results are shown in the Table-1. The TGA thermograms were recorded on DuPont model 951 thermogravimetric analyzer at a heating rate of 10 ^{0}C/min under nitrogen atmosphere. The DSC data were obtained from DuPont 900 thermal analyzer.

The polyetherketones thus synthesized were tested with different microorganisms that are commonly employed for the biodegradability tests. Bacterial strains (*Escherichia coli, Bacillus subtilis, Staphylococcus citreus, Pseudomonas fluorescens, Protecus vulgaris),* fungi *(Aspergillus niger, Sporotichum pulverulentum, Trichoderma lignorum, Penicillium chrysogenum* and *Rhizopus stolonifer)* and yeast *(Candida utilis, Sacharomyces cerevisiae, Pichia stipitis, Rhodotorula minuta)* were selected and grown in the Nutrient-broth, Sabourad's dextrose broth and YEPD (yeast extract peptone dextrose) medium respectively to study the microbial properties. The content of the flasks were incubated in a shaker at room temperature at a specific time intervals between 20 to 48 hrs. The optical density was measured at 660 nm for bacterial and yeast cultures. The percentage inhibition (I) was obtained from the equation:

$$\mathbf{I = 100\,(X\text{-}Y)\,/\,X}$$

Where,

X=optical density of bacterial suspension in the control set

Y= optical density of bacterial suspension in the test set

The percentage inhibition was found to be maximum after 48hr. The fungal culture was harvested after 48hrs and the dry cell mass was determined gravimetrically. The percentage inhibition was calculated using the same equation where,

X=weight of the fungal cell mass in the control set.
Y= weight of the fungal cell mass in the test set.

The details of the experimental procedures have already been reported [24-25].

Result And Discussion

Polyetherketones prepared by different experimental conditions are presented in Table-1. All are highly colored ranging from brown to black and are soluble in acetone, dimethylformamide and dioxane.

The IR spectra confirmed the structure of polyetherketones in all the aspects. The important IR frequencies are assigned and are listed in the Table-2. A broad band in the region of 2930-2948 cm^{-1} could be due to C-H stretching vibration of methylene group, whereas the bands at about 1345 and 1455 cm^{-1} could be due to C-H bending vibration of methyl or methylene group. The 835 cm^{-1} peak in all the resins may be due to C-H out of plane bending vibrations of tetra substituted aromatic ring, whereas C-H in plane bending is observed at around 1150 cm^{-1}. A sharpe band at around 670 cm^{-1} has been assigned to C-Cl stretching in the monomer 1,4-PDC [26]. This band is expected to be disappearing on the formation of polymer. The C=O stretching vibration in polymers appears around 1700 cm^{-1} [27]. In all the polymers the fairly strong absorption band around 1235 cm^{-1} is attributed to C-O-C stretching band [28]. The vibrations due to aromatic ring are assigned to absorption in the range of 1500-1600 cm^{-1}.

Thermal properties of all the resins have been determined by thermogravimetric analysis (TGA) and differential scanning calorimetry(DSC) measurements. The thermal data and various kinetic parameters of the thermal degradation are presented in Tables-3 and 4. The resins degrade between 170-595 ^{0}C and show moderate thermal stability. Broido method [29] was used for the TGA data evaluation for activation energy (E_A) for the degradation reaction and was found to be 93-137 $kJmol^{-1}$. The values of the characteristic degradation temperatures and integral procedural decomposition temperature (IPDT) were determined by Doyle's method [30]. IPDT expresses the overall stability of the sample and it in the range of 559-490 ^{0}C. From the DSC thermogram the heat of fusion was obtained as 22-29 Jg^{-1}.

Polyetherketones prepared from the different monomers listed in Table-1, when tested for their response against microorganisms showed interesting observations. Figures 3, 4, 5 provide comparative account of the effect of polyetherketones on the growth of bacteria, yeast and fungi. The results indicate that the polyetherketones inhibit significantly the growth of microorganisms. The control culture (without resin) exhibits the maximum growth during 48hrs. Resin-1 appears to be least effective to prevent the growth of bacteria, fungi and yeast. Resin-2 is the most effective antimicrobial agent. The presence of chlorine in the resin is the important component to prevent the growth of microorganisms [31-34]. Resin-1 is not having chlorine and Resin-2 has the maximum chlorine content, whereas the other resins have more or less chlorine content. Thus the variation in the microbial properties is not the only essential requirement for the resin to have antimicrobial property.

Conclusion

Seven polyetherketones were synthesized as shown in Table 1 and were characterized. All the resins showed antimicrobial activity. Although the chlorine content of the resins does not vary drastically, the antimicrobial activities are significantly different amongst these resins.

Refrences

1 Critchley J.P., Knight G.J.,Wright W.W., *Heat Resistant Polymers*, Plenum Press, New York (1983).

2 Rose J.B., *High Perf. Polymers*, Their Origin and Development, Ed. Seymour R.B.,Kirshnbaum G.S., Elsevier, New York (1986).

3 Johnson R.N., Farnham A.G., Clendinning R.A., Hale W.F., Merriam C.N., *J. Polym. Sci., Part A-1*, **5(9)**, 2375 (1967), Chem. Abs., **68**, 40159u (1968).

4 Hergenrother P.M., Jensen B.J., Havens S.J., *Polymer*, **29**, 358 (1988).

5 Olah G.A., Cupas C.A., *Kirk Othmer Encycl. Chem. Technol.*, 2nd Ed., **10**, 135 (1966), Chem. Abs., **66**, 10292e (1967).

6 Bonner W.H.,U.S.Pat.:3,065,205 (1962), Chem. Abs., **58**, 5806f (1963).

7 Goodman I., McIntyre J.E., Russell W., Brit. Pat. : 9,71,227 (1964), *Chem. Abs.*, **61**, 14805b (1964).

8 Swedo R.J., Marvel C.S., *J.Polym. Sci., Polym. Lett.* Ed., **15**, 683 (1977).

9 Sutter A., Schmutz P., Marvel C.S., *J.Polym. Sci., Polym. Chem. Ed.*, **20**, 609 (1982).

10 Lee J., Marvel C.S., *J. Polym. Sci., Polym. Chem. Ed.*, **21**, 2189 (1983).

11 Niume, F.Toda, Uno K., Iwakura Y., *J.Polym. Sci. Polym. Chem. Ed.*, **20(7)**, 1965 (1982).

12 Baek Jong-Beom, Tan Loon-Seng, *Polymer,* **44(2)**, 3451-3459 (2003), *Chem. Abs*., **139(9)** 133892c (2003).

13 Baek Jong-Beom, Tan Loon-Seng, *Polymer Preprints*, **42(2)**, 469-470 (2001), *Chem. Abs*., **135(25)**, 358278z (2001).

14 Baek Jong-Beom, Tan Loon-Seng, *Polymer Preprints*, **43(1),** 514-515 (2002), *Chem. Abs*., **137(1),** 6505n (2002).

15 Nandan B., Lal B., Pandey K.N., Alam S., Kandpal L.D., Mathur G.N., *Europe. Polym. Jr.,* **37(10),** 2147 – 2151 (2001).

16 Brostow Withild, Cassidy Patrick E., Macossay Javiour, Paola Candanedo, Venumbaka Sreenu R., Hagg Haley E., Montemartini Pablo E., *Polym. Mater. Sc. and Eng*., **84**, 618-619 (2001), *Chem. Abs*., 1**38(22)** 339003b (2003).

17 King Richard, Eur.Pat.Appl.EP 1,348,454, (2003), *Chem. Abs*., **139(18)** 281315g (2003).

18 Aesculap Ag & Co. kg, Germany, Ger. Gebrauchsmusterschrift DE 20,015,355, (2001), C*hem. Abs*., **134(14),** 198144b (2001).

19 Gebelein G.C., Carraher C.E Jr., *Perspectives in bioactive polymers*, ACS Symp. Ser., **186,** 1-9 (1982). *Chem.Abs***., 97,** 2332m (1982).

20 Patel S.A., Patel M.V., Ray A., Patel R.M., *J. Polym. Sci. Part A : Polym. Chem.* **41**, 2335-2344 (2003).

21 Srinivasan M., Scariah K.J., Krishnamurthy V. N., Rao K.V.C., *J. Polym. Sci. Part A : Polym. Chem.,* **22**, 1743-1756 (1984).

22 Morrison R.T., Boyd R.N., *Organic Chemistry,* Prentice Hall of India, 5th ed., 510 (1989).

23 Bance S., *Handbook of Practical Organic Microanalysis*, Ellis Horwood, Chichester, England, 101 (1980).

24 Patel N.Z., Patel J.N., Ray R.M., Patel R.M., *Die Angew Makromol.Chem*., **192**, 103-111 (1991).

25 Patel P.M., Mehta Y.M., Patel R.M., *Res. J.Of Chem. And Environ*.,**2**, 29-33 (1998).

26 Colthup N.B., Wibereley S.E., *Introduction to Infrared Spectroscopy*, Academic Press, New York, 110, (1990).

27 Bellamy L.J., *Advances in Infrared Group Frequences*, Methuen, London, 25-27 and 43, (1968).

28 Williams D.H., Fleming I., *Spectroscopic Methods in Organic Chemistry*, 4th ed., Tata McGraw Hill, New Delhi, 56 (1988).

29 Broido A., A simple Sensitive Graphical Method of Treating Thermogravimetric analysis data, *J.of Polym. Sci. Part-A-2: Polym. Phys*., **7,** 1761-1774 (1969).

30 Doyle C.D., Estimating thermal stability of experimental polymers by empirical thermogravimetric analysis, *analy. Chem.,* **33**, 77-79, (1961).

31 Sang T.O., Chang S.H., Won J.C., *Pollimo.*, **18**, 309-315, (1994), *chem..Abst.***121,** 134905z (1994).

32 Sang T.O., Yoo C.S., Chang S.H., Won J.C., *Pollimo.*, **18,** 276-281, (1994), *chem.Abst.***121,** 84081e (1994).

33 Shah B.V., Patel M.B., Patel R.M*., Int. J. Of Polym. Mat*.,**53**,609-620 (2004).

34 Lein E.J., Hansch C., Anderson S.M., *J. of Med. Chem*., **11,** 430-441, (1968).

TABLE: 1

Conditions for the preparation of poly(etherketone)s

Resin No.	Phenetole (mol)	1,4-PDC (mol)	CAC (mol)	DCE (mol)	DCM (mol)	$AlCl_3$ (mol)	Yield (%)	Physical state and softening range[a] (^0C)	Chlorine (%)	Remarks[b]
1	0.03	0.03	-	-	-	0.06	40.7	Brown Powder 134-145	-	1,4-PDC+CS_2 +$AlCl_3$ was mixed and phenetole was added within 10 min.
2	0.03	0.015	0.015	-	-	0.06	39.5	Dark Brown Powder 125-132	5.1	To, 1,4-PDC +CS_2+$AlCl_3$, phenetole was added, content was kept at0^0C for 1h. and to this CAC was added.
3	0.03	0.015	-	0.015	-	0.06	38.9	Brown Black Powder 135-142	4.5	To,1,4-PDC +CS_2 +$AlCl_3$, phenetole was added, content was kept at0^0C for 1h. and to this DCE was added.
4	0.03	0.015	-	-	0.015	0.06	37.3	Black Brown Powder 128-136	4.4	To, 1,4-PDC+CS_2 +$AlCl_3$, phenetole was added, content was kept at 0^0C for 1h. and to this DCM was added.
5	0.03	0.01	0.01	0.01	-	0.06	38.1	Light Brown Powder 132-143	4.9	To,1,4-PDC +CS_2 +$AlCl_3$, phenetole was added, content was kept at 0^0C for 1h. and to this CAC was added. After 1h., DCE was added.
6	0.03	0.01	0.01	-	0.01	0.06	37.6	Dark brown Powder 131-142	4.7	To,1,4-PDC+CS_2 + $AlCl_3$, phenetole was added, content was kept at 0^0C for 1h. and to this CAC was added. After 1h., DCM was added.
7	0.03	0.01	-	0.01	0.01	0.06	40.4	Reddish Brown Powder 128-141	4.3	To,1,4-PDC+CS_2 +$AlCl_3$, phenetole was added, content was kept at 0^0C for 1h. and to this DCE was added. After 1h., DCM was added

Reaction temperature: 60 ^0C ; Reaction time : 6h. ; Solvent : CS_2 (25 ml.)

a From DSC thermograms.

b The general method of preparation is already given in the text . Here specific changes for each preparation are indicated.

TABLE: 2

Assignment of Infrared Frequencies of poly(etherketone)s prepared from phenetole

Resin No.	CH of aromatic ring and CH_2 of bridge (cm^{-1})	Phenyl vibration (cm^{-1})	Ph-O-CH_2 (cm^{-1})	Substituted aromatic ring		CH_2 bending		Aromatic O-C_2H_5 group		C=O stretching (cm^{-1})	C-Cl stretching (cm^{-1})
				CH in plane (cm^{-1})	CH out of plane (cm^{-1})	Scissoring (cm^{-1})	Rocking (cm^{-1})	Assym. stretching (cm^{-1})	Symmetric stretching (cm^{-1})		
1	2930	1510	1228	1160	832	1465	738	1350	1025	1712	675
2	2935	1490	1225	1175	830	1455	730	1320	1029	1705	685
3	2940	1503	1236	1162	838	1448	728	1340	1045	1660	680
4	2948	1505	1229	1158	842	1445	735	1340	1015	1658	675
5	2945	1510	1228	1155	835	1450	730	1352	1042	1665	670
6	2938	1505	1230	1162	832	1454	738	1378	1025	1710	675
7	2932	1518	1225	1159	825	1460	740	1358	1035	1718	685

TABLE: 3

Characteristic Temperature For Thermal Degradation of Poly(etherketone)s Evaluated From TGA

Resin number	Weight loss (%) at temperature up to					IPDT[a] (^{0}C)	IDT[b] (^{0}C)	T_S[c] (^{0}C)
	250 ^{0}C	350 ^{0}C	450 ^{0}C	550 ^{0}C	650 ^{0}C			
1	5	25	39	94	94	480	201	468
2	2	31	43	85	95	465	228	494
3	13	29	38	83	95	459	173	491
4	14	34	40	84	93	479	185	489
5	10	34	67	92	92	485	312	435
6	13	31	37	85	94	490	170	487
7	12	27	36	83	93	480	198	490

[a] Integral procedural decomposition temperature.
[b] Initial decomposition temperature.
[c] Half-volatilization temperature.

TABLE: 4

Kinetic Parameters for the Decomposition of Poly(etherketone)s (prepared from Phenetole) from TG and DSC

Resin number	Temperature range for step-1 (^{0}C)	Weight loss for step-1 (^{0}C)	Temperature range for step-2 (^{0}C)	Weight loss for step-2 (^{0}C)	Decomposition temperature range (^{0}C)	ΔT (^{0}C)	Energy of activation[a] 'E_A' (kJ.mol^{-1})	Order of reaction 'n'	Heat of fusion[b] 'ΔH_f' (J.gm^{-1})
1	201-370	26	370-545	94	201-545	344	89	1	22
2	228-411	38	411-594	95	228-594	366	103	1	25
3	173-377	31	377-604	96	173-604	431	93	1	23
4	185-381	36	381-591	93	185-591	406	125	1	28
5	312-418	43	318-515	92	312-525	312	137	1	28
6	170-375	32	375-592	95	170-592	422	134	1	29
7	198-370	28	370-595	94	198-595	397	111	1	23

Rate of heating: 10 ^{0}C/min.

[a] Broido method.

[b] From DSC thermograms

Figure - 1

For Resin No. 1

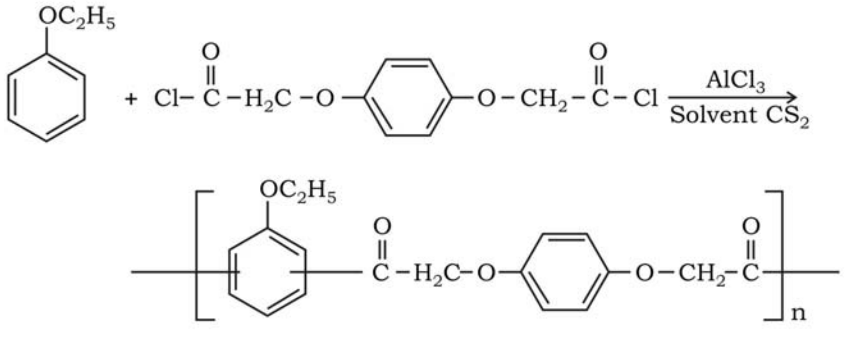

For Resin No. 2

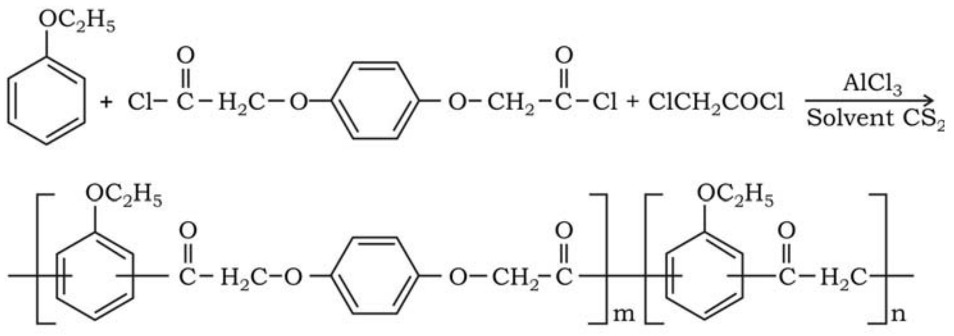

For Resin No. 3, 4

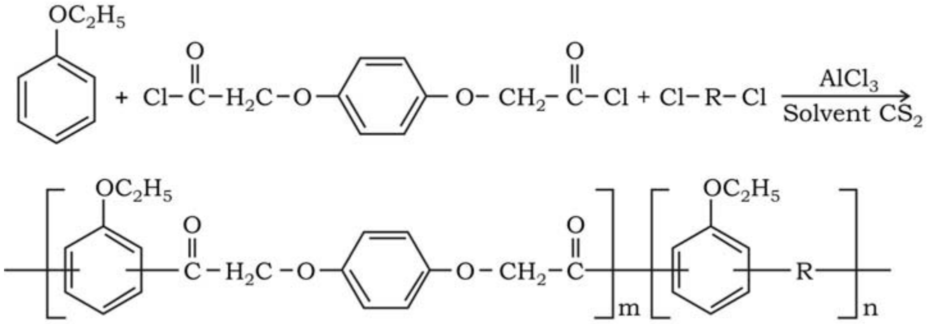

For Resin No. 3 : R = $-CH_2-CH_2-$

For Resin No. 4 : R = $-CH_2-$

Figure - 2

For Resin No. 5, 6

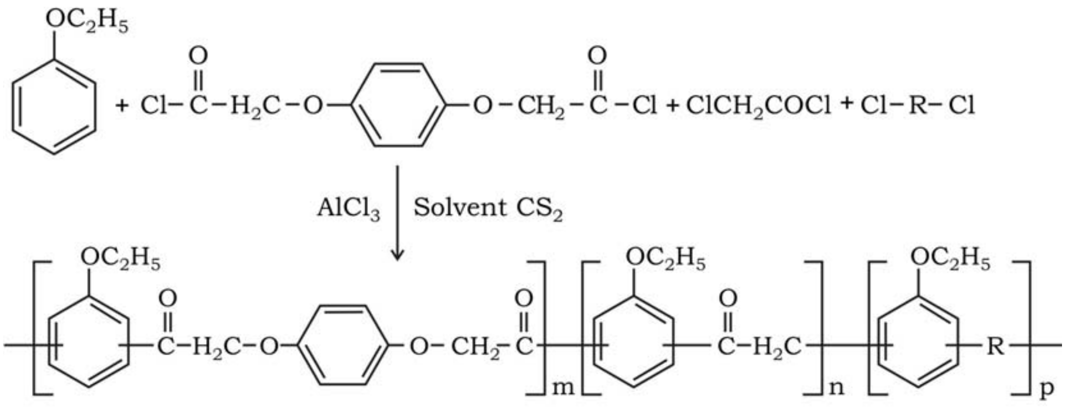

For Resin No. 5 : R = $-CH_2-CH_2-$

For Resin No. 6 : R = $-CH_2-$

For Resin No. 7

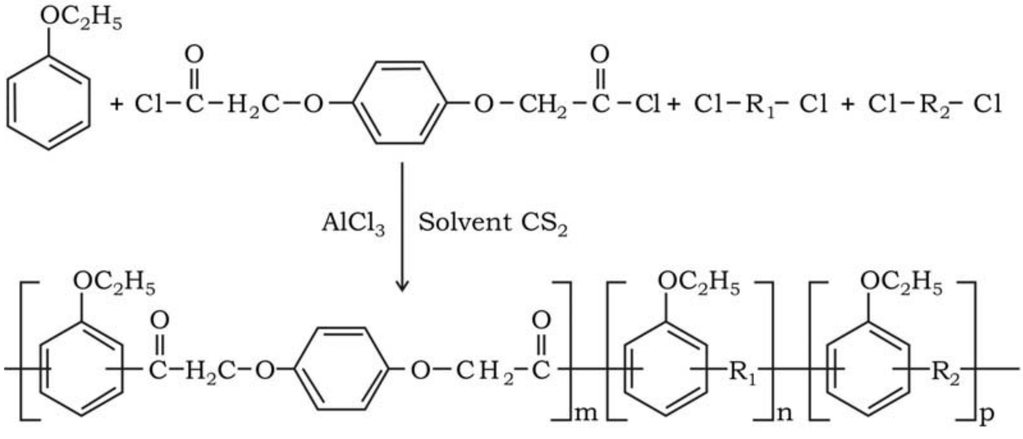

$R_1 = -CH_2-CH_2-$

$R_2 = -CH_2-$

Figure -3

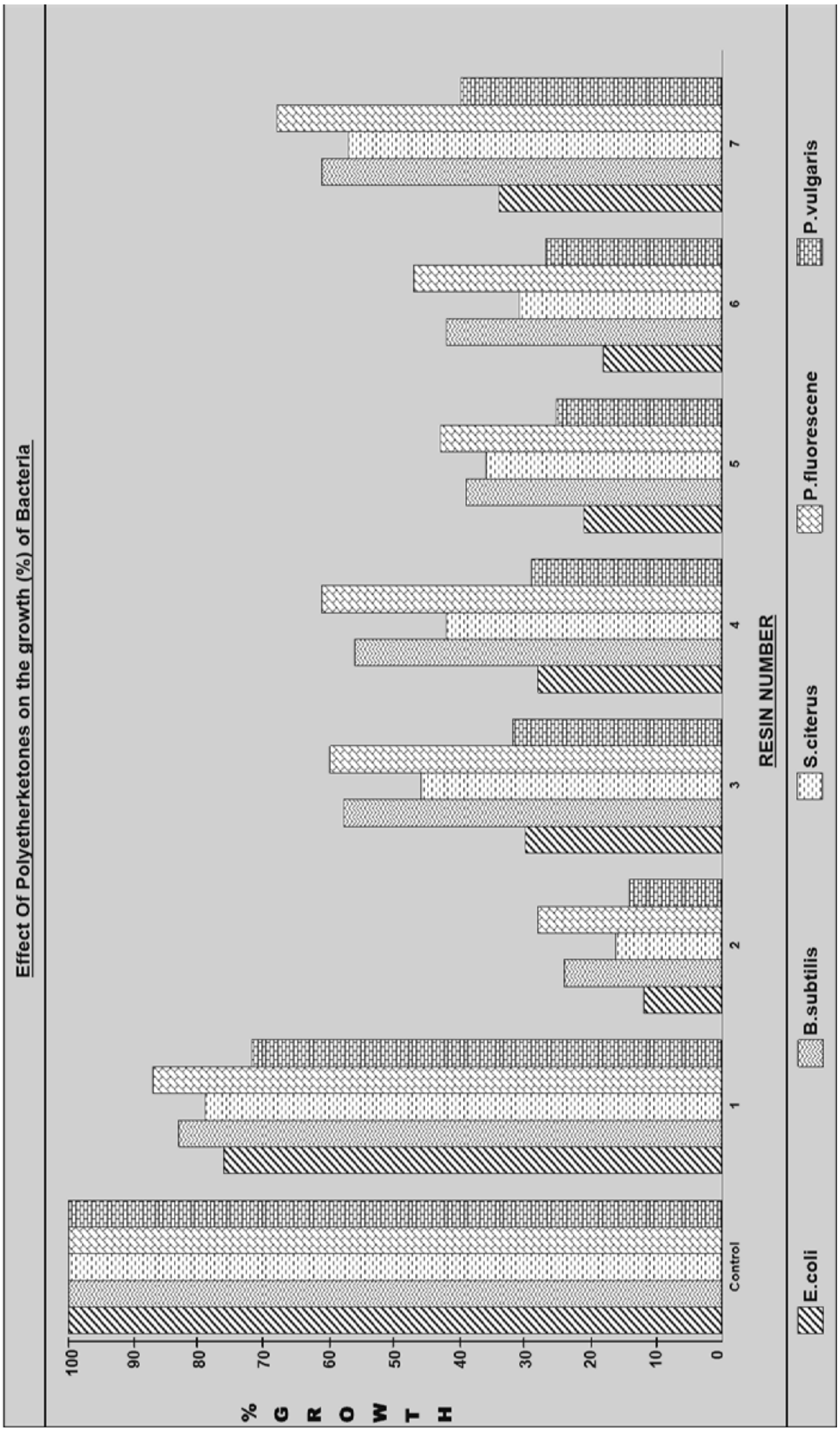
Effect Of Polyetherketones on the growth (%) of Bacteria
% GROWTH
100
90
80
70
60
50
40
30
20
10
0
Control
1
2
3
4
5
6
7
RESIN NUMBER
E.coli
B.subtilis
S.citerus
P.fluorescene
P.vulgaris

Figure-4

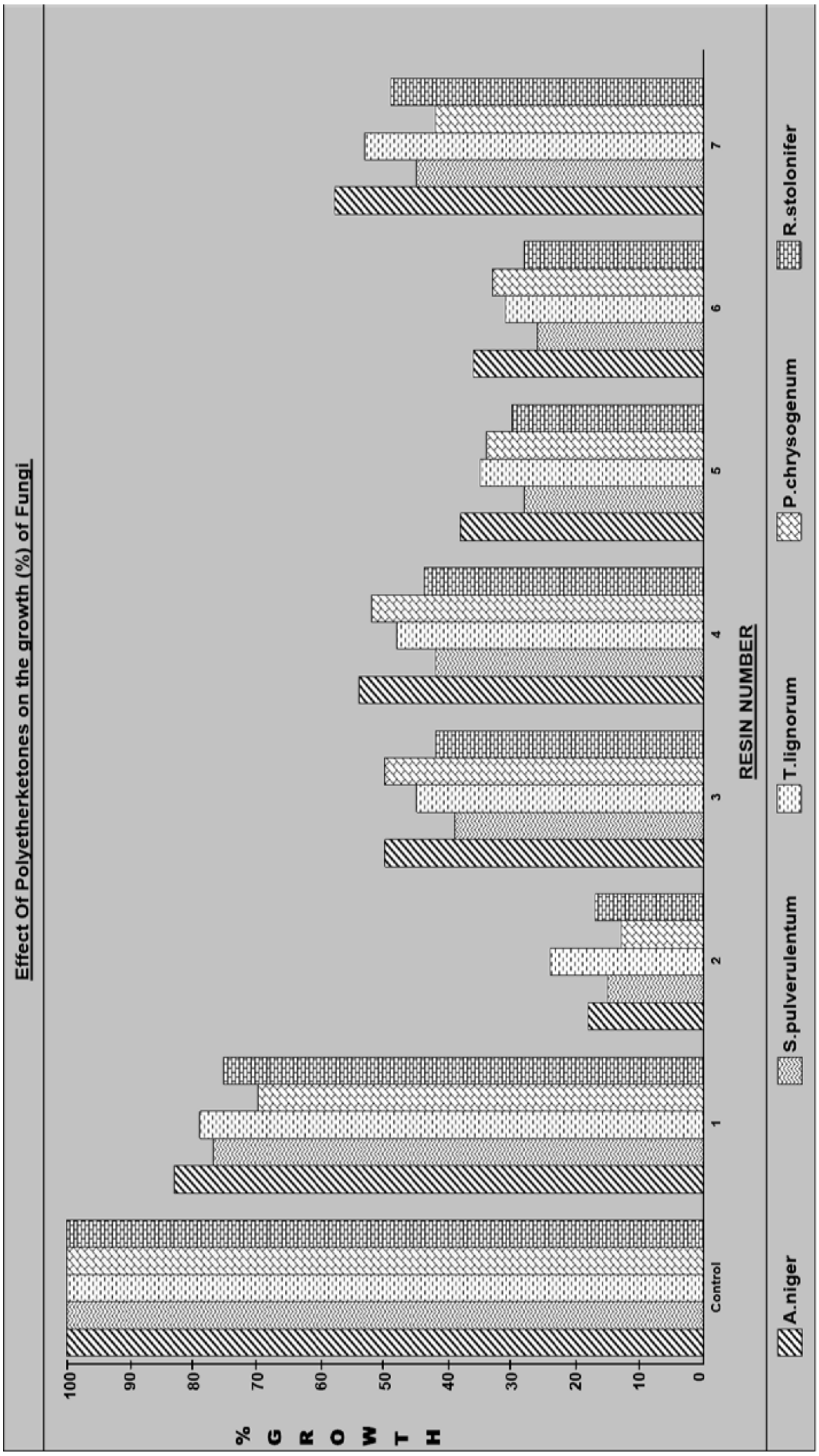
Effect Of Polyetherketones on the growth (%) of Fungi
% GROWTH
100
90
80
70
60
50
40
30
20
10
0
Control
1
2
3
4
5
6
7
RESIN NUMBER
A.niger
S.pulverulentum
T.lignorum
P.chrysogenum
R.stolonifer

Figure -5

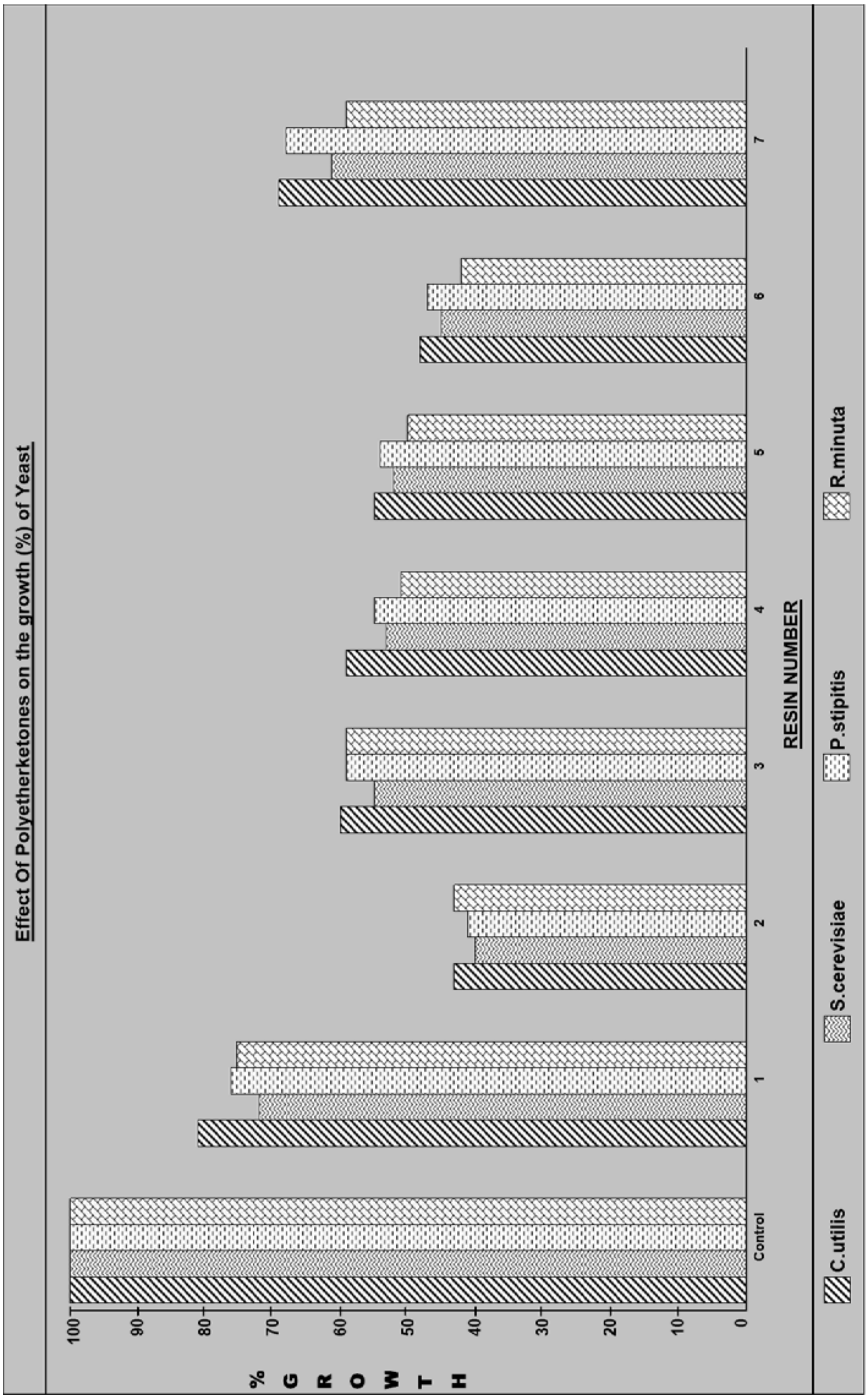
Effect Of Polyetherketones on the growth (%) of Yeast
% GROWTH
100
90
80
70
60
50
40
30
20
10
0
Control
1
2
3
4
5
6
7
RESIN NUMBER
C.utilis
S.cerevisiae
P.stipitis
R.minuta

'Prajna' - Jounal of Pure & Applied Sciences, 14 (2006) 17-24

PARICHAY: AN AGENT FOR ADULT LITERACY

Priti Sajja
GH Patel PG Department of Computer Science and Technology
Sardar Patel University, Vallabh Vidyanagar 388 120, Email: priti_sajja@yahoo.com

Abstract

This paper describes an autonomous agent named Parichay for adult literacy through multimedia that introduces alphabet, words, numbers, phrases and statements in Gujarati language enriched with examples from daily life. It begins by explaining the need of a user-friendly computer programme to provide adult education in native language, and discuss the utilization of technologies to address the challenges of adult literacy. It explains how education must be so designed as to incorporate the most suitable technology that provides effective learning, motivates, teaches a user in the absence of experts, and assists the user to accelerate the pace of learning. Many agents like Parichay can be integrated with a base of proposed Knowledge Based System, which provides advantages like intelligent behaviour, documentation and cloning of knowledge, self learning and explanation, user friendliness, flexibility and reusability. Successful research in this area would enable a large-scale development effort in many languages nationwide.

Introduction

“Illiteracy is a curse in our country”, said Mahatma Gandhi. Literacy and education have been termed as the best form of defence that a society can put to use against rising population, poor health, social strife and tensions, poor economic conditions and higher child mortality rate.

Eradication of illiteracy has been one of the major national concerns of the Government of India since independence. Despite nearly six decades of development planning in independent India, the rate of illiteracy continues to be high, perhaps, leading to a higher incidence of poverty. The literacy rate in India was 65.38% as per the census of 2001 compared to about 16% at the time of independence in 1947. However, vast section of adult population in India remains to be made literate.

Alarmed at the number of illiterate adults in the country and need to make them literate, has led to unprecedented activity in adult literacy in the nation in recent years. Adult education programme endeavours to upgrade adults functionally, and improve their economic skills so that the participants are able to earn more and use their money effectively as well as cultivate basic literacy skills of reading and writing so as to benefit from all that they read and thus raise the level of their own awareness with regard to social, cultural and political life.

Government and NGOs are utilizing different media aids for adult literacy namely TV, radio, film projector, computer etc. A more systematic approach is required to accelerate the process of learning so that an individual learner or a group of learners may achieve the desired objectives more effectively and efficiently. Each learner should have an individualized learning path. Learning should be enjoyable, and such that a learner feels encouraged to spend more time in learning. These goals can be better achieved through application of knowledge-oriented multimedia computer technology.

Presently, a few computer programmes dedicated to adult literacy are available in India. These programmes have yet to yield good results if only due to shortage of experts to teach in rural areas, understanding the language that is being used, and the absence of an alternative approach for creating interest in the learners.

An effort has been made to address these limitations by developing an agent named Parichay for adult literacy.

Agents and Their Impact

The term agent can be loosely defined as a component of software and/or hardware, which is capable of acting exactly like user in order to accomplish tasks on behalf of its user. Adaptivity, autonomy, collaborative behaviour, inferential capability, “knowledge-level” communication ability, mobility, reactivity and temporal continuity are few characteristics of agents [1]. Since agents tend to focus on a particular domain, they can be very good means for breaking down a problem into solvable sub-units. Though agents are all autonomous their scope is wide because they possess capability to work independently in conjunction with a given system. This yields benefits like increased modularity, structuredness, reusability, flexibility and reduced complexity [1]. When an agent is autonomous, it can be easily detached from the base system and integrated with another system where needed. Also, the approach provides high opportunities to isolate and test the agent that improves overall quality of the system.

Parichay: Characteristics and Design

Parichay is an autonomous agent and can be executed independently in a typical personal computer with Windows 95/98 or advanced technology. Touch screens with symbols are recommended, as the users are illiterate. To make learning more effective and allow for ease in understanding, the instruction provided to users is in their native language and presented mainly in voice/picture/animation form. The current version of the system needs minimum keystrokes and mouse movement, which are totally optional.

The CD containing Parichay package is set with auto-run facility so that the moment the source CD is inserted, the software would get started in multimedia. The major screen outputs of the developed agents (in Visual Basic 6 mainly with an animation tool) are briefly illustrated in Figure 1.

Emphasis is laid on developing reading and writing skills of adults. Only static presentation of the letters of alphabet would not give the learners the ability to reproduce them. Hence, continuous patterns are generated using animations for the letters of the alphabet (with an imaginary pen). The presentation will be repeated continuously till the user is satisfied. The gradual formation of an alphabet is shown in Figure 2. So learners can observe the correct starting position and path of alphabet or symbol generation. The agent is designed in such a way that it facilitates learning without any help from a tutor. The developed agent is thoroughly tested.

The agent Parichay gives introduction to different letters of the alphabet, words, numbers, phrases, and simple statements in Gujarati language. The agent is enriched with examples of daily life in the form of pictures, animations and sound (prompts and instructions, jingles, music and other information) specially designed for the illiterate adult so as to generate interest in the adult learners.

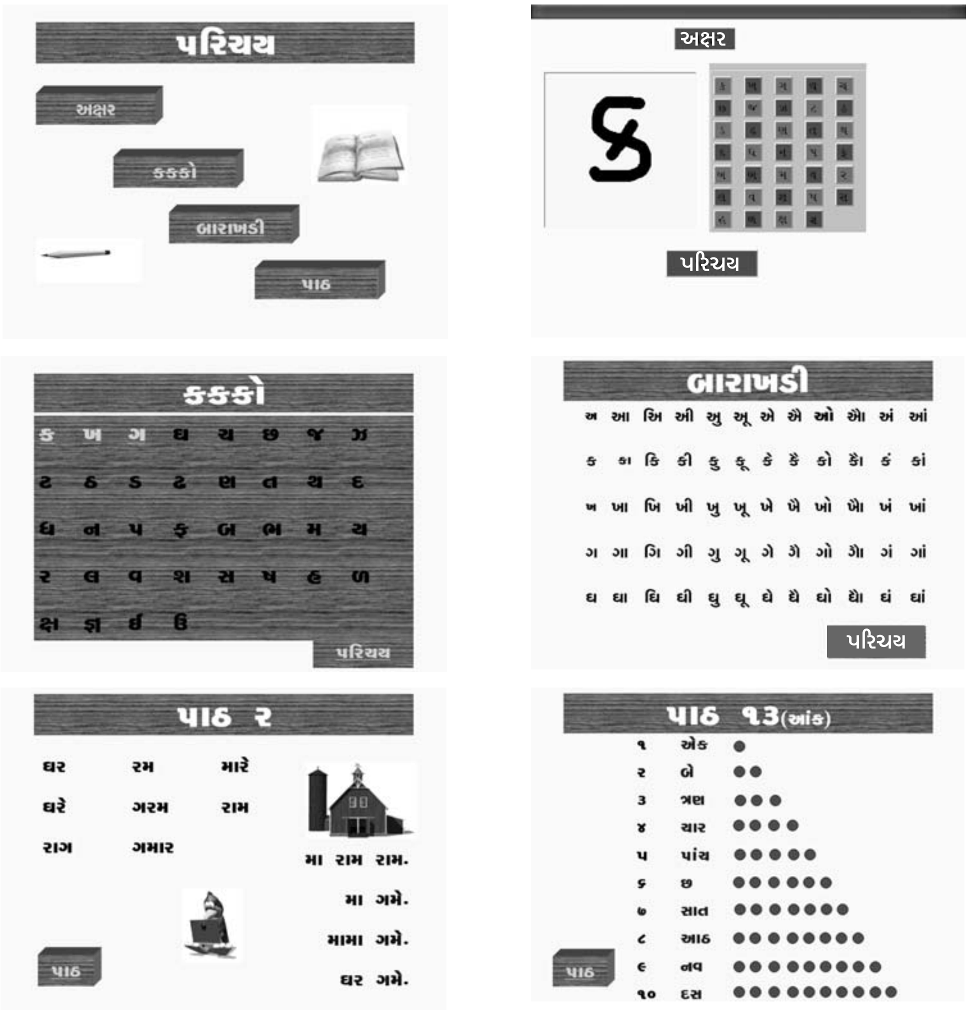

ક ખ ગ ઘ ચ છ જ ઝ
ટ ઠ ડ ઢ ણ ત થ દ
ધ ન પ ફ બ ભ મ ય
ર લ વ શ સ ષ હ ળ
ક્ષ જ્ઞ ઈ ઉ

અ આ ઇ ઈ ઉ ઊ એ ઐ ઓ ઔ અં આં
ક કા કિ કી કુ કૂ કે કૈ કો કૌ કં કાં
ખ ખા ખિ ખી ખુ ખૂ ખે ખૈ ખો ખૌ ખં ખાં
ગ ગા ગિ ગી ગુ ગૂ ગે ગૈ ગો ગૌ ગં ગાં
ઘ ઘા ઘિ ઘી ઘુ ઘૂ ઘે ઘૈ ઘો ઘૌ ઘં ઘાં

ઘર રમ મારે
ઘરે ગરમ રામ
રાગ ગમાર

મા રામ રામ.
મા ગમે.
મામા ગમે.
ઘર ગમે.

૧ એક ●
૨ બે ●●
૩ ત્રણ ●●●
૪ ચાર ●●●●
૫ પાંચ ●●●●●
૬ છ ●●●●●●
૭ સાત ●●●●●●●
૮ આઠ ●●●●●●●●
૯ નવ ●●●●●●●●●
૧૦ દસ ●●●●●●●●●●

Figure 1 : Few screens while executing Parichay

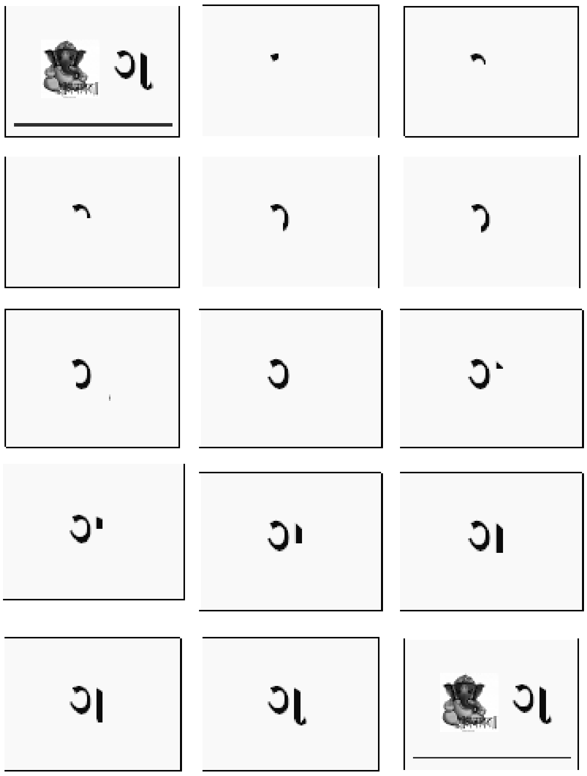

Figure 2 : Gradual increment of the selected symbol in Parichay

Multi Agent Knowledge Based System (MAKBS)

Traditional computer-aided software is typically a full-fledged system based on database providing only static presentation of information. Such systems are meant for literate young students and lack personal attention that illiterate adults need. Shortage of experts and trainers in rural areas is also a concern. Learners do not get motivated as there is a lack of guidance. The literacy software should be user friendly, easy to operate (mainly in native language), able to present information dynamically in multimedia and capable to explain its own decision-making. In short, the agent needs to satisfy different user groups in different ways by identifying the user's interest and level.

The agent Parichay partly satisfies the criteria. Since the developed component is an agent, many such other detachable components can be developed further for ensuring progress in an area, and when task is over, a new component can be attached to the system. This gives advantage of reusability. To achieve the remaining characteristic of intelligent behaviour, it is proposed that the agent Parichay should be integrated with other system that supports multiple agents and behave in an intelligent manner. A Knowledge Based System (KBS) can be used, which works on Knowledge Base instead of databases and offers advantages of intelligent behaviour and replaces expert, for this purpose. In rural areas, where experts are few and not easily available, the system with multiple agents can act as an intelligent expert to accelerate the process of development and meet the exact need by identifying the users' level and requirements. This can be considered as one of the reasons why traditional computers have failed in rural and/or remote areas. Other reasons can be problem of availability of technology, training and language/interface. For tasks like literacy and awareness in rural development, imparting such intelligent system does not seems feasible at a first glance. It should be noted that the set up cost of such system may be high and require some extra development effort, but facilities like good user interface in users' native language in multimedia, cloning of system and documentation of knowledge make it cost effective, flexible and reusable [6]. Government has established computers both within various states and within these at district and block levels. Such basic infrastructure can be utilized for the purpose.

Besides a Knowledge Base, such KBS has a search programme called Inference Engine (IE) to infer and generate new knowledge from the existing knowledge. The knowledge base contains Knowledge about domain, Knowledge about knowledge (meta knowledge), Knowledge about the learner and Knowledge about the process.

KBS may be automatically updated by itself (machine learning)[5]. In addition to all these, there is an appropriate User Interface, which may have the Natural Language Processing and multimedia facility. Since the system is multi agent system, other agents like translation agent, query agents, reporting agents and agents related to the rural development programme (like identifying suitable beneficiaries to different Government schemes) can be attached on demand. Figure 3 shows the structure of the system.

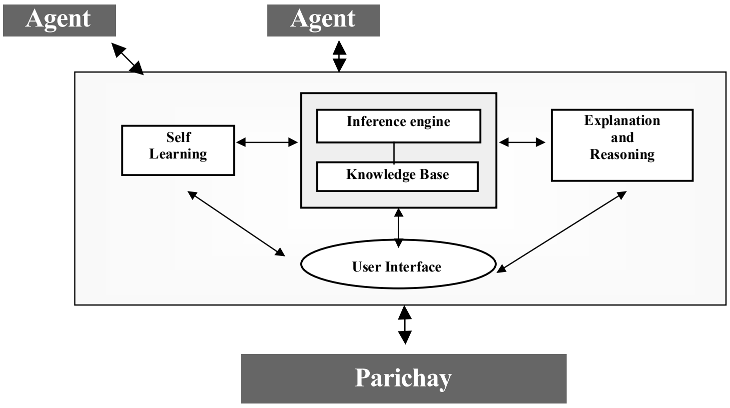

Figure 3: Parichay in conjunction with Knowledge Based System

As far as knowledge about learner is concerned, one can design user profile and heuristic (rule of thumb to exhibit intelligent behaviour) [4] to identify slow learners and arrange the presentation sequence for the user in the knowledge base of the system. Such knowledge about users can be dynamically learned while creating users' profile when system is in use. By analyzing responses by users at different stages, the user profile can be created to evaluate the learner level. Alternatively, one or more drills/quizzes will be prepared from the question bank on the related topics and the results from these can be used to determine the level. Attributes like user's interest in a particular material, number of repeats, speed of attending drill questions per minute and correct question per drill along with the history about user if any, play an important role to determine the grasping level of learner. An example frame of a heuristic function of range [0,1] that determines the level of user (L_Level) depending on the user's speed-correctness ratio (S/C) is given below.

L_Level = High if S/C >=0.70
= Medium if 0.70< S/C >= 0.55
= Low if 0.55< S/C >= 0.30
= Poor if 0.30< S/C

The speed correctness ratio from 0 to 5 questions per minute is described graphically in Figure 4 A along with a heuristic function based on it in Figure 4 B. Based on this, the next presentation material and its style (representation scheme) can be chosen. Responses of the user, history and temporary results can be stored in the user profile for history and backup purpose. Some standard can be developed and a learning matrix can be formed for different groups of learners. Once the learner level is identified, its value can be utilized with the rules of the system stored in the knowledge base. Some sample rules are given in the Table 1. Similarly, knowledge about process and knowledge about knowledge (meta knowledge) heuristics and rules can be defined.

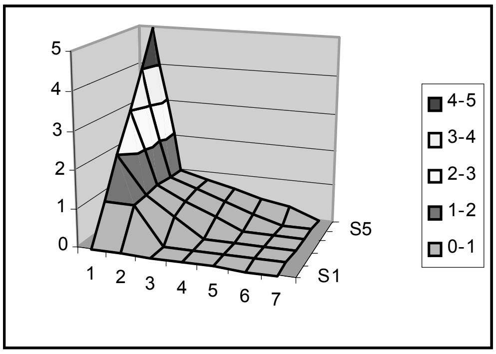

Figure 4 A: Speed correctness ratio upto 5 questions per minute

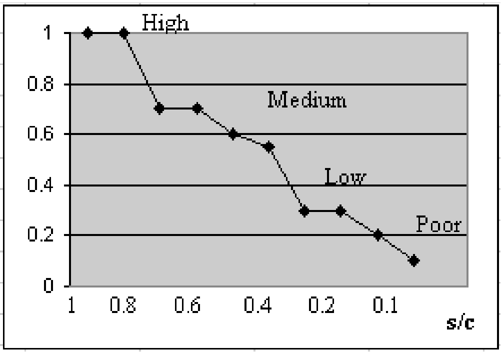

Figure 4 B: Heuristic function L_Level based on speed correctness ratio

(R1) Presentation for High Grasping Users If L_Level = High Unless previous-repeat-count < 2 Generally present-next-information Specifically select medium-to-high level questions	**(R2) Slow Information Presentation** If L_Level = Low Unless previous-repeat-count <= 4 Generally present-current-info-again Specifically select low level questions
(R3) Simulated Example Presentation If L_Level = Medium with value 0.6 And previous-repeat-count >= 2 Generally change-present-information Specifically select simulated-example-information	**(R4) Dumb Student Support** If L_Level = Low with value 0.8 And previous-repeat-count <= 4 Generally restart with previous-repeat-count MAX Specifically []

Table 1. Few sample rules for the system

Such system can be placed at the block level or *panchayat* level to allow the users to seek optimum advantage out of it. Existing centers like '*Jan Sewa Kendra*' in Ahmedabad model of Gujarat Government for e-Governance [2,3] and Citizen Facilitation Centers at *Taluka* and District Head Quarters can be considered as centers for the project implementation. The system can be used simultaneously at multiple places as multiple copies of such system can be easily done. Farmers, teachers, *gramsevaks*, retired people, women and children can be trained to use the system and the same people can work as resources persons thereafter. The Government of Andhra Pradesh has employed the same strategy for the Project of Chiluvuru called RAJiv internet village (RAJiv) [7]. The system can be enhanced in future, from a single PC based system to web based multi user system with minor changes and no change in the agent Parichay, which is already developed and successfully implemented. Once the system is successfully achieves its objective, one may think of additional agents to be attached to the system such as: health awareness programme, technical education and distance learning, Rural e-Seva like services giving information about various Government welfare schemes, awareness agents for girl child, population control agents, translation agents, animal husbandry and crop-land pattern matching type agricultural support information agent. This makes the system multi purpose, flexible, reusable and modular.

Conclusion

Adult education can be significantly modernized and made more effective if knowledge-oriented multimedia programmes can be designed more thoroughly on the basis of predefined instructional design. The agent parichay is an effort in utilizing the technology in best manner possible to help achieve adult literacy. Such tutoring is more effective because the agent can respond to the specific needs of a user, guide slow learners, challenge rapid learners and monitor the progress of each user at a time.

Acknowledgement

Author is thankful to Prof. DB Choksi, Incharge Head, GH Patel PG Department of Computer Science and Technology, Sardar Patel University for providing guidance in preparation of this paper.

References

[1] Bradshaw, J.M. An Introduction to Software Agents. In: Software Agents, AAAI Press, p. 3 (1997)

[2] Government resolution dated 28 March 2003 of the Government of Gujarat, with respect to replicating Ahmedabad model (2003)

[3] Karwal Anita, "E-Governance and Citizens' Charter – An Agenda for an Effective Delivery Mechanism- the Ahmedabad Experience, ICT for National Development, Proceedings of 40th Annual National Convention of Computer Society of India, Hyderabad, p. 121-135 (2005)

[4] Rich Alain: Artificial Intelligence, McGraw Hill (2001)

[5] Rolston David, Principles of Artificial Intelligence and Expert System Development, McGraw Hill Book Company (1988)

[6] Turban Efraim, Decision Support and Expert System, Macmillan Publication Ltd., (1990)

[7] www.ieg.gov.in/chiluvuru, Government of Andhra Pradesh, Project of Chiluvuru-RAJiv Internet Village

'Prajna' - Jounal of Pure & Applied Sciences, 14 (2006) 25-38

GROWTH OPTIMIZATION OF $AgGaTe_2$ COMPOUND THIN FILMS

Shahera S. Patel[1] **and B. H. Patel**[2]

[1] University Science Inst. Centre (U.S.I.C.), Sardar Patel University, Vallabh Vidyanagar-388 120
E-mail : swamibhavin@yahoo.com
[2] Department of Electronics, Sardar Patel University,Vallabh-Vidyanagar-388 120

Abstract

Bulk $AgGaTe_2$ was prepared by melting pure constituents in stoichiometric proportions. Thin films of this material were grown by flash evaporation technique at different substrate temperature. The bulk material and the films were characterized by X-ray and electron microscope techniques. The effect of substrate temperature on the structural properties – grain size, film orientation, composition, and stoichiometry of the films have been studied. It was found that the polycrystalline, stoichiometric films of $AgGaTe_2$ can be grown in the substrate temperature range of $473K < Ts < 573K$. The deposition temperature also had a significant influence on the electrical properties of $AgGaTe_2$ thin films. Data are presented indicating the effects of substrate temperature on the resistivity and activation energy of the films. The implications are discussed.

Introduction

The thin film deposition of ternary I-III-VI_2 compound with a defined structure is an important problem in the semiconducting technology related to the search for new devices. Most of the I-III-VI_2 compounds are direct gap semiconductors and they crystallize with the chalcopyrite structure [1-6]. They have attracted a lot of attention in the past decade due to their potential applications in Opto-electronics, photovoltaic conversion and non-linear optics [7-11]. Although the Cu–III-VI_2 compound have been studied extensively, information on Ag compound of this family is rather scarce [12-15].

However, these compounds are relatively less investigated in the form of thin films. From this point of view and considering their applications in opto-electronic devices, it is necessary to grow the films and to investigate their characteristics. It is well known that the properties of thin films are highly sensitive to small changes in their chemical composition and to crystallographic imperfections which in turn are controlled by the detailed mode of preparation and conditions of growth. Hence, the purpose of this present investigation is to obtain information on the growth and structural characteristics – grain size, film orientation, composition and stoichiometry of the vaccum deposited $AgGaTe_2$ thin films prepared by flash evaporation technique. The effect of substrate temperature on the crystallization behaviour, composition and structure of $AgGaTe_2$ films are discussed.

Experimental

Bulk $AgGaTe_2$ ingot was prepared by mixing pure (99.999 % koch-light) individual elements in stoichiometric proportions in a sealed quartz ampoule evacuated to a pressure of $\approx 133 \text{ X } 10^{-5}$ Pascal. The sealed ampoule was placed in a furnace at a temperature of ≈ 1200 K and was rotated by a mechanical arrangement to ensure complete mixing of the constituents so that a complete reaction of the constituents may occur. The rotation was continued for 13 hours at the same temperature. Special care has been taken to avoid cracking of the ampoule by a step-wise slow cooling technique [16]. It was then cooled slowly in the furnace to room temperature. The ingot thus obtained was powdered and subjected to X-ray Diffraction and Energy Dispersive Analysis of X-ray to confirm the homogeneity and stoichiometry.

Film Preparartion

Thin films of $AgGaTe_2$ were grown by flash evaporation technique in a vacuum of $\approx 133 \text{ X } 10^{-5}$ Pascal. The source material was single phase $AgGaTe_2$ with grain size of 100-150 μm. The evaporation was carried out from a molybdenum boat maintained at sufficiently high temperature (≈ 1400K) in order to evaporate the material instantaneously. Freshly cleaved NaCl crystal surfaces were used as substrates. The deposition rate was ≈ 10 nm.s^{-1} and the thickness of the deposits were kept at $30 \overset{0}{A}$ in all cases. The composition of the bulk and films were analysed by EDAX using Model : XL 30; ESEM. The structural properties of these films were examined by transmission electron microscopy (TEM) using EM : Philips Model : Tecnai 20 TWIN. The electrical resistivity of the films was measured using a high impedance electrometer EA 814.

Results And Discussion

Small portions of grown compound were taken from different parts of the ingot and subjected to EDAX and X-ray diffraction studies. The X-ray diffractometer trace as shown in Fig.1(a) could be indexed on the basis of a tetragonal unit cell [17]. The interplanar spacings computed from the diffractogram are in good agreement with the calculated values obtained from the lattice parameter data reported by Hahn et.al.[1] [Table-1]. The very strong and sharp (112) peak indicates a highly preferred orientation of the crystallites. No peak other than $AgGaTe_2$ was evident in this pattern. The X-ray diffraction [Fig.1(b)] was carried out on the $AgGaTe_2$ film deposited at substrate temperature 523K (thickness 3500 $\overset{0}{A}$) in order to confirm the crystallinity. No reflections corresponding to the free elements were detected in the diffraction pattern. The EDAX studies [Fig.1(c)] indicate that the bulk consisted of near - stoichiometric $AgGaTe_2$ with a maximum deviation of 0.05 wt %.

The substrate temperature has been found to have significant influence on the quality and orientation of the $AgGaTe_2$ thin films. Electron diffraction patterns for films grown at T_{sub}= (a) 323K, (b) 473K, (c) 523K, (d) 573K & (e) 673K are presented in Fig.2. From the micrographs, it is revealed that the grain size increases with increasing substrate temperature. As deposited films obtained by evaporation in vacuum of the stoichiometric bulk onto NaCl substrates maintained at ambient temperature (300K) were essentially amorphous in nature and had a fine grain structure [Fig.2(a)]. The initiation of crystallization was noticed when the substrate temperature was raised to 473K [Fig.2(b)]. It is worth to mention that the film deposited at this temperature has random orientation with many chalcopyrite reflections e.g. (112), (204) & (221) present. At T_{sub}=523K [Fig.2(c)], a stronger (112) & (221) orientation is noted with decrease in intensity of (204). Film deposited at still higher substrate temperature T_{sub} = 573K, diffraction lines become sharp and intense and ultimately develop a strong (112) orientation as shown in Fig.2(d). When the substrate temperature was raised to values higher than 600K, the films were found to be dissociating as can be seen from the diffraction pattern of the film deposited at 673K [Fig.2(e)]. Several additional reflections were noted, which were identified to be due to Ag_2Te* and $Ag_xGaTe_{1-x}^{\blacktriangle}$. The crystallinity of the films can not be improved because the compound decomposes at higher substrate temperature. Films grown in the substrate temperature range of $473K \leq T_{sub} \leq 573K$ are single phase, polycrystalline and showed a stronger (112) preferred orientation. Patel et.al.[18] and Kazmerski et.al.[17,19] have reported similar significant influence of the substrate temperature on the quality and orientation of $AgGaSe_2$ and $CuInTe_2$ thin films.

The compositional analysis of the films presented in graphical form is shown in Fig.3 which shows that the elemental weight percentages of Ag, Ga & Te depend critically on the substrate temperature. The EDAX data reported in this work are the averages of a large number of individual analyses on different identical samples and are accurate up to ± 0.3 wt %. The film deposited at ambient temperature is Tellurium rich. Attention may be drawn to the fact that the films deposited in the substrate temperature range $473K \leq T_s \leq 573K$ are nearly stoichiometric. Further increase in the substrate temperature above 573K resulted in a gradual decrease in Tellurium content in the films. This Tellurium deficiency may be attributed to re-evaporation of mobile Te adatom from the substrate surface, since Te has a high vapour pressure. Patel et.al.[20] have reported deficiency of Te in $AgInTe_2$ thin films at higher substrate temperatures.

The films grown on glass substrates have the same orientational properties as those discussed for films grown on NaCl substrates. However, the films had a smaller grain size than those deposited on NaCl substrates.

Thus, single phase, polycrystalline, stoichiometric films of $AgGaTe_2$ can be grown in the substrate temperature range $473\ K \leq T_{sub} \leq 573\ K$.

The variation of the electrical resistivity of $AgGaTe_2$ films with different substrate temperature (Ts) is shown in Fig.4. It is observed that the resistivity decreases as the substrate temperature increases and is at a minimum for 573 K. The decrease in resistivity of the as-deposited films with increase in the substrate temperature up to 573K can be explained using Petritz's barrier model [21]. Since the crystallites do not grow sufficiently large at low substrate temperature, the intercrystalline regions are wide offering a high resistance to the movement of charge carriers. Nucleation theory [22,23] shows that higher substrate temperature favours the formation of a fewer nucleation centres resulting in larger crystallite size which ultimately is effective in decreasing the intercrystalline barrier size. Also, a large grain size material has fewer grain boundaries and therefore the electrons scattered less effectively. The charge carriers, therefore, have to cross comparatively narrow intercrystalline barriers which may be responsible for the decrease in the resistivity.

The increases in resistivity of the films deposited above 573K may be attributed to the deviation from the stoichiometric composition of the films, since the films grown at temperature above 573K are Te deficient. Moreover, the formation of additional phases Ag_2Te and Ag_XGaTe_{1-X} may be responsible for this deviation. Fray et.al. [24] and Patel et.al. [25] reported that $CuInSe_2$ and $AgInSe_2$ films grown at higher substrate temperatures were found to be Se defficient which showed high resistivity. Similar dependence of the resistivity on the substrate temperature has also been reported in other silver ternary compound films [18,20]. Kazmerski et.al.[19] have observed the presence of additional phases in $CuInTe_2$ films at higher substrate temperatures .

Fig.5 shows the plot of Log of Resistance (R) versus reciprocal Temperature (1/T) for

$AgGaTe_2$ films deposited at different substrate temperatures. The P-type nature of the films as indicated by the hot probe method showed that the conduction was primarily due to holes. It is observed in Fig.5 that each curve consists of two linear portions with a break at certain temperature which does not appear to remain constant. It can not be attributed to any change of structure or phase of the deposit but to the changing over from extrinsic to intrinsic region. The calculated values of activation energy were found to be Eg =1.155eV, 1.171eV, 1.191eV & 1.27eV for substrate temperatures (Ts) = 473K, 523K, 573K & 673K respectively. It is seen from the figure that as the substrate temperature increases, initially the resistance slowly decreases and then rapidly increases, suggesting the approach in the intrinsic region . The activation energy of the films grown at different substrate temperatures are found to be slightly higher than the value reported for bulk $AgGaTe_2$ (1.1eV)[3]. At higher substrate temperature (Ts = 673K), the higher value of activation energy may be due to the additional phases in the film.

Conclusions

The flash evaporation of stoichiometric bulk $AgGaTe_2$ yield polycrystalline, single phase, stoichiometric compound films in the substrate temperature range $473\ K \leq T_{sub} \leq 573K$. The films deposited at lower substrate temperature (Tsub < 473K) are amorphous in nature. At higher substrate temperature (Tsub > 623K) the films are of polyphase. The electrical resistivity of polycrystalline $AgGaTe_2$ films is found to be minimum grown at substrate temperature of 573K. The properties of the films have been shown to depend critically on the deposition temperature. Grain boundary scattering mechanisms dominates the electrical properties.

References

[1] Hhan H., Frank G., Klinger W., Meyer A.D. and Stroger G., Z.Anorg. Allg.Chem. **27**, 153 (1953)

[2] Shay J.L., Tell B., Kasper H. M. and Schiavone L. M. Physics Review **B7**, 4485 (1973)

[3] Zhuze V. P., Sergeeva V.M. and Shtrum E. L., Soviet Phys.Tech.Phys., **A2**, 1925 (1958)

[4] Neumann H. , Kuhn G. and Schumann B., Progr.Crystal Growth Charact. **3**,157 (1981)

[5] Tell B., Shay J. L. and Kasper H. M., J. Appl. Phys. **43**, 2469 (1972)

[6] Zonaghi M.C.,Nasrallah T. B., Marsillac S.,Bernede J. C. and Belgacem S., Thin Solid Films **382**,39 (2001)

[7] Bodnar I.V., Rud V.Yu. and Rud Yu. V. Semicond.Sci. Technol. **17**, 1044 (2002)

[8] Boustani M. et al., Semicond.Sci.Technol. **12**,1658 (1977)

[9] Shay J.L. and Wernick J.H., Ternary Chalcopyrite Semiconductors: Growth,Electronic properties and Applications (New York: Pergamon) 1975

[10] Siemer K., Klaer J., Luck I., Braunig D., Thin Solid Films **387**, **No.1-2** 22 (2001)

[11] Rechid J. and Reineke-Koch R.,Thin Solid Films **387**, **No.1-2** 243(2001)

[12] Pamplin B. and Feiglson R. S. 1979 Thin Solid Film **60**, 141 (1979)

[13] Hong W., Neumann H., Schumann B. and Kuhn G., Phys. Stat. Sol. **85b**, K57 (1978)

[14] Metzner H., Hahn T., Thin Solid Film **361-362**, 504 (2000)

[15] Shfarman W.N., Zhu J.,Thin Solid Film **361-362**, 473 (2000)

[16] Kanellis G., Kambas C. and Spyridelis J., Mater. Res. Bull.**11**, 429 (1976)

[17] Kazmerski L.L., Ayyagri M.S., Sanborn G.A.,White F.R. and Merrill A.J., Thin Solid Films **37**, 323 (1976)

[18] Patel S.M., Kapale V.G., Materials Letters **3**, 440 (1985)

[19] Kazmerski L.L.and Juang Y.J., J.Vac.Sci.Technol. **14**, No.3 769 (1977)

[20] Patel S.M.,Patel B.H., Materials Letters **2**, 424 (1984)

[21] R.L.Petritz, Phys.Rev.**104**, 1508 (1956)

[22] Burke J.,“ The Kinetics of Phase Transformation in Metals ”, Pergoman, Oxford, 143 (1965)

[23] Rybka V., Sevcik Z., Krejci P. and Dudrova E., Thin Solid Films **9**, 83 (1971)

[24] Fray A.F. and Lloyd P., Thin Solid Films **58**, 29 (1979)

[25] Patel S.M., Patel A.D., Thin Solid Films **111**, 53 (1984)

Table -1. Calculated and Observed d spacing data for AgGaTe_2

hkl	Calculated(a) d-spacing $\overset{0}{(A)}$	Angle (2θ)	Observed d-spacing from X-ray diffraction pattern of powder(b) sample $\overset{0}{(A)}$	d-spacing-spacing $\overset{0}{(A)}$ of diffraction rings of thin films(c) observed at various deposition temperatures (Ts)		
				Ts = 473 K	Ts = 523 K	Ts = 573 K
112	3.55	24.91	3.57	3.44	3.34	3.58
200	3.16	28.33	3.14		3.12	3.18
220	2.23	40.41	2.23		2.35	2.00
221	2.18	41.55	2.17	2.22	2.38	2.32
204	2.16	41.72		2.08		
312	1.88	48.17	1.88		1.90	1.88
313	1.78	50.01	1.82			1.64
441	1.55	58.43	1.57			
332	1.44	64.47	1.44			
333	1.39	69.47	1.35			
500	1.25	76.58	1.24			1.33
512	1.20	78.85	1.21			
532	1.06	92.90	1.06			
600	1.05	94.42	1.04			

(a) d values are calculated from the reported lattice parameters [1] and possible chalcopyrite reflections [17]

(b) From the X-ray diffraction pattern of the bulk.

(c) From the Electron diffraction patterns of the thin films.

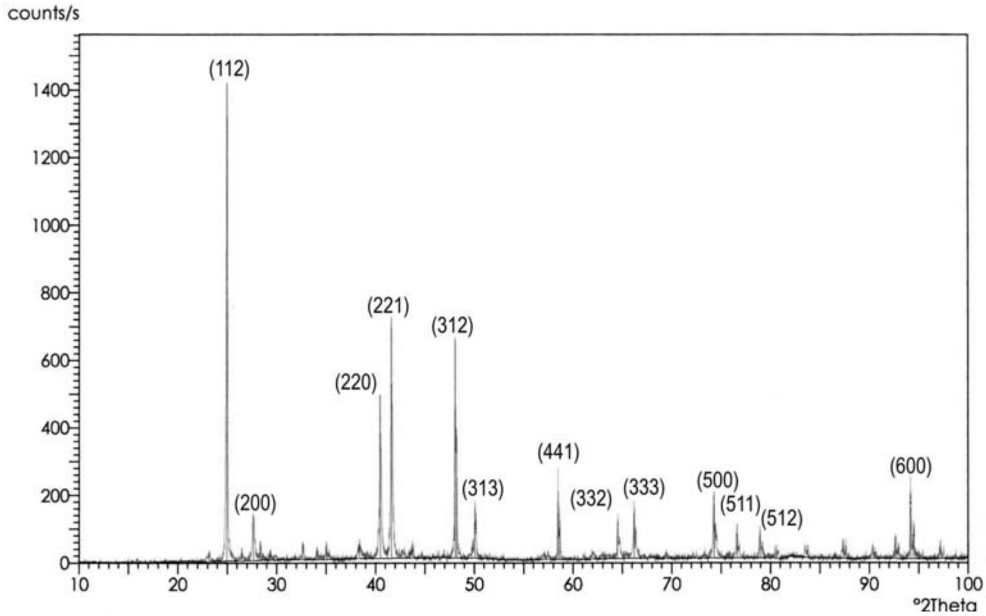

Fig. 1 (a) X-ray diffractogram of the bulk $AgGaTe_2$ (compound).

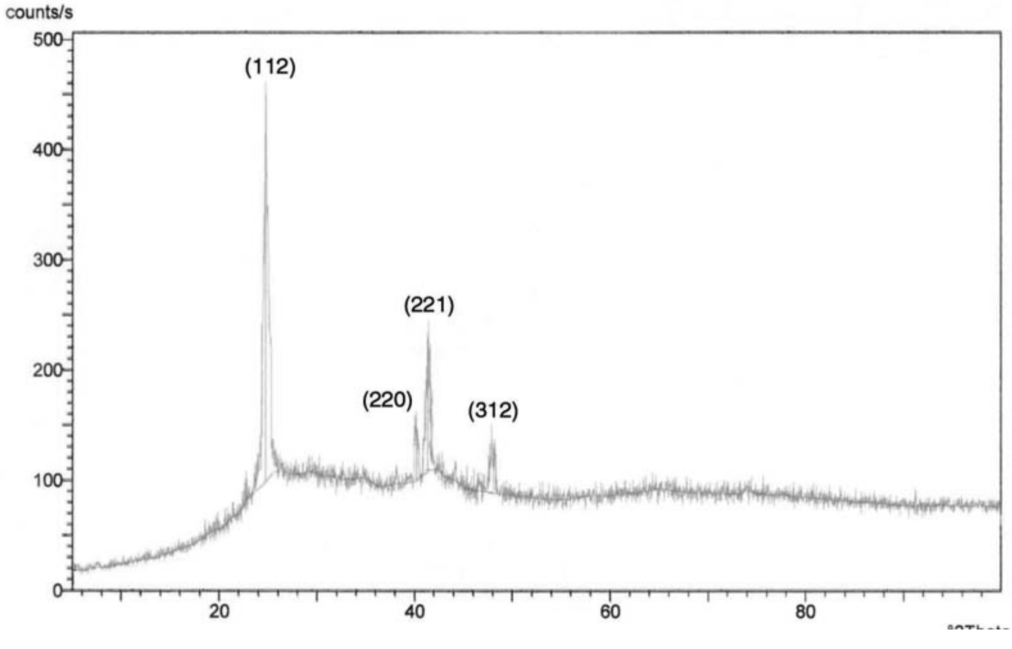

Fig. 1(b) X-ray diffractogram of $AgGaTe_2$ thin film deposited on glass substrate at substrate temperature Ts=523K.

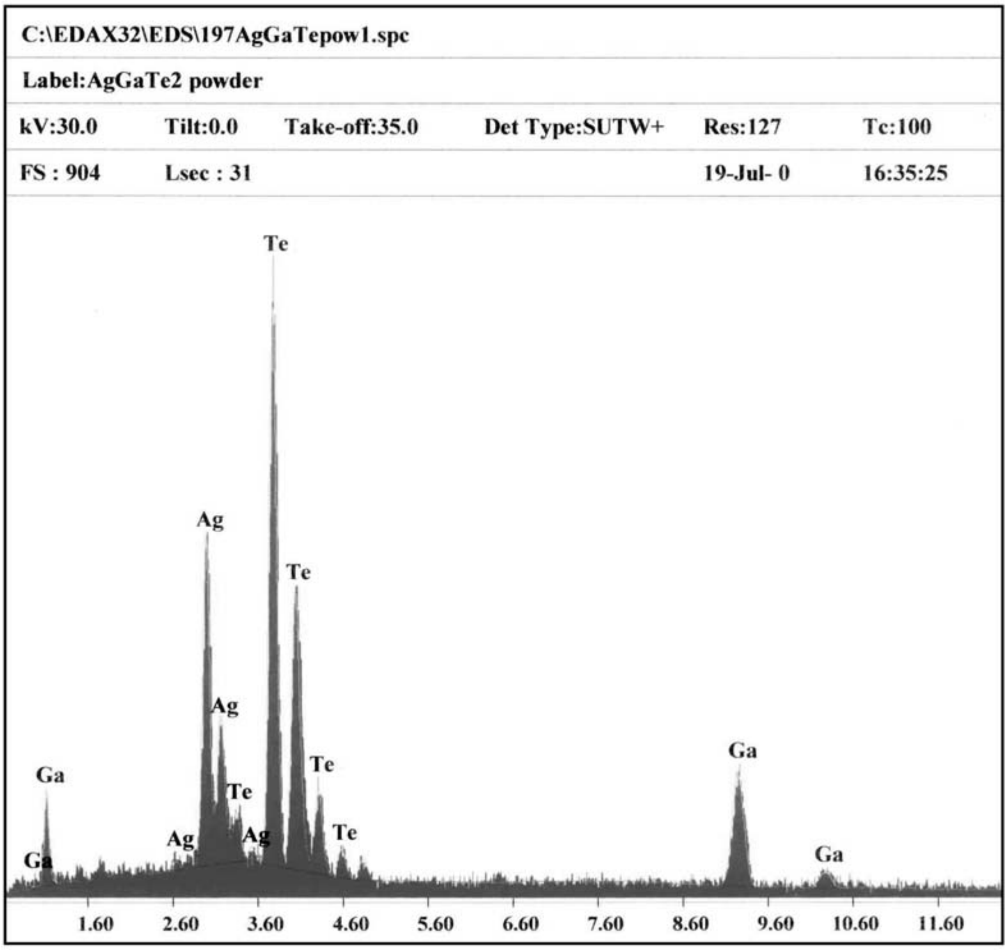

C:\EDAX32\EDS\197AgGaTepow1.spc

Label:AgGaTe2 powder

kV:30.0 Tilt:0.0 Take-off:35.0 Det Type:SUTW+ Res:127 Tc:100

FS : 904 Lsec : 31 19-Jul- 0 16:35:25

EDAX ZAF Quantification

Element	Wt %	At %	K-Ratio	Z	A	F
AgL	25.02	25.02	0.2244	1.0325	0.8470	1.0256
TeL	58.50	49.46	0.4547	0.9626	0.8076	1.0000
GaK	16.48	25.51	0.1611	1.0748	0.9092	1.0000

Fig. 1(c) EDAX Analysis of the bulk $AgGaTe_2$ (compound)

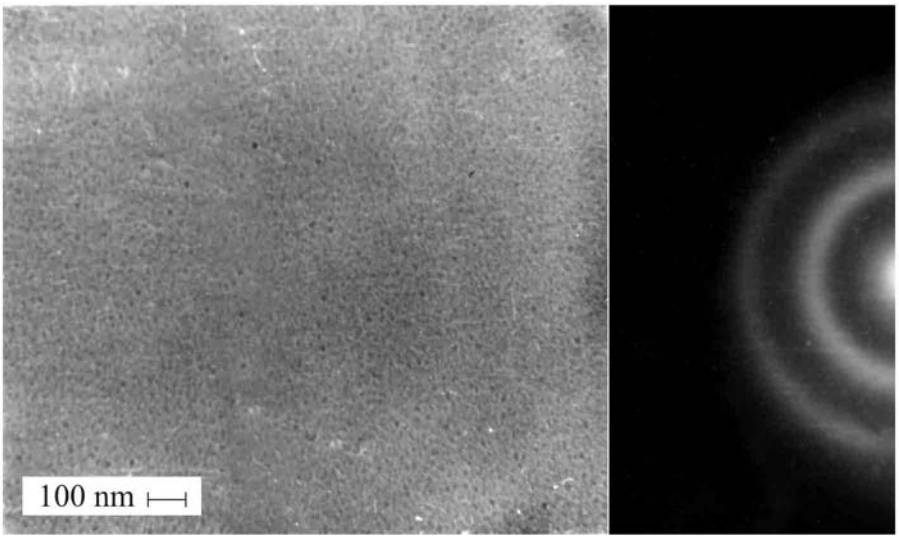

(a) Ts = 300K

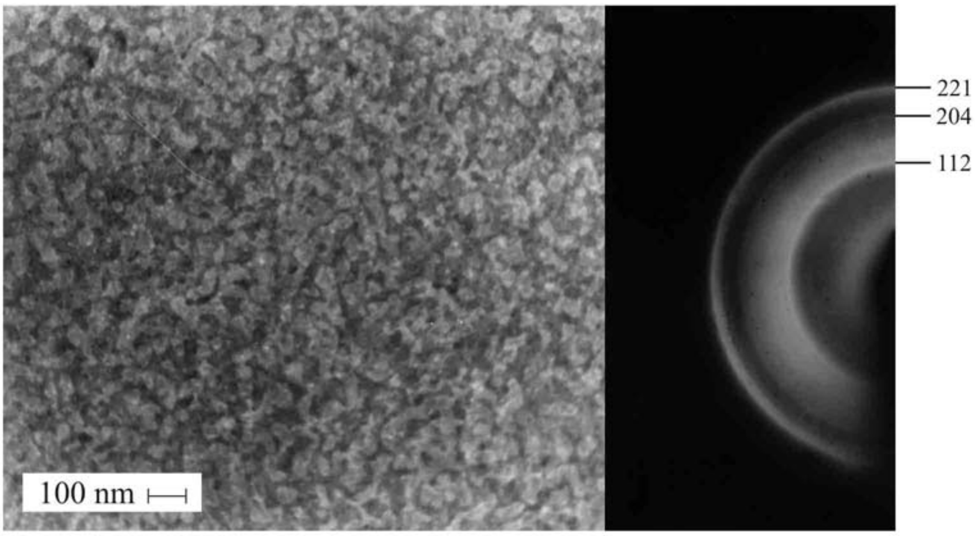

(b) Ts = 473K

Fig. 2 Transmission Electron Micrographs and the Corresponding Diffraction patterns of AgGaTe$_2$ thin films deposited on NaCl at substrate temperatures (a) 300K (b) 473K.

Fig. 2 Transmission Electron Micrographs and the Corresponding Diffraction patterns of $AgGaTe_2$ thin films deposited on NaCl at substrate temperatures (c) 523K (d) 573K.

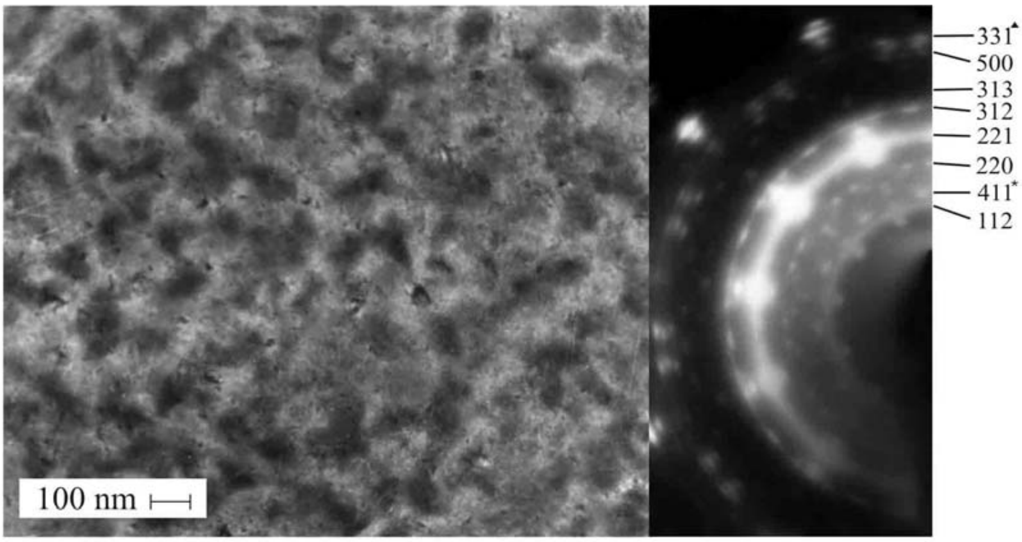

(e) Ts = 673K

Fig. 2 Transmission electron micrographs and the corresponding diffraction pattern of $AgGaTe_2$ thin film deposited on NaCl at substrate temperature (e) 673K.

▲ Indicates the d value may be due to the Ag_XGaTe_{1-X} compound.

* Indicates the d value matching with the Ag_2Te compound.

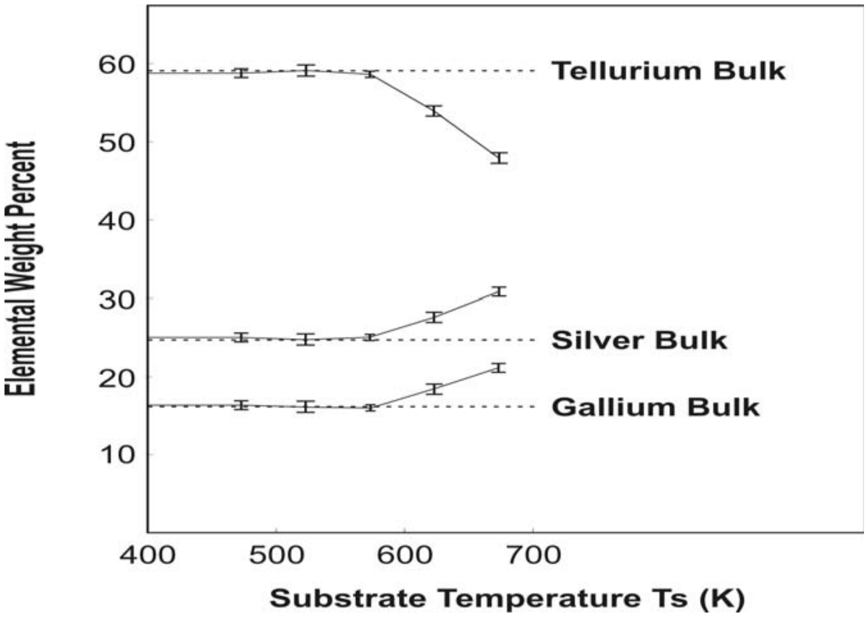

Fig.3 Graphical representation of variation of Elemental Weight Percent in the $AgGaTe_2$ thin films deposited at different substrate temperatures. The stoichiometric composition in the bulk material is shown by dashed lines.

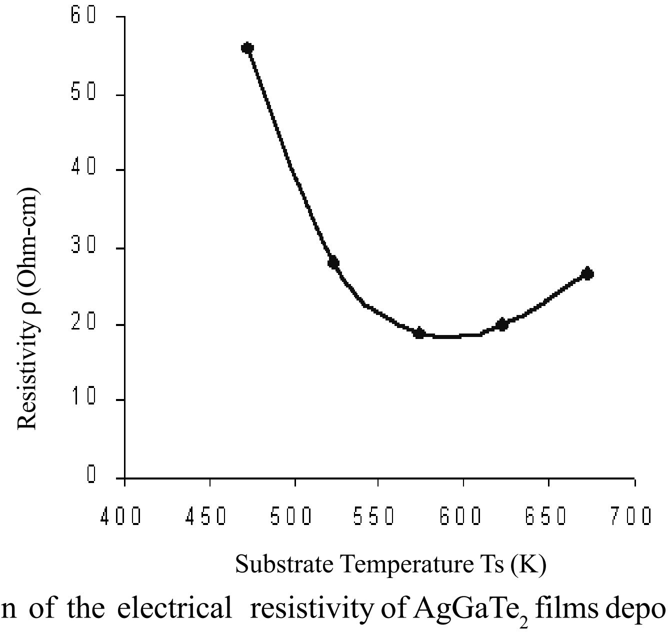

Fig. 4 Variation of the electrical resistivity of $AgGaTe_2$ films deposited on glass at different substrate temperatures.

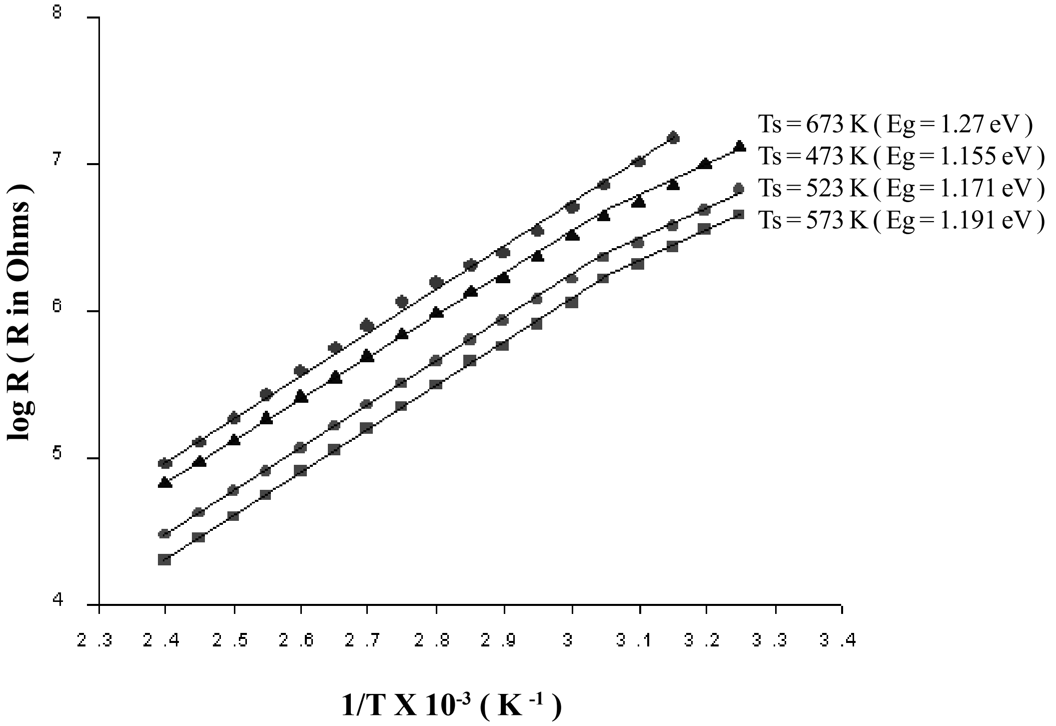

Fig. 5 Temperature dependence of resistance for AgGaTe$_2$ films deposited at (a) Ts = 473K (b) Ts = 523K (c) Ts = 573K (d) Ts = 673K

'Prajna' - Jounal of Pure & Applied Sciences, 14 (2006) 39-46

STUDIES ON CHEMICAL BIOCHEMICAL AND NUTRITIONAL ASPECTS OF WHEAT PRODUCTS PROCESSED FOR DAILY CONSUMPTION

Harshada J. Shah

Department of Biochemistry. M.B.Patel Science College. Anand.388001.

Abstract

Wheat is a main cereal consumed through out India as a part of main diet. Chemical composition of the wheat alters due to cooking. Preparation of the products for human consumption is responsible to change in its nutritive and nutritional value. Present investigation was aimed to study the effect of processing on chemical constituents of the wheat and of the selected traditional products on biochemical constituents of the weanling rats. Phulka ,Thepla and Poori are main food items of a traditional menu were prepared and fed to the rats. Total fat, thiamine and riboflavin content of the diet were altered on processing. Blood , plasma and liver parameters of the weanling rats for these constituents were also altered on feeding trials.

Key Words: Phulka ,Thepla , Poori , Protein, thiamine riboflavin , PER, FER, cholesterol, lipid..

Introduction

Wheat is extensively cultivated and important cereal used throughout the world for consumption. Wheat flour is used to produce Bread stuffs, which is superior to other cereals because of Gluten (Clark A.1956). Nutritive value of the wheat varies slightly from year to year (Shrinivas A. L.1984). Bread, Biscuits, Toast, Wheat flakes, Shredded wheat, Semolina, Wheat germ, Cake, Noodle, Macaroni, Spaghetti are industrial products Obtained from wheat. Among all the products Phulka, paratha and Poori are prepared, both in household and in commercial establishments (Saxena and Haridas.1995). Wheat flour is also processed at home scale for the preparation of the Chapati and Poori. Chapati is a traditional recipe for Gujarat but a new for Southern coastal families, also for the people of hilly region, in West Bengal, Orissa and Bihar (Govilker M.1984). About 80 to 90 % of wheat consumption in India are in form of Chapati (Austin and Ram.1979).

Present study was planed to prepare the products from wheat as a first part of the experiment, which are used as a main part of the diet. Phulka , Thepla and Poori , were prepared and analyzed freshly to find out changes in their nutrient content on cooking . Availability of the nutrients was studied by feeding these products to the weanling rats, as the second part of the experiment.

Experimental

Raw material – Wheat were procured from the local market, cleaned and made in to the fine flour. Groundnut oil, pure Ghee, Salt ,Turmeric powder and Chillies powder of the Standered mark were also procured from local market.

Preparation of recipes: To minimize variation in nutrient content physical parameters such as thick ness, size, temperature and duration of cooking were kept constant for the preparation of each product. .

Pulka: In 100 gm. of the wheat flour 4 gm. of oil was added as shortening. Dough was kneaded by adding 2 gm. salt and 75 ml. of water. Dough balls were rolled in 0.069 cm. thick and 12.4 cm. circular disk. Both the sides were roasted on iron pan for 15 second then grilled on fire to obtain Phulka.

Thepla: : In 100 gm. of the wheat flour 4 gm. of oil,2 gm. salt,1 gm turmeric powder and 1 gm. chilly powder were mixed, dough was kneaded using 75-ml water. Dough balls were rolled in 0.095 cm. thick and 11.2cm. circular disk. Both the side were shallow fat fried on iron pan for 15 sec. to obtain golden brown product.

(3) Poori: Dough balls prepared from Thepla dough were rolled in 0.069cm. thick and 4.4 cm. circular disk. They were deep fat fried in groundnut oil to obtain soft raised and golden brown product.

Chemical Analysis of the Products

Freshly prepared products were divided in different parts to study various nutrient content such as total protein (Oser and Hawks.1956), Fat, Thiamine and Riboflavin (A.O.A.C. 1984).

Animal Experiment

To study the effect of wheat products on growth, total 24 weanling rats were divided in to four groups. The rats were fed on raw wheat flour, freshly prepared Phulka, Thepla and Poor for a period of 28 days. Records for dietary intake, gain in weight and PER were made according to Swaminathan M.(1985) , FER was calculated using formula- Gain in weight (g)/ Food intake(g) .

At the end of the experiment animals were sacrificed under mild anesthesia. Blood was collected from the heart in the heparinised tubes. A small portion of the blood was used for Haemoglobin estimation (Van Kampen et al 1961.), remaining blood sample was transferred to centrifuge machine for the plasma separation . Plasma was used for the analysis of Protein (Rein hold J. A. 1953) and Cholesterol (Zlatkis, Zan and Boyle.1953).

Liver Prossesing

Liver tissue were excised blotted of blood and tissue fluids on a filter paper, cleared of extraneous tissue and weighed on a pre weighed aluminum foil. The known gm. of the liver tissue were divided for the estimation of total protein (Lowry.et.al. 1951), Lipid , Riboflavin and Thiamine (AOAC .1984) .

Results And Discussion

Freshly prepared products Phulka , Thepla and Poori were analysed along with raw flour. Chemical analysis showed 12.9 % protein content which match with the reported value of Gopalan. et. al.(1978). Protein content of the wheat ranges from 11.31 to 12.7 gm.%. (Chopra et .al. 1978). Protein content of the wheat flour decreased on processing as in Phulka (9.6 gm. %), Thepla (12.3 gm. %) and Poori (9.23 gm. %). All represents decreased value in the final product. Decrease was 25%, 4.5% and 26.7% respectively on preparing Phulka , Thepla and Poori. This may be due to greater time required for cooking. Martin C. (1985) mentioned that higher temperature unless of extremely short duration is a matter of the seconds, results in breakdown of the protein. Among the amino acids, lysin and tryptophan may get destroyed during the preparation of poori and phulka. (Yasodadevi and Geervani 1978). Higher temperature during cooking is responsible to decrease the protein content.(Veena et.al.1963)

During the preparation of the dough 4.0 gm. % of the oil was added, therefore fat content of the wheat flour was 6.4 gm. %. After preparation of phulka ,ghee applied on the surface of the phulka increased the initial value to 23.4 gm. % fat in a final product. Thepla contained 24.24 gm. % fat, due to use of the oil for shallow fat frying. Maximum fat content was observed for poori (30.2 gm. %) due to deep fat frying.

Wheat analysis showed 0.52 mg. % thiamine and 0.33 mg. % riboflavin, which is higher then the reported value (Gopalan et.al.1978). The difference may be due to the variety of the wheat used in the experiment. Thiamine content was 0.45 mg. %, 0.51 mg. % and 0.27 mg. % for Phulka Thepla and Poori respectively. Products showed 14 %, 1 % and 48 % loss respectively. Results are in agreement with the reported values 11-33% loss in chapati (Pal. B.P.1956) 40 –90 % loss in poori (Ahmed et al.1948). Riboflavin content of the products were 0.30mg%, 0.24mg% and 0.18mg% for phulka, thapla and poori represents 9%, 25% and 48% loss from the initial value respectively. Observations are related with the values 29% - 41% loss as reported by Ranhotra. et. al.(1983) during cooking of the pasta products. Results for chemical analysis are presented in table-1.

Considering above changes, selected products were fed to the weanling rats to study biological and biochemical parameters. Food intake and nutrients intake were calculated from the record book and presented in table-2. Food intake of phulka was maximum 205.19 gm. compared to wheat flour (180.9gm), thepla (175.7gm) and poori (204.4gm). Dietary intake of Phulka is correlated with the value obtained on feeding "kalyansona" wheat chapatti. Nutrients intake also changes on the basis of the dietary intake. Efficiency of the diet fed is represented in terms of gain in weight, PER and FER. Gain in weight of the rats fed wheat flour was 28.3 gm which slightly increased on feeding phulka (29.25gm), were as decreased on feeding thapla (18.9gm) and poori (15.15gm). Chawala et al (1982) reported 23.7 gm. gain in weight on 148.5 gm. chapati intake, which is very well related with present study indicating 29.5 gm. gain / 205 gm. of phulka intake. Gain in weight of 27.88 gm. reported for wheat fed rats by Kappor A .C. and Gupta. V. P. (1992). Poori fed rats represents 45.9 gm. decreased in weight compared to raw flour fed rats. Retarded growth may be due to destruction of the some nutrients like riboflavin and amino acids like lysin or tryptophane or cystine during deep fat frying (Stilling and Hackler 1965) or may be due to decrease in pancreatic digestibility as reported by Vidya sager et. al. (1973) that heated oil produced growth depression .

Phulka group had slightly higher PER (1.48) compared to raw (1.2). The result suggest that the quality of the protein was improved due to roasting. Decreased in PER for Poori and Thepla may be due to loss of certain amino acids during deep fat frying and shallow fat frying. Chandrasheker et al (1978) and Charangeet et al. (1995) both, had reported higher PER for chapatti is due to roasting. PER for raw flour reported by Geeta et al (1995) is 1.04 and for chapatti by Anita et al (1994) is 1.3, values are supportive for results obtained in present study. As the level of oil increases FER found to decrease. However rats fed same level of Ghee in Phulka had better FER; this may be due to high palatability of Ghee compared to ground nut oil. Observations are presented in table-3.

Blood, plasma and Liver Parameters

Blood and plasma Parameters: Haemoglobin content was studied to confirm the biological availability of the iron. Preparation of the wheat products found to increase blood hemoglobin value. Compared to the raw flour the increase was 18.7%, 33% and 29.1% respectively for Phulka , Thepla and Poori .The 4% increase in haemoglobin on roasting of the grains is reported by Kapoor and Mehta. (1992). Plasma protein for the wheat flour fed rats was 8.16gm% which decreased on the feeding of Phulka , Thepla and Poori (5.6%,1.8 %and 9.2%) respectively. Diet containing high fat showed increase in total Cholesterol .The rats fed Poori (147.86mg%) and Phulka (148.4mg%) indicates highest value compared to Thepla (123.7mg%), even though source of fat was differ. Results are reported in table-4.

Liver Parameters: Liver protein store indicates 5.7%,9.4% and 7.2 % decrease respectively for Phulka , Thepla and Poori compared to raw flour fed rats. Phulka containing ghee had lowest lipid storage (8.9mg%) where as thepla (11.66mg%) and poori (13.29mg%) and had higher lipid content. Results reveals that groundnut oil leads to higher amount of the liver lipid accumulation compared to the pure ghee. This may be due to linolic-acid, which is a metabolic precursor of w_6 group, which deposits directly in to the tissues. Connor et. al. (1986) Liver store for thiamine and riboflavin were decreased with increasing intake of fat from prepared products. This may be due to increased demand of "B complex " vitamins on increasing fat content of the diet (Kosuke and Yoshinori 1977) .Higher liver store for both vitamins for Phulka group may be due to higher dietary intake . Values for Liver parameters are mention in table-5.

Acknowledgement: Author is grateful for research facility and guidance provided by Dr. S.S.Sail. Ex. Prof. Dept. of Foods and Nutrition. S.P. University. V.V. Nager.

Table : 1. Chemical composition of wheat flour and its products.

Product	Protein(g)	Fat(g)	Thiamine (mg)	Riboflavin (mg)
What flour	12.9±0.01	6.41±0.14	0.52±0.007	0.88±0.003
Phulka	9.6±0.01	24.3±0.17	0.45±0.009	0.30±0.008
Thepla	12.3±0.02	22.2±0.29	0.51±0.007	0.24±0.006
Poori	9.2±0.01	30.2±0.25	0.27±0.006	0.18±0.007

Mean of six replication.

Table : 2. Diet and nutrients intake of the rats.

Four weeks intake				
Product	**Diet (g)**	**Protein (g)**	**Thiamine (mg)**	**Giboflavin (mg)**
Wheat flour	180.9±6.7	23.34±0.7	0.958±0.06	0.57±0.04
Phulka	205.2±12.0	19.72±1.2	0.923±0.05	0.69±0.03
Thepla	175.7±2.4	21.62±0.9	0.891±0.01	0.42±0.04
Poori	204.4±7.4	18.87±0.7	0.552±0.04	0.36±0.02

Mean of six replication

Table : 3 Weight gain, PER and FER for the rats fed on wheat flour and its products

Four weeks record			
Product	**Weight gain (g)**	**PER**	**FER**
Wheat flour	28.03±1.8	1.20±0.08	0.155±0.01
Phulka	29.25±3.5	1.48±0.11	0.149±0.02
Thepla	18.91±1.9	0.87±0.04	0.108±0.01
Poori	15.15±1.1	0.82±0.10	0.072±0.01

Mean of six replication

Table : 4 Blood and plasma parameters for the rats fed on wheat flour and its products.

Product	Heamoglobin (g%)	Protein (g%)	Cholesterol (mg%)
Wheat flour	9.31±0.4	8.2±0.2	98.8±5.6
Phulka	11.06±0.4	7.7±0.4	148.4±10.2
Thepia	12.39±0.5	8.1±0.3	123.6±4.6
Poori	12.02±0.6	7.4±0.2	147.9±5.7

Mean of six replication

Table : 5 Liver parameters for the rats fed on wheat flour and its products.

Product	Protein (gm%)	Lipid (gm%)	Thimine (mg%)	Riboflavin (mg%)
Wheat flour	18.6±0.8	10.98±0.5	0.33±0.97	1.94±0.01
Phulka	17.54±1.7	9.93±0.6	0.24±0.08	2.17±0.15
Thepla	16.85±0.5	11.65±1.0	0.25±0.05	1.93±0.15
Poori	17.27±2.0	13.29±0.7	0.16±0.01	1.06±0.0

Mean of six replication.

References

B. Ahmad ,S. Mohra and G. Bharihoka. A study of the thiamine content of different varieties of wheat and wheat products of the Punjab in relation to the dietary habits of the people. *Ann.Biochem.Exp.Med.*8:4 :54-56. (1948).

Anita, Rawat, Gurmakh, Singh, Mital, B.K and Mital S.K. Effect of soy fortification on quality characteristic of chpaties. *Jr. Fd. Sc and Tech.* 1: 2: 114 –116. (1994)

A.O.A.C. Official methods of analysis of association of official agricultural Chemist. D. Williams .S. 14 th ed. Virginia U.S.A. (1984).

A. Austin and A.Ram. Study on chapati making quality of wheat. I.C.A.R. New Delhi.*Tech. Bull.* 31:39 - 41. (1979).

J. O.Ayaste,.O,V. Eka, and E. T. Ifon.. Chemical evaluation on the effect of roasting on nutritive value of maize. *Fd.Chem.*12 : 135 - 147. (1983).

T.M.Chandrasekhar, J.M.Howe and H.E.Clark.The complementary value of cooked Bengal gram and opaque-2 corn for the growing rats. *Nutr. Rep Inter.* 5:119-123 (1972).

K. Charangeet, Hira and Nupur, Chopra. Effect of roasting on protein quality of chickpea and peanuts. *Jr. Fd. Tech.* 32:6:501-503. (1995).

U. K. Chawla and A. C. Kapoor Chemical composition and protein quality of wheat triticale chapaties. Jr. Fd. Sc. 47 : 4:2015-2018. (1982).

A. Clark. Changing food habits in context of wheat. Indian miller. XV : 3. (1956).

K. Chopra, A. K. Chopra and C. M. Bhat. Protein qualities of chapaties prepared from high yielding varieties of wheat. *Jr. Rese. P.A.U.* Vol. XV : 4 : 478 - 480. (1978).

W. L Connor. Hypo-lipidemic effect of dietary omega –3 fatty acids in normal and hyper lipidemic humans. *Ind. Food Tech.*:124. (1986).

Geeta,Luthra and Balwinder, Sadana. Potential improving protein quality of Wheat chapati by addition of bhatu, Carrot and Radish leaves. *Jr. Fd. Sc. Tech.*32: 6 :5 0 – 60. (1995).

C.Gopalan, B.V.Ramasastri and S.C.Bal Subramanian.Nutritive value of Indian foods. N.I.N.Hyderabad.6065(1984).

M.Govilker . World Wheat situation. *Indian miller.* Vol. XV : 2 – 29. (1984).

A.C.Kappor and V.P. Gupta . Note on effect of roasting on nutritional quality of soy protein. *Ind. Jr.Agri.Sci.* 47: 360-367. (1977).

R.Kappor and V. Mehta. Iron bio-availability from Spirulina platensis, whole egg and whole wheat. *Ind. Jr. of Exp. Biology*. 30 : 904 – 907. (1992).

Kosuke, Nichino and Yoshinori, Itokawa.Thiamin metabolism in vitamin B_6 or vitamin B_{12} deficient rats. *Jr. Nutri.* 107:775-782. (1977).

O.H. Lowry, N.J.Rosebrough,A.L.Forr and R.J.Randall. *J.Biol.Chem*. 193 : 265.(The original method). (1951).

C.R.A.Martin. The effect of the food processing on nutritional value. *Br. Fd. Jr*. 87 : 106 – 107. (1985)

B.Oser and B. Hawks.Hawks physiological chemistry.13thedition.T.M.H.Publishing company Ltd. New Delhi. (1956)

B.P.Pal. Grain quality. VIII wheat. *Indian council of Agri. Res*. New Delhi. 178-180. (1956).

G.S.Ranhotra, J.A. Gelroth, Novak and Bock. Losses of enrich vitamins during the cooking of pasta products. *Nut Rep. In* 28:2: 423-425. (1983).

D.C.Saxena and P. Haridas, Rao. Survey of the quality characteristics of Tandoori dough and Tandoori roti. *Jr. Fd. Sci. Technol*. 32 :1 : 74-76. (1995).

B.R.Stilling and L.R. Hackler. Amino acids studies on effect of fermentation time and heat processing of Temphon. *Jr. Fd.Sci*. 30: 1047- 1048. (1965).

A.L. Shrinivas. World Wheat Situation. Indian *miller*. Vol . XV. 2 – 17. (1984).

M. Swaminathan.Essential of food and nutrition.Vol.I.Fundamental aspects.II.ed 158.Ganesh pub.Co.Benglor. (1984).

E.L.Van – Kampen. And W.G.Zijiska . Clinical chem. Acta. 6 : 538. C.F. *Brit. Jr. Haemat*.(1967). Supple.13. (1961).

K.Veena and B. Puri . Effect of processing on nutritive value of wheat, Bajara and Barley. *In studies in Nutrition*. Lady Irwin college. Delhi. 50-51. (1963).

K.Vidyasager, S. S. Arya, K. S. Premavalli, D.B. Parihar and N. NathChemical and nutritive changes in refined groundnut oil during deep fat frying. *Jr. Fd. Sci. and Tech*. 11: 73-75. (1973).

M.Yasodadevi and P. Geervani . Effect of different heat treatment on lysine, tryptophane content of wheat based products. *ICFOST*.78: 45. (1978).

Zaltkis,B.Zak and A.J.Boyled. A new method for direct determination of serum cholesterol. Jr.Lab.Clin.Med.41:486- 488. (1953).

'Prajna' - Jounal of Pure & Applied Sciences, 14 (2006) 47-52

COMPARATIVE STUDIES ON THE COMPOSITION OF Bt AND NON Bt COTTONSEED AND SEED OIL

Sini Alex, M. B. Tadhani and S. Rema
Food Biotechnology Laboratory, Post Graduate Department of Home Science,
Sardar Patel University, Vallabh Vidyanagar-388 120, Gujarat, India.

Abstract

Several new crop varieties protected against insect, fungal and viral diseases are being developed using biotechnological interventions. One of these is cotton which is protected throughout the season against damage by some of the most devastating insect pests- the cotton bollworm, the tobacco bollworm and the pink bollworm. Cottonseed oil is used for human consumption while cottonseed and processed cottonseed meal are used for animal feed. In the present study, a comparison of the proximal composition of Bt-cottonseed and seed oil with non Bt-cottonseed and seed oil, respectively, were carried out. Nutrients analyzed included moisture, fat, protein, ash and carbohydrate. Oils were analyzed for their saponification, iodine and acid value. Quality of protein was compared by electrophoresis. The study indicates that Bt cottonseed is compositionally equivalent to and similar in nutrient content to seed from the parental variety.

Keywords: Bt cottonseed, Bt cottonseed oil, proximal composition

Introduction

Cotton as a crop provides livelihood to more than 60 million people in India by way of support in agriculture, processing and use in textiles [1]. Approximately 80% of the 11-13 million acres that are under cultivation of cotton annually are infested with one or more insect pests, which amount to an expenditure of $ 100 million annually on insecticides [2-3]. Cotton plants have been developed with the stable introduction of a gene encoding an insecticidal protein from *Bacillus thuringiensis* subsp. kurstaki. These plants have season-long protection against cotton bollworm, tobacco bollworm and pink bollworm [4]. The first genetically modified crop in India - Bt cotton has been introduced to address bollworm infestation [1]. As an effective and environmentally superior approach to control these insect pests, a gene initially derived from a naturally occurring bacterium, *Bacillus thuringiensis* (Bt) has been stably inserted into the chromosome of cotton, enabling the production of a protein that is active against these insect pests. Producing this protein within the cotton plant itself provides effective and season-long control of these insect pests [5]. *Bacillus thuringiensis* has been used safely for over 30 years in microbial formulations [6]. This organism and the insecticidal proteins produced have been shown to be very specific to the targeted insect pests and to cause no deleterious effects to non target organisms such as beneficial insects, birds, fish and mammals including humans [7].

Cottonseed is an important source of oil for human consumption and processed cottonseed meal is used as animal feed [8]. Therefore, the composition of cottonseed needs to be studied to confirm that these products derived from insect protected cotton varieties are equivalent to those of parental varieties as well as conventional cotton lines. With this objective the levels of various nutrients (fat protein, ash and carbohydrate) were analyzed in Bt cottonseed and non-Bt cottonseed in the present study. In addition, the composition of oil (saponification value, iodine value and acid value) was also analyzed. These analyses were used to study whether cottonseed produced from Bt cotton is compositionally equivalent to that from the parental variety.

Materials and Methods

The present investigation was carried out to compare MECH-162 (non-Bt seeds) and MECH-162 (Bt cotton seeds), which is marketed by Mahyco Monsanto Biotech (India) Ltd. Both were grown in Panchavada Village, Gujarat in the same field with similar agro climatic conditions.

The following parameters were analyzed for comparison of Bt cottonseeds and non-Bt cotton seeds. Size of both types of seeds was compared. Cottonseeds were decoated and crushed before biochemical analysis. Estimation of moisture and ash content was carried out according to the method given by AOAC (1984) [9]. Oil content was analyzed by the Soxhlet method. Estimation of protein from cotton seed was carried out using the Kjeldahl method [10].

Determination of saponification value [11], acid value [12] and iodine value [11] were carried out. Qualitative analysis of oil from Bt and non-Bt cottonseeds were carried out by Thin Layer Chromatography (TLC) [13] using the solvent system hexane: diethyl ether: formic acid (80:20:2). Electrophoretic patterns of Bt and non Bt cotton seed protein was carried out by SDS-Polyacrylamide Gel Electrophoresis [14]. For this sample was prepared as follows: total soluble protein were extracted by adding 30 mg of defatted ground seeds to 1 ml of 50mM tris HCl (pH 7.5) at 4^{o} C for 60 minutes. It was then frozen immediately in the deep freezer. This was thawed thrice during 24 hrs to disrupt the tissue and to release the proteins and followed by centrifugation at 10000 rpm for 10 minutes [15]. Samples were prepared for electrophoresis by mixing 10 μl of supernatant (extracted protein), 2.5 μl of 2- mercaptoethanol and 7.5 μl of 0.002% bromophenol blue in 0.0625 M tris HCl (pH 6.8) containing 10 % glycerol and 2% SDS. Protein staining was performed using 50 mg Coomassie blue to water: methanol: acetic acid (45:45:10) for four hours. Destaining was carried out using the same without the dye.

Statistical Analysis: Appropriate statistical analysis (paired 't' test) was carried out whenever necessary.

Results and Discussion

Analyzed parameters for Bt cotton were compared with that of the parental variety as well as the values reported by researchers for other commercial cotton varieties.

5.0 g of Bt cottonseeds contained 53 seeds and that of non-Bt cottonseeds contained 41 seeds. This showed that Bt seeds were smaller in size than non-Bt cottonseeds.

Proximal composition : The proximal composition of Bt cottonseed and non Bt cottonseed is presented in Table-1. Moisture content was found to be 10% in both the varieties. The reported value for moisture content in different varieties ranged between 5.4 to 10.1% [16]. The percentage of fat present in cottonseed by Soxhlet method showed that fat content was significantly higher ($p \leq 0.01$) in Bt seeds compared to non-Bt seeds. The results obtained in the present study are similar to those reported by Cherry and Leffler [17] which ranged from 16.1 to 26.7%. The protein content of Bt cottonseeds was slightly higher than non-Bt cottonseeds, both of which were found to be within the range (12-32%) reported by Turner et al [18]. Ash content of Bt cottonseed was slightly higher when compared to non-Bt cottonseeds. These results reveal that non-Bt seeds had a slightly higher mineral content than Bt seeds. Both the values were found to be within the range reported by Cherry et al [19]. Carbohydrate content was significantly lower ($p \leq 0.001$) in Bt cottonseed compared to non-Bt cottonseed.

Biochemical parameters in seed oil : Biochemical parameters were carried out on oil extracted from Bt-cottonseed and non-Bt cottonseed to evaluate the quality of oil. These oils were estimated for different parameters (e.g. saponification value, iodine value and acid value). The results obtained for these parameters are presented in Table 2. Saponification value showed the presence of small chain fatty acids present in the sample. Saponification value of Bt seed oil was significantly higher ($p \leq 0.001$) when compared to non-Bt seed oil. This indicates that the percentage of small chain fatty acids is higher in the Bt seed oil. The normal saponification value of cottonseed oil ranged from 191 to 195. In the present study, the saponification value of both the varieties was found to be lower than the normal range. Iodine value indicates the presence of unsaturated fatty acids in the oil. Bt seed oil showed significantly lower value ($p \leq 0.001$) compared to non Bt seed oil. This shows that Bt seed oil contained lower amount of unsaturated fatty acids than non Bt seed oil. Acid value is an index of the presence of free fatty acids and thereby the freshness of the oil. Oil extracted from Bt cottonseed showed significantly higher ($p \leq 0.006$) acid value compared to non-Bt seed oil indicating higher amounts of free fatty acid in Bt seed oil.

A difference in the colour of both oils was also observed. Appearance indicated that Bt seed oil had a lighter colour compared to the non-Bt seed oil. The lighter yellow colour of the oil extracted from Bt seed oil may be due to the lower concentration of colored pigments when compared to non-Bt seed oil. Qualitative analysis of the extracted oils was evaluated using TLC. One of the fractions that appeared in non Bt seed oil chromatogram was absent in that of Bt seed oil (this showed a yellow colored band of R_f value 0.39). Other band patterns were similar in both the varieties.

Qualitative analysis of protein from defatted cottonseed was carried out using electrophoresis (SDS-PAGE). Both the samples showed five bands of protein fractions which indicated no differences in the protein composition. Overall the study indicates that Bt cottonseed and seed oil showed similarity for all parameters studied when compared to non-Bt cottonseed and seed oil, respectively.

References

1. Barwale R. B., Gadwal V. R., Zehr U. and Zehr B., AgBioForum, **7,** (1&2) 23-26 (2004).
2. Head R. B., Cotton losses to insect-1992, In Proceedings, Beltwide Cotton Conferences; Herber D J, Ed; National Cotton Council of America, Memphis T N 655-660 (1993).
3. Williams M. R., Cotton insect losses-1993, In Proceedings, Beltwide Cotton Conferences; Herber D J, Ed; National Cotton Council of America, Memphis T N 743-762 (1994).
4. Berberich S. A., Ream J. E., Jackson T. L., Wood R., Stipanovic R., Harvey P., Patzer S. and Fuchs R. L., J. Agric. Food Chem. **44,** 365-371(1996).
5. Wilson F. D., Flint H. M., Deaton W. R. and Buehler R. E., Crop Sci. **34**, 38-41 (1994).
6. Luthy P., Cordier J. L. and Fischer H. M., *Bacillus thuringiensis as a bacteria insecticide: basic considerations and application, In Microbial and Viral Pesticides*. Kurstak E Ed. Dekker: New York 35-71 (1982).
7. EPA (Environmental Protection Agency) Guidance for the registration of pesticide products containing *Bacillus thuringiensis* as active ingredient, U S Government Printing Office, Washington DC NTIS PB 89-164198 (1988).
8. Anonymous A. E., Cottonseed and its products, 9th Ed., National Cottonseed Products Association, Memphis, TN (1989).
9. AOAC, *Official Methods of Analysis*. 14th ed., Association of Official Analytical Chemists, Washington, D C (1984).

10. Oser, B. L., *Hawk's Physiological Chemistry.* 14th ed., T.M.H. Publishing Company Ltd. New Delhi, 1373-1376 (1976).

11. Jacobs M. B., *The chemical analysis of food products* III Ed. 375-393 (1959).

12. Plummer D. T., *An Introduction to Practical Biochemistry* 184 (1971).

13. Christie N.W. (1982) c. f. AOAC *Official Methods of Analysis.* 14th ed., Association of Official Analytical Chemists, Washington, DC (1984).

14. Laemmli U. K., Nature **227**, 680-685 (1970).

15. Miller M. K., Schonhorst M. H. and Mc Daniel R. G., Crop Science **12**, 535-537 (1972).

16. Cherry J. P., Simmons J. G. and Kohel R. J., *Nutritional Improvement of Food and Feed Proteins*, Friedman M Ed, Plenum Press, New York 343-364 (1978).

17. Cherry J. P. and Leffler H. R., In Cotton, Kohel R. J. and Lewis C. F. Eds. AGRONOMY Series 24: American Society of Agronomy, Crop Science Society of America, Soil Science of America; Madison, WI, Chapter 13, Seed, 511-558 (1984).

18. Turner J. H., Ramsey H. H. and Worley S., Crop Science **16,** 407-409 (1976).

19. Cherry J. P., Simmons J. G. and Kohel R. J., Cottonseed composition of national variety test cultivars grown at different Texas locations, In proceedings of the Beltwide Cotton Production Research Conference, Dallas, TX, Brown J. M., Ed. National Cotton Council, Memphis T N 47-50 (1978).

Table 1 : Proximal composition of Bt cottonseed and non-Bt cottonseed.

Sr No.	Parameter	Non-Bt cottonseed	Bt cottonseed	Reported value
1	Moisture (%)	10.00	10.00	5.4-10.1[16]
2	Fat (%)	24.8±0.21	25.25±0.35*	16.1-26.7[17]
3	Protein (%)	27.97±1.2	29.25±0.27	12-32[18]
4	Ash (%)	4.2±0.2	4.0±0.5	4.1-4.9[19]
5	Carbohydrates (%)	33.03±0.53	31.50±0.37*	-

Values are the mean of three determinations ± S.D.

*indicates significant difference ($p \leq 0.05$) compared to non-Bt cottonseed

Table 2 : Saponification, iodine and acid values of oil extracted from Bt seed and non-Bt seed oil

Sr. No.	Parameters	Non-Bt cottonseed	Bt cotton seed	Normal ranges
1	Saponification value	142.96±1.4	171.33±0.61*	191-195
2	Iodine value	116.62±0.7	102.61±0.5*	101-121
3	Acid value	0.07±0.002	0.09±0.002*	< 0.5

Values are mean of three determinations ± S. D.

*indicates significant difference ($p \leq 0.05$) compared to non-Bt cottonseed

'Prajna' - Jounal of Pure & Applied Sciences, 14 (2006) 53-61

EFFECT OF DIFFERENT LEVELS OF DIETARY VITAMIN E ON THE BIOCHEMICAL ALTERATIONS INDUCED BY N-DIMETHYLNITROSAMINE INTOXICATION

Patel V. H. and Sail S. S.

P.G. Department of Home Science, Sardar Patel University, Vallabh Vidyanagar 388 120. India.
E-mail: patelvh2004@yahoo.co.in

Abstract

The effect of varying levels of vitamin E on some biochemical and hematological changes induced by N-dimethylnitrosamine intoxication were investigated. Albino rats were fed low, normal and high amounts of vitamin E in the diet for 28 days and thereafter, injected a dose of N-dimethylnitrosamine (30% of LD_{50}). After 48 h of intoxication, blood was collected and analyzed for hemoglobin, protein, various enzymes (aspartate transaminase, alanine transaminase, alkaline phosphatase, and superoxide dismutase), bilirubin, vitamins A, C and E, glutathione, uric acid and ceruloplasmin. Study shows the different degrees of fluctuation of these biomolecules in N-dimethylnitrosamine intoxicated animals, reared on low, normal and high vitamin E diet. Fluctuations of biochemical changes were minimum in high vitamin E fed rats indicating its protective role against N-dimethylnitrosamine intoxication.

Key words : Vitamin E, N-Dimethylnitrosamine, Plasma antioxidants

Introduction

Vitamin E is a fat soluble vitamin that occurs naturally in eight different forms, including four tocopherols (α-, β-, γ-, δ-) and four tocotrienols (α-, β-, γ-, δ-) Each of the four tocopherols, including α-tocopherol, has eight possible stereoisomer forms due to the presence of three optically active sites, each with two possible configurations (R and S).However, the RRR-stereoisomer is the only form that occurs naturally in plant foods. Most of the synthetic vitamin E preparations, which are included in fortified foods and vitamin supplements, contain equal amounts of all eight stereoisomes [1]. α- tocopherol is the most abundant form of vitamin E in plasma and most tissues [2]. Vitamin E is the major hydrophobic chain-breaking antioxidant that protects membrane lipids, including polyunsaturated fatty acids, from oxidation [3]. α-tocopherol has several other important physiological functions that are independent of its antioxidant activity, including inhibition of protein kinase C (PKC) activity, which plays an important role in cell proliferation, adhesion, immune responses, free radical production, and gene expression [3]. In addition, α-tocopherol has been shown to regulate several antioxidant defense genes [4]. Vitamin E deficiency promotes oxidative stress in CCl_4 and dehydroepiandrosterone induced hepatotoxicity [5,6]. Studies have shown that supplementation of vitamin E reduces the chemically induced oxidative stress [7], which is one of the mechanisms in the development of liver fibrosis [8].

Hepatic fibrosis induced by N- Nitrosodimethylamine (NDMA) in rat appears to be a good and reproducible model accompanied with many decompensating features of human alcoholic fibrosis [9,10]. NDMA is a widely spread nitroso-compound in the environment. It is a well recognized teratogen and carcinogen in animals and human beings [11,12]. Although food and tobacco products are important sources of exposure, these compounds appear to originate mainly from the *in vivo* reaction of nitrate with amines [13]. About 5.0% of ingested nitrates are reduced to nitrites in saliva [14]. Nitrites can subsequently react with secondary and tertiary amines, as well as N-substituted amides, carbamates and other related compounds to form N-nitroso compounds mainly in gastric juice. NDMA can be hydorxylated by cytochrome P450 while CYP2E1 has been described to be involved in it's metabolism yielding formaldehyde [15].

Literature review reveals that both low and high levels of vitamin E play a significant role in hepatotoxicity. Therefore, the present study was planned to screen the therapeutic effect of varying (low, normal and high) levels of vitamin E on plasma marker enzymes and antioxidant compounds (vitamin E, A, C, glutathione, uric acid and ceruloplasmin) altered due to acute toxicity induced by N-Dimethylnitrosamine.

Materials and Methods

Chemicals: N- Nitrosodimethylamine (NDMA), glutathione reductase (GR), pyrogallol and {3-[Tris-9-hydroxymetyl] methyl] amino) propane sulfonicacid} (TAPS) were purchased from sigma chemical company, U.S.A. All other chemicals were of AR grade, purchased from Indian companies.

Animals: Thirty young adult male albino rats (*Charles Foster* strain) weighing about 178.0 to 197.0 g were used for the study. Animals were divided into six groups consisting of five animals in each group and were caged separately. Food and drinking water were provided *ad libitum* during the study period. Basal diet was prepared by mixing corn starch 74.5 gm with 12.5 gm of casein (containing 80% protein), 2.0 gm salt mixture and 1.0 gm vitamin mixture [16,17]. Fat soluble vitamins viz., vitamin A, vitamin D, vitamin E and vitamin K were added to 10.0 g of groundnut oil at a concentration of 200 I.U, 20.0 I.U, 12.0 mg and 100 µg, respectively. The application of diet with different concentrations of vitamin E is detailed in Table 1. Animals were fed for 28 days and on the 29th day the carcinogen treatment was given.

Carcinogen Treatment : 1.0 g dimethylnitrosamine (Sigma chemicals, U.S.A) was dissolved in 100 ml of distilled water and further diluted to give a final concentration of 5.0

mg/ml and injected (i.p.) at a dose of 12 mg/kg body weight (30% of LD_{50}) to groups II, IV and VI as shown in table 1. Group-I, III and V served as control group to toxicated animals and were injected the same amount of distilled water.

Biochemical assay: After 48 hours of NDMA treatment, rats (fasted for 16 hrs.) were weighed and sacrificed under mild anesthesia. Blood was collected directly from the heart and used for haemoglobin estimation using auto kit method. Remaining blood was centrifuged under refrigeration to obtain blood plasma. The plasma was analyzed for aspartate transaminase (AST), alanine transaminase (ALT), alkaline phosphatase (ALP), uric acid and bilirubin using the Autopak kit supplied by Miles India Ltd., Baroda. Plasma superoxide dismutase [18], protein [19], vitamin E [20], vitamin A [21], vitamin C [22], glutathione [23] and ceruloplasmin [24] were analyzed by standard methods.

Statistical analysis: Results are expressed as mean ± SEM. Student "t" test and regression analysis were calculated using "Microsta" software and the levels of significance was accepted at $p<0.05$. Values of NDMA-treated animals were compared with their respective controls.

Results

The detailed results of the body and tissue weights are presented in Table 2 and briefly discussed here. Body weight gain did not show any significant change but highest gain in weight was observed in the group supplemented with high vitamin E in the diet. Tissue weights were increased after 48 hrs. of NDMA toxication in all the groups. The results of various biochemical parameters are depicted in Table 3. Haemoglobin and plasma protein levels decreased significantly in NDMA intoxicated animals as compared to their respective controls. Study also shows a tremendous increase in plasma marker enzymes (aspartate transaminase, alanine transaminase and alkaline phosphatase) and bilirubin in all the three NDMA treated groups and the raised levels were highest in low vitamin E fed animals. The plasma levels of SOD showed decreasing trend in NDMA induced animals in low and normal vitamin E fed groups. However, it clearly evident from the table that high concentrations of vitamin E in the diet showed protection against NDMA toxicity, indicating that vitamin E has a neutralizing effect on the toxicity.

The levels of antioxidant compounds (vitamin E, A, C, glutathione, uric acid and ceruloplasmin) are presented in Table 4. Vitamin E, C, and vitamin A levels were decreased in NDMA toxicated animals. Decrease of plasma vitamin A level was more in low vitamin E fed rats than in normal and high vitamin E fed animals. Some inconsistent changes were observed for GSH, uric acid and ceruloplasmin. GSH and ceruloplasmin levels were reduced maximally in low vitamin E fed animals. Uric acid was increased significantly in animals fed low vitamin E.

Discussion

In the present study, acute hepatic toxicity (evaluated by plasma marker enzymes) and the change in plasma antioxidant status in response to NDMA toxicity was studied in animals fed different levels of dietary vitamin E. It is evident that plasma marker enzymes (aspartate transaminase, alanine transaminase, and alkaline phosphatase) levels were increased significantly in all NDMA induced animals compared to their respective control animals which confirmed the hepatic toxicity. Increased plasma bilirubin in all the experimental groups suggests abnormal liver function particularly related to bile. Plasma superoxide dismutase levels were reduced in NDMA treated animals in LVE and NVE groups. Plasma antioxidant vitamins (vitamin E, C and A) were reduced significantly in NDMA toxicated animals but the reduction was minimum in HVE group. Reduced GSH, which is an important antioxidant, showed a reduction in the LVE group, but increased in NVT and HVT groups. The ceruloplasmin level too, showed a similar trend. Uric acid showed a significant increase in LVE group. NDMA is a potent hepatotoxin and it causes damage to DNA [25], which may be considered the cause for the reduction of haemoglobin and protein levels in blood.

Plasma aspartate transaminase and alanine transaminase are useful indicators of hepatocellular damage while alkaline phosphatase is a reliable indicator of biliary obstruction; hence their increase in plasma indicates the severe liver cell damage by NDMA after 48 hours. Enzyme activities in plasma are regulated by the releasing mechanism across cell membranes rather than by the intracellular enzyme content [26]. Lin and Wang [27] reported that necrosis of only 1.0% of liver cell population could account for a doubling of the enzyme activities in the plasma. George et al. [28] also reported similar results in rats intoxicated with NDMA. Supplementation of high levels of vitamin E protects against hepatic toxicity which may be attributed to it's antioxidant activity. NDMA is metabolized by cytochrome p-450 enzymes and this also produces ROS [29]. Thus increase of ROS can lead to damage of the liver cells and simultaneously various biomolecules and liver tissue. These results are very well supported by the results of plasma SOD levels as they are decreased in NDMA injected animals which confirmed the production of superoxide radical.

Plasma vitamin E levels showed a positive and significant relationship with dietary vitamin E in the control and experimental animals. The decreased vitamin E in plasma in NDMA induced animals may possibly be due to excessive conversion of vitamin E to its quinone form after reacting with the free radicals. Lathia and Blum [30] reported that vitamin E is a very good nitrosation inhibitor. One more possibility is related to the lipoproteins in plasma, as these act as carriers for vitamin E. Lipoproteins are synthesized in the liver and when liver functions are affected in response to NDMA, synthesis of lipoproteins may also be affected. Irshad [31] also found reduced lipoproteins in liver disease caused by hepatitis in humans. The plasma vitamin E reduction may be a result of any one of these possibilities or may be due to their combined effects.

Plasma vitamin A levels in all the three groups were reduced significantly. The reduction in vitamin A level is possibly due to reduction in the plasma albumin level which is a result of reduced plasma protein. Frankul [32] reported a significant correlation between serum vitamin A and protein in the blood. Another possibility for reduced plasma vitamin A in this study may be due to the immobilization of liver vitamin A as a result of enhanced NDMA metabolism to protect the liver itself. Chapman et al. [33] reported similar results in alcohol and CCl_4 induced hepatotoxicity in rats.

Glutathione, ceruloplasmin and vitamin C levels were reduced in NDMA intoxicated animals but the changes were non-significant indicating that vitamin E was able to maintain their levels in plasma, inspite of their functions to neutralize the free radicals formed in response to NDMA treatment. Glutathione itself is involved in detoxification by making conjugation with toxins or with it's metabolites. Plasma uric acid levels were also increased in NDMA intoxicated animals, which suggests that purine metabolism is affected possibly due to a higher nucleotide breakdown.

It is concluded from the data that depletion of antioxidant systems, as well as increase in free radical generation during N-dimethylnitosamine intoxication are the major factors in reducing various biomolecules in blood plasma. Against this vitamin E decreases oxidative stress and protects the animals from toxic effect of NDMA since vitamins E is an important antioxidant.

References

[1] Food and Nutrition Board, Institute of Medicine. Dietary reference intakes for vitamin C, vitamin E, selenium, and carotenoids: Washington, D.C.: National Academy Press, 2000.

[2] Freeman VL, Meydani M, Yong S, *et al.* : Am J Epidemiol, 151: 109-18 (2000).

[3] Ricciarelli R, Zingg JM, Azzi A.: Faseb J, 15: 2314-25 (2001).

[4] Azzi A, Gysin R, Kempna P, *et al.* : Biol Chem, 385: 585-91 (2004).

[5] Ng, H.P, Wang, Y.F, Lee. C.Y and Hu, M.L: Food Chem Toxicol, 37:503-508 (1999).

[6] Campo, G.M, Squadrito,F, Ceccarelli S, Calo, M, Avenoso A, Campo S, Squadrito, G and Altavilla, D. : Free Radic Res., 34:379-393 (2001).

[7] MacDonald-Wicks, L.K and Garg, M.L.: J Nutr Biochem.,14:211-218 (2003).

[8] Svegliati Baroni, G., D'Ambrosio, L., Ferretti, G., Casini, A., Di Sario, A., Salzano, R., Ridolfi, F., Saccomanno, S., Jezequel, A., and Benedetti, A..: Hepatology 27: 720–726 (1998)..

[9] Jenkins SA, Grandison A, Baxter JN, Day DW, Taylor I, Shields R.:J Hepatol, 1: 489–99 (1985).

[10] George J, Chandrakasan G.: J Clin Biochem Nutr, 22: 51–62 (1997).

[11] Walker, R.: Food Add. Contam., 7: 717-718 (1990).

[12] George, J., Rao, K.R., Stern, R., and Chandrakasan, G.: Toxicology, 156: 129-138 (2001).

[13] Hotchkiss, J.H.: Relative exposure to nitrite, nitrate, and N-nitroso compounds from endogenous and exogenous sources. In: Food Toxicology, a Perspective on the Relative Risks. (Taylor, S.L and Scanlan, R.A. eds),. Marcel Decker, NewYork. pp.57-100 (1988).

[14] NRC: Nitrate and Nitrite in Drinking Water. National Research Council. National Academy Press, Washington, D.C. (1995).

[15] Guengerich, F.P: Cancer Res.: 48: 2946-2954 (1988).

[16] Hawk P.B and Osar B.L: *Hawk's Physiological Chemistry*,14th Ed. Tata Megrraw Hill Book Company, New Dalhi (1964).

[17] Osar, B.L and Osar, M.: *Hawk's Physiological chemistry*,14th Ed. Tata Megrraw Hill Book Company, New Dalhi (1954).

[18] Marklund, S. and Marklund, G. : Euro. J. Biochem.: 47: 469-474 (1974).

[19] Reinhold JG. *In*: Reiner M, (editor) Standand Methods of Clinical Chemistry. New York: Academic Press, Vol. I p 88 (1953)

[20] Desai, I.D.: Methods Enzymol., 105: 138-144 (1984).

[21] Neeld, J.B. and Pearson, W.N.: J. Nutr., 79: 454-462 (1963).

[22] Roe, J.H. and Kuether, C.A.: J. Biol. Chem., 147: 399-407 (1943).

[23] Griffifth, O.W.: Anal. Biochem., 106: 207-212 (1980).

[24] Raghuramulu, M K., Nair, M.K. and Kalansundram, S.: A manual of Laboratory techniques. National Institute of Nutrition, Indian Council of Medical Research, Hyderabad (1983).

[25] Jorquera, R., Castonuay, A. and Schuller, H.M.: Carcinogenesis.,15: 389-394 (1994).

[26] Dortman, R. B. and Lawhorn, G.T.: Drug Chem Toxicol.,1:163-171 (1978).

[27] Lin, J.K. and Wang, C.J.: Carcinogenesis, 7(4): 595-599 (1986).

[28] George, J., Mikihiro, T. and Shujiro, T.: The International Journal of Biochemistry & Cell Biology.,36: 307-319 (2004).

[29] Alaa, E. D. ELSISI, Earnest, D.L and Sipes, I.G.: Toxicol and Applied Pharmaco.,119:295-301 (1993).

[30] Lathia, D. and Blum, A.: Intemat J Vit Nutr Res.,59: 430-438 (1989).

[31] Irshad, M.: Indian J Med Res.,120 : 542-545 (2004).

[32] Frankul, W.: J.of Faculty of Medicine Baghdad, 31(2): 135-143 (1989).

[33] Chapman, K.M., Prabhudesai, M. and Erdman, J.W.: Alcohol Clin.Exp.Res., 17:637-642 (1993).

Table 1: Vitamin E supplementation and carcinogen treatment given to different groups.

No.	Group	Levels of Vitamin E supplemented to groundnut oil (mg /100 g diet)	Carcinogen treatment
I	Low vitamin E treated group (LVC).	Not added	Not injected
II	Low vitamin E treated group post toxicated with NDMA (LVE).	Not added	NDMA
III	Normal vitamin E treated group (NVC).	12.0	Not injected
IV	Normal vitamin E treated group post toxicated with NDMA (NVE).	12.0	NDMA
V	High vitamin E treated group (HVC).	48.0	Not injected
VI	High vitamin E treated group post toxicated with NDMA (HVE).	48.0	NDMA

Table 2 : Body weight gain, relative liver and kidney weights of rats fed different levels of vitamin E, treated with and without NDMA.

Parameter	Low vitamin E		Normal vitamin E		High vitamin E	
	LVC	LVE	NVC	NVE	HVC	HVE
	Group-I	Group-II	Group-III	Group-IV	Group-V	Group-VI
Weight gain (g)!	89.4 ± 10.4		93.0 ± 3.9		104.5 ± 7.7	
Liver weight@	2.90 ± 0.1	3.46* ± 0.11	2.70 ± 0.06	3.54* ± 0.13	3.06 ± 0.16	3.45* ± 0.23
Kidney Weight@	0.56 ± 0.01	0.58 ± 0.03	0.54 ± 0.02	0.57 ± 0.02	0.54 ± 0.01	0.57 ± 0.02

Values are mean ± SEM (n=5)

! - Values are mean ± SEM (n=10) of animals fed different diets.

@ - g/100g of body weight

* Significantly different ($p<0.05$) from their respective control.

Table 3: Blood haemoglobin, plasma protein and plasma marker enzyme levels in rats fed different levels of vitamin E, treated with and without NDMA.

Parameter	Low vitamin E in diet		Normal vitamin E in diet		High vitamin E in diet	
	LVC	LVE	NVC	NVE	HVC	HVE
	Group-I	Group-II	Group-III	Group-IV	Group-V	Group-VI
Blood haemoglobin (g %)	13.4 ± 0.2	12.0*± 0.3	13.1± 0.3	11.9*± 0.3	13.2± 0.4	12.7*± 0.5
Plasma protein (g %)	6.5± 0.2	5.9*± 0.1	6.4± 0.3	5.9± 0.3	6.6± 0.1	5.9*± 0.1
Aspartate transaminase IU/L)	156.6 ± 23.8	297.5*± 44.1	242.3± 41.8	424.8± 91.7	195.0 ± 10.3	258.0*± 14.9
Alanine transaminase (IU/L)	79.8±7.6	152.9*±28.5	87.3± 4.3	177.4± 54.1	74.2± 6.0	87.8± 4.0
Alkaline phosphatase (µM/ml/ min)	1.6± 0.5	2.6± 0.5	2.00± 0.5	3.20± 0.7	2.0± 0.2	2.6± 0.7
Bilirubin (mg %)	0.70± 0.05	0.87± 0.06	0.72± 0.05	0.91*± 0.06	0.77± 0.06	0.86± 0.05
Superoxide dismutase (U/ml)	48.4±5.4	37.3±7.0	44.6± 4.3	38.5± 3.6	45.6± 5.4	46.9±7.4

Values are mean ± SEM (n=5),
* Significantly different ($p<0.05$) from their respective control

Table 4: Plasma nutrient and non-nutrient antioxidant compounds in rats fed with different levels of vitamin E, treated with and without NDMA.

Parameter	Low vitamin E in diet		Normal vitamin E in diet		High vitamin E in diet	
	LVC	LVE	NVC	NVE	HVC	HVE
	Group-I	Group-II	Group-III	Group-IV	Group-V	Group-VI
Vitamin E (mg%)	0.86[a]± 0.06	0.51*± 0.06	1.29± 0.11	0.93* ± 0.08	1.85[a] ± 0.13	1.41* ± 0.19
Vitamin A (µg%)	40.57±2.59	28.14* ± 2.95	42.2± 2.69	33.76*± 1.49	50.52± 2.03	39.01*± 2.67
Vitamin C (mg%)	1.41± 0.19	0.94± 0.12	1.49± 0.22	1.18± 0.16	1.69± 0.30	1.27± 0.22
GSH (mg%)	1.65± 0.16	1.50± 0.16	1.44± 0.13	1.90± 0.25	1.65± 0.13	1.94± 0.28
Uric acid (mg%)	1.90± 0.14	2.78*± 0.35	1.98± 0.18	2.53± 0.20	2.48± 0.34	2.37± 0.13
Ceruloplasmin @	0.40± 0.03	0.36± 0.03	0.40± 0.05	0.42± 0.03	0.45± 0.05	0.45± 0.04

Values are mean ± SEM (n=5),
@ O.D of PPD oxidase activity
* Significantly different ($p<0.05$) from their respective control.
[a] Significantly different ($p<0.05$) from normal control group (NVC)

'Prajna' - Jounal of Pure & Applied Sciences, 14 (2006) 62-69

PRINTING OF COTTON AND POLYESTER FABRICS WITH KIKAR FRUITS AND BHANGRA LEAVES AS NATURAL DYES

Namrita Kola
P.G.Deartment of Home Science, Sardar Patel University, Vallabh Vidyanagar-388 120
E-mail: knamrita@yahoo.com

Abstract

Due to environmental awareness, it has become necessary to revive the art of dyeing and printing with natural dyes. Their application on both natural and manmade fibres has become essential today. It is to this effect that the present study was undertaken to study the block printing application of two locally available natural dyes, fruits of kikar and leaves of bhangra on cotton and polyester fabrics. The incorporation of certain mordants in the printing paste has resulted in colour retention.

Introduction

In every civilization, from the remote ages to the present day colour has played an important role in adding beauty to the world. Colours fascinated human beings and this made them use colours in clothes by way of dyeing. Primitively, only natural dyes were used for the purpose. India has a long tradition of dyeing textiles with dyes obtained from plants and animal sources. Ancient dyes were extracted from leaves, fruits, flowers, berries, roots, barks of various local plants, as well as from certain insects and shellfishes. Natural mordants like urine, saliva, egg albumin and tannins from barks were used to make the dyes fast and to get a range of colours (Bahl and Gupta [2])

The first synthetic dye was discovered by Perkin in 1856 (Trotman [11]). With this there was no looking back for the dye industry. Slowly all the natural dyes were replaced by the synthetic dyes because these dyes gave good fastness, were easily made and had quick dyeing process. Thus, the knowledge and expertise of natural dyes which was traditionally passed down by word of mouth from the master craftsman to his disciple is lost. Consequently, documentation on sources of such dyes, the technique of extraction and application is meager (Srivastava [9]).

Natural dyes have been neglected for about 150 years but currently they have again come into limelight, they have the potential to change the textile scenario (Gulrajani [5]). The synthetic dye industry is facing a very critical problem of not being eco-friendly. These dyes cause pollution at each stage of production and use and disposal after use. Many chemicals have to be phased out from dye manufacturing and many have been banned. In the advanced countries, Eco-Tex labels are insisted upon by foreign buyers. With these developments, the need for exploring natural/forest wealth to extract dyes has increased (Venugopal[12])

Extensive research and development work has been already carried out in the recent past. Khan et.al. [6] has reported the application of tesu, dolu and amaltas on wool. Pre and post mordanting treatments were given with alum, copper sulphate, ferrous sulphate and potassium dichromate. Tesu and dolu gave red-yellow colour while amaltas gave yellow-green colour. Use of tea, turmeric, majistha and tamrind were studied as natural dyes on jute by Teli et. al. [10]. Pre, post and metamordanting techniques were used with copper sulphate, tartaric acid, tannic acid and ferrous sulphate. Out of the three mordanting techniques studied, post mordanting gave the maximum colour depth.

Babool bark as natural dye on cotton was used by Patel et. al. [8]. Ferrous sulphate, copper sulphate, stannous chloride and combination of ferrous sulphate + copper sulphate were used for pre and meta mordanting. The colours obtained varied from pale cream to dark creamish brown depending on the mordant used. The dye uptake increased with the increase in the concentration of the dye. Application of madder and cochineal on wool, silk and cotton fabrics by premordanting technique has been reported by Micheal et. al. [7] . Pre mordanting was done with alum, potassium dichromate, stannous chloride, copper sulphate and ferrous sulphate. A wide range of colours were obtained with different mordants. Dyed samples mordanted with copper sulphate and ferrous sulphate gave deeper colours. Stannous chloride and alum increased the redness of the dyed samples.

Mostly all the work reported has been concentrated on the use of natural dyes on natural fibres, also only dyeing aspect has been explored in most of the studies. If natural dyes are to succeed then their application on synthetic fibres is also to be established along with applications in printing. The present study is an effort in this context.

Materials And Methods

(1) Dyes used: Two dyes were used; they were fruits of kikar (*Acacia nilotica*) and leaves of bhangra (*Eclypta prostrate*). Kikar, known as Bavaria and Bhangra known as kalo-bhangra in the local language are wild plants found in non-agricultural dry land. The fruits of kikar grow during the months of May to June, dry fruits were collected, the seeds were removed and the fruits were dried and powdered. Mature leaves of bhangra were collected and dried in shade for dye extraction.

(2) Fabrics used: 100% cotton and 100% polyester fabrics were used for the study, which were purchased from the local market. The fabrics were tested for fibre content, weave, fabric count, fabric thickness, weight per unit area as per standard methods. The fibre content was identified as per standards of AATCC test method no. 20-

1976 [1]. Both the fabrics were of plain weave, the weave was identified by visual examination through a pick glass (Blinav and Belay [3]). Fabric count, fabric weight and fabric thickness were determined using standard methods given by Booth [4]. It was 132 x 46, 200 gms./sq.mt. and 0.21 mm respectively for cotton; 146 x 76, 160 gms./ sq.mt. and 0.19 mm respectively for polyester.

(3) Chemicals used: Potassium dichromate and ferrous sulphate were used in the print paste as mordants. Carboxy methyl cellulose (CMC) was used as a thickener for the print paste. All chemicals used were of laboratory grade.

(4) Preparation of fabrics: Cotton and polyester fabrics were scoured with 2 gms./lit. soap and soda ash in boiling water for 45 minutes with M:L ratio of 1:30. Both the fabrics were then washed in running water and dried.

(5) Dye extraction procedure: Dye from kikar fruit and bhangra leaves was extracted on percent soluble matter basis by boiling in water for 45 minutes. A 10% extract was prepared.

(6) Preparation of the print paste: To determine the influence of dyes and mordants (potassium dichromate and ferrous sulphate) three different print pastes were prepared for each dye. The use of ingredients is specified in table 1. The ingredients as per requirement were mixed and a homogenous paste was prepared by stirring the ingredients continuously for 15 minutes with an electric stirrer.

(7) Printing of fabric samples: A wooden block with an engraved stylized natural design was selected for the printing process. The ink pad and the printing table were prepared as per conventional procedures. The samples were printed with the block and dried flat. Polyester fabric samples were given heat treatment at 110°C for 10 minutes in an oven. This dry heat treatment was given to soften the fibres, this result in the movement of polymers in the amorphous region for the entry of the dye molecules. All the samples were washed in running water to remove the thickener and other printing paste constituents which have not entered the polymer system of the fibre. The samples were dried flat and ironed.

(8) Colour fastness tests: Washing, ironing, crocking and perspiration fastness tests were performed on the samples as per standard methods of AATCC test method no. 61-1968 was used for washing, test method no. 133-1976 for dry and wet ironing, test method no. 8-1974 for crocking fastness and test method no. 15-1976 for perspiration were used. After the fastness test, the samples were evaluated for colour change and staining, the effect was expressed and defined by reference to the grey scale [1].

Results

Natural dyes-kikar fruits and bhangra leaves can be successfully applied on cotton with block printing. Application of these natural dyes is also possible even on synthetic fibres like polyester by after treatment with heat.

The printed samples of cotton and polyester with all the six print pastes are presented in photographs 1 to 3. Photograph 1 presents samples which have been printed with paste A and D, this paste does not contain any mordant. Photograph 2 present samples printed with paste B and E, photograph 3 represents samples printed with paste C and F.

Cotton and polyester samples, in photograph 1 shows that only in case of kikar dye on cotton, the colour has been retained. Maximum loss in colour is on polyester printed with bhangra dye.

On comparing photograph 1 with 2 and 3, the role of mordant is very clear. Both the fabrics have retained the colour and the print is very clear with even lines. Potassium dichromate gives brown colour while ferrous sulphate gives grey colour. Kikar has given better results than bhangra after the first wash.

Colour fastness of all the samples: The results of all the colourfastness tests are presented in table 2. Amongst all the colourfastness tests, washing fastness showed maximum loss in colour. Most of the samples fell in class 3 and 4 which shows that noticeable or slight change in colour and staining was observed. Samples printed with paste A and D (i.e. without mordant) showed poor fastness in comparison with samples printed with a mordant in the print paste.

Conclusion

From the present study it can be concluded that with the use of heat treatment synthetic fibres (polyester) can be printed with natural dyes: fruits of kikar and leaves of bhangra. The incorporation of mordants like potassium dichromate and ferrous sulphate can give different colours, the mordants also influence colour retention for cotton as well as polyester fabrics. Use of potassium dichromate gives brown colour to kikar and bhangra dyes, while grey colour is obtained with ferrous sulphate. Kikar showed better results than bhangra.

Kikar and bhangra being wild plants are easily available, the fruits of kikar and dry leaves of bhangra which go waste can be used for block printing. Traditional designs created by skilled craftsmen can be created and sold in the local market or even exported. Thus modern demand of using natural products can facilitate the survival of the dieing art of block printing apart from generating employment.

References

(1) AATCC technical manual, **52**, American Association of Textile Chemists and Colourists, p. 57-72,103,105,122,159,265 (1976)

(2) Bahal D. and Gupta K.C., Colourage, **37**,22-24 (1988)

(3) Bilinav I. and Belay S. *Design of woven fabrics,* (Mir Publishers-Moscow) p.28-30 (1988)

(4) Booth J.E. *Principles of textile testing*, (Newness Butterworths-London) p. 210-215,229-231,289 (1966)

(5) Gulrajani M.L. *Book of papers Convention on natural dyes* (Department of textile technology, IIT-Delhi) p. 3-22 (1999)

(6) Khan M, Khan M.A., Srivastava P.K. and Mohammad F, Colourage, **48**,33-38 (2004)

(7) Micheal M.N., Tera F.M. and Aboelanwar S.A., Colourage, **50**, 31-42 (2003)

(8) Patel B.H., Agarwal B.J. and Patel H.M., Colourage, **50**, 21-26 (2003)

(9) Srivastava, M.G.,*Compendium of the first national seminar on natural dyes,*(NHDC-Lucknow) p.1 (1989)

(10) Teli M.D., Adiverekar R.V., Bhagat M and Manjrekar S.G., J. of the Text. Ass., **63**, 129-134 (2002)

(11) Trotman E.R, *Dyeing and Chemical Technology of Textile fibres,*(Charles Griffin and Co.-London) p. 1,4, (1975)

(12) Venugopal B.R., Colourage, **40**, 7,8 (1993)

Table 1: Ingredients of print paste

Sr. No.	Ingredients	Paste					
		A	B	C	D	E	F
1.	Dye extract of kikar (ml.)	100	100	100	-	-	-
2	Dye extract of bhangra (ml.)	-	-	-	100	100	100
3	CMC (gms.)	4.6	4.6	4.6	4.6	4.6	4.6
4	Potassium dichromate (gm.)	-	1	-	-	1	-
5	Ferrous sulphate (gm.)	-	-	1	-	-	1

Table 2: Colour fastness of samples

Print paste	Dye used	Fabric	Washing fastness		Ironing fastness				Crocking fastness		Perspiration fastness	
			CC	SC	Dry		Wet		CC	SC	CC	SC
					CC	SC	CC	SC				
A	Kikar	Cotton	4	4	5	5	4	4	4	4	4	4
A	Kikar	Polyester	3	3	5	5	4	4	5	5	5	5
B	Kikar	Cotton	5	4	5	5	5	5	5	5	5	5
B	Kikar	Polyester	4	4	5	5	5	5	5	5	5	5
C	Kikar	Cotton	4	4	5	5	4	4	5	5	4	4
C	Kikar	Polyester	5	5	5	5	4	4	5	5	5	5
D	Bhangra	Cotton	4	4	4	4	4	4	4	4	4	4
D	Bhangra	Polyester	5	5	5	5	5	5	4	4	4	4
E	Bhangra	Cotton	3	4	5	5	5	5	5	5	4	4
E	Bhangra	Polyester	3	3	5	5	5	5	5	5	5	5
F	Bhangra	Cotton	3	4	5	5	4	4	5	5	3	3
F	Bhangra	Polyester	3	3	5	5	5	5	5	5	5	5

CC = Colour Change SC = Colour Staining

Key:
5 = negligible or no change/staining
4 = slight changed/staining
3 = noticeable changed/stained
2 = considerable changed/stained
1 = much changed/stained

Photograph 1

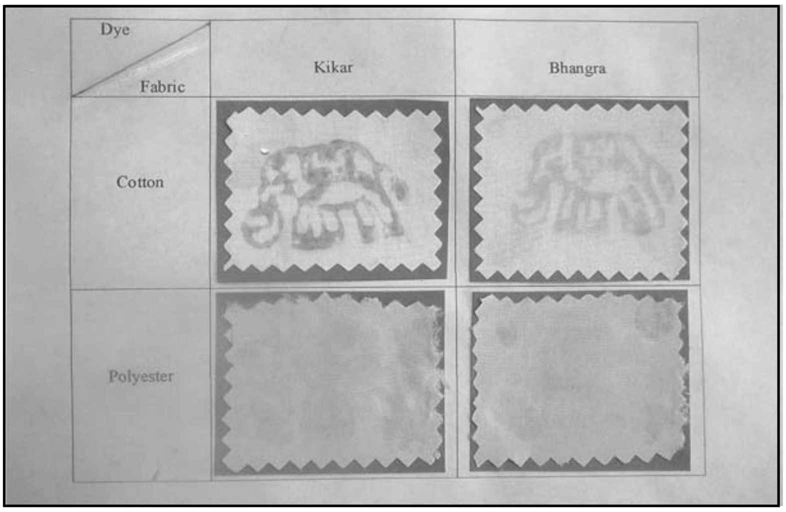

Cotton and polyester samples printed with kikar fruits and bhangra leaves

Photograph 2

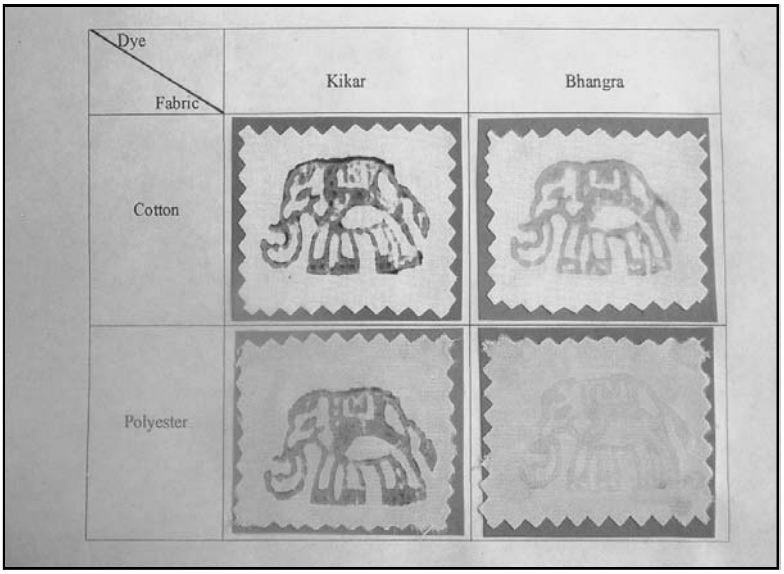

Cotton and polyester samples printed with kikar fruits and bhangra leaves with potassium dichromate in the print paste

Photograph 3

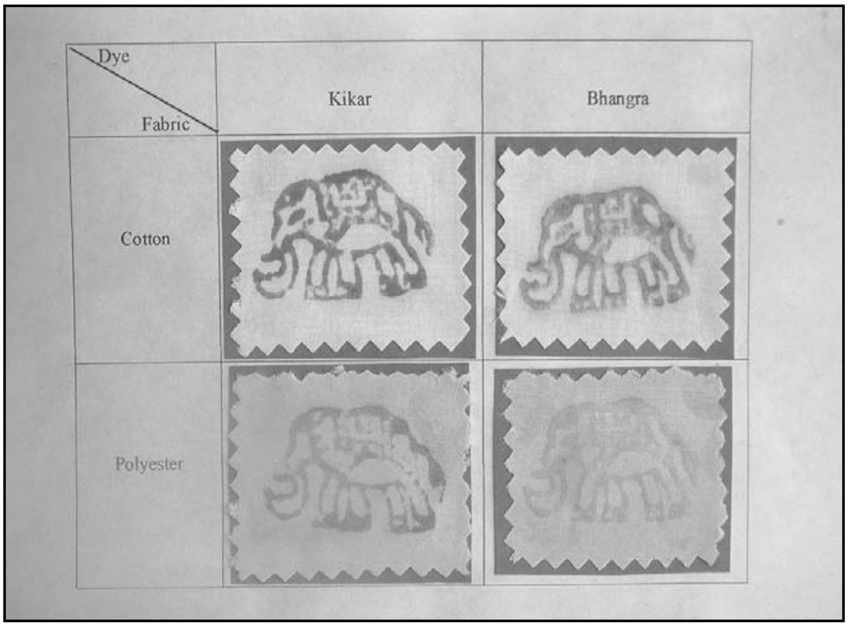

Cotton and polyester samples printed with kikar fruits and bhangra leaves with ferrous sulphate in the print paste

'Prajna' - Jounal of Pure & Applied Sciences, 14 (2006) 70-78

STUDIES ON FLAME RETARDANT POLYURETHANES BASED ON BISPHENOL A MONOPHOSPHATE

R. H. Patel* and H. B. Patel

*G.H.Patel Institute of Materials Science, Sardar Patel University, Vallabh Vidyanagar-388120

Abstract

Phosphorous containing flame retardant polyurethanes were prepared and characterized by various chemical and instrumental analysis techniques. Various physical and thermal properties of the polymers were established . Flame retardant characteristics of polymers in the form of film were found out. Resistancy of the polymer films towards uv light and various chemical agents were also determined. Polyurethanes have good flame retardant and chemical resistance properties.

Introduction

Phosphorous containing polymers are generally flame retardant in nature [1, 2]. It is also thought that the combination of phosphorous with nitrogen on a polymer backbone may enhance the flame retardant characteristics of polymer. With this idea , attempts were made to synthesize intrinsic type flame retardant polyurethanes. These types of polymers can be useful in coating, adhesive formulation, in certain military and mining applications[3 - 6] where flame retardant property is in great demand. The advantage of these systems is due to their intrinsic nature, the elements do not bloom or migrate to the surface very easily. Among the different types of flame retardants, phosphorous containing polymers with predominantly aromatic structure are more effective because they have good thermoxidative stability, char yield and chemical stability [7].

In the present work we have described the synthesis of different flame retardant polyurethanes by reacting the monomer having aromatic ring in the structure of bisphenol A monophosphate with various diisocyanates. Polymers are characterized by chemical and instrumental analysis techniques. Thermal, flame retardant and chemical stability of the polyurethanes have also been evaluated.

Experimental

Materials

The reagents bisphenol A, phosphorous oxychloride, toluene diisocyanate, hexamethylene diisocyanate, diphenyl methane diisocyanate and isophorone diisocyanate were obtained from Fluka and were used as such without further purification. Castor oil obtained from local market was found to contain hydroxyl value 127 corresponded to 2.12 hydroxyl groups per one mole of castor oil [8]. Solvents such as methyl ethyl ketone (MEK), ethanol, dimethyl formamide (DMF) were used after distillation.

Synthesis of Monomer : Bisphenol A monophosphate

The monomer bisphenol A monophosphate [9] was synthesised by reacting bisphenol A(3.0 mole) and phosphorous oxy chloride (1.0 mole) at a temperature of 130°c for 8 hours in presence of N, N - dimethyl aniline (0.0132 mole). The resultant mass was washed with ether and dissolved in acetone. The resultant product was obtained by neutralizing and precipitating in cold water.

Synthesis of phosphorous containing polyurethanes

Polyurethane (PU-1) was synthesised in two steps.

In the first step a prepolymer was prepared by reacting bisphenol A monophosphate (BPMP,1.0 mole) with toluene diisoisocyanate (TDI ,3.0 mole) in methyl ethyl ketone solvent at 55 °c temperature with continuous agitation of 2.5 hrs.

In the next step this prepolymer was further reacted with excess monomer at 70 °c for 4.5 hrs in the same medium with excess monomer to get a hydroxyl terminated polyurethane. The product was vacuum distilled to obtain pure polyurethane.

Polyurethanes with isophorone diisocyanate (IPDI, PU-2), diphenyl methane diisocyanate (MDI, PU-3) and hexamethylene diisocyanate (HMDI, PU-4) were also prepared following the above method.

These polyurethanes are blended with conventional castor oil based polyurethane to improve the latter's flame retardant as well as the hardness properties.

Scheme 1:

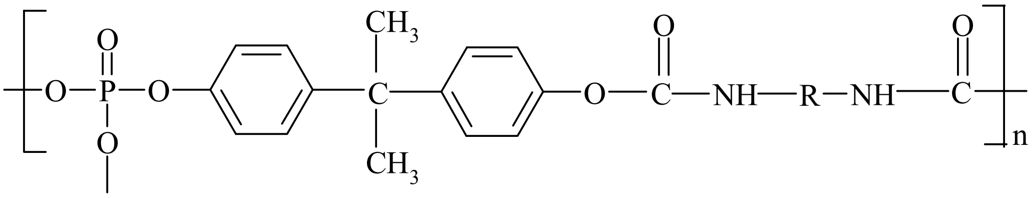

Polyurethane

Where R represents

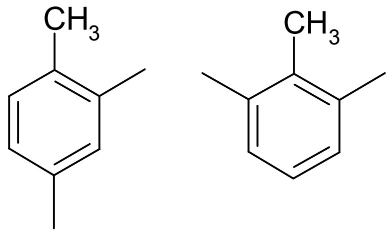

PU-1

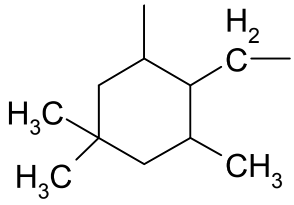

PU-2

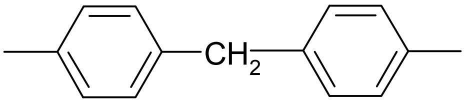

PU-3

$-(CH_2)_6-$

PU-4

Synthesis of castor oil based polyurethane

Castor oil based polyurethane (COPU) was prepared following a reported method [10]. Castor oil (0.054 mole) was allowed to react with toluene diisocyanate (0.0946 mole) at 45^{o}c for 1 hour with continuous stirring. The isocyanate terminated polyurethane was vacuum distilled at 45^{o}c to isolate pure polymer.

Characterization

Number of hydroxyl group of the monomer and the polyurethane was determined by hydroxyl group estimation [11]. Intrinsic viscosity of the soluble polymers was measured using ubbelohde suspended level viscometer in suitable solvent. Percentage yield of monomer and polymers are in the range of 70-74%. Elemental analysis was carried out in Perkin Elmer USA (Model 2400 series II). These data are reproduced in Table 1. The infra-red spectra of the monomer and polymers were recorded in KBr pallet on Perkin Elmer USA (Model Spectrum GX ,FT-IR) spectrophotometer. Molecular weight of the polyurethanes were determined by vapour pressure osmometry technique using vapour pressure osmometer model K-7000, KNAUER instrument.

Measurement of Thermal Properties

The heat flow data of the polyurethanes was obtained by differential scanning calorimetric technique (DSC) using TA Instrument USA (Model 5000/2920) at a heating rate 10^{o}c. min^{-1} using empty cell as reference. Thermogravimetric analysis (TGA) of the polymers were done on Perkin Elmer USA (TGA-7) thermal analyzer in air at a heating rate 10^{o}c min^{-1}.

Preparation of Films

A teflon sheet of 2.5 mm thickness was punched to the required size (0.2 x 5 x 9 cm). This sheet was placed on a triangular leveling plate and leveled by moving the rotating screw of the leveling plate. Required amount of polyurethanes based on bisphenol A monophosphate were mixed thoroughly with castor oil based polyurethanes (COPU) and 0.01 percent ethylenediamine to obtain different films shown in Table 3. The mixtures were poured on the prepared site of the teflon sheet. The plate was kept inside an oven at 50^{o}c. After 24 hours films were obtained.

Testing of the Films

Dimension of the films were measured with the help of micrometer screw. Shore A and Shore D hardness of the films were measured using hardness tester TSE testing machine. The chemical resistance properties in various chemicals were also determined. The ultra violet spectra of the polymer films were recorded on a Perkin Elmer (Model Lambda-19) spectrophotometer. The limiting oxygen index (LOI) data of the films were obtained on an apparatus as per standard ASTM D2863.

Results And Discussion

The elemental analysis for the determination of percentage of carbon, hydrogen and nitrogen for monomer and all the polyurethanes were carried out and the observed values are in good agreement with the calculated value as shown in Table 1.

The IR spectra of the monomer shows a broad absorption band at 3410 cm^{-1} due to the presence of H-bonded hydroxyl species, the band at 1262 cm^{-1} corresponds to Ar-OH symmetric stretching frequency, C=C stretching of aromatic ring is obtained at 1494 cm^{-1}, the band at 1235 cm^{-1} is due to the presence of P=O group and the band at 975cm^{-1} is due to the P-O-C stretching frequency.

The IR spectra of polyurethanes in Figure 1 show absorption band around 1595-1643 cm^{-1} for-OCONH asymmetric stretching vibration. The band for P=O group appears around 1224-1237 cm^{-1}. P-O-C stretching frequency is observed around 970-973 cm^{-1}. The broad band around 3294-3337 cm^{-1} attribute to >N-H bond.

DSC scans for all the polymers show a step down in heat capacities corresponding to the glass transition temperature varying from 150-190^{o}c depending on the nature of the polyurethanes. Thermal stability of the polymers were obtained by TGA analysis. Percentage weight loss data, integral procedure decomposition temperature (IPDT) and char yield values are shown in Table 2. The thermograms in Figure 2 show that polymers are stable upto 220 – 255^{o}c in air with 10% weight loss and start degrading afterwards. Polyurethane prepared with toluene diisocyanate shows highest char yield in the series. Polyurethanes have moderately good LOI value in the range of 24-30%.

The polyurethane films were exposed to UV radiation for 5 hours. UV spectra of films were obtained at a time interval of every one and half hours. After exposure no change in the spectra has been observed. Thus it may be inferred that polymers are stable to UV light.

The polyurethane films also possess good hardness properties. The shore D hardness value of the polymer films is in 30-70 range while the shore A hardness ranges in 80-90 as shown in Table 3.

The chemical resistancy of the polymers were measured by dipping the films in methanol, 10% sodium hydroxide, 20% sodium hydroxide, 10% hydrochloric acid and in water. After five days only minor change in the weight was observed while there was no change in the dimension of the films. A slight discoloration of the films was observed in sodium hydroxide solution but the color of the film remained unchanged in other medium. The weight change data are given in Table 4. These data reveal that the polymers have good chemical and hydrolytic stability.

Conclusion

From the above study it can be concluded that the polymers have moderately good thermal stability, flame retardancy and chemical resistance properties.

Acknowledgement

The financial assistance from University Grants Commission, New Delhi is gratefully acknowledged.

References

[1] Sandler S.R. and Karo W. *Polymer Synthesis ,* 2nd Ed.,(Academic Press Inc.-New York) (1992)

[2] Weil F.D., Fearing R. B. and Jaffe F. , *J. Fire Retardant Chem.* **9**, 39 (1982)

[3] Jianzong L. and Shiyuan C. , *J. Appl. Polym.Sci,* **40**,417-426 (1990)

[4] Kemmlein S . , Hahn O . and Jann O. , *Atmos . Env .* **37**, 5485-5493 (2003)

[5] Modesti M . , Loronzetti A . , Simioni F . and Camino G. , *Polym . Degrad . Stab.* **77** , 195 – 202 (2002)

[6] Spirckel M, Regnier N, Mortaigne B, Youssof B. and Bunel C. , *Polym.Degrad. Stab.* **78**, 211-218 (2002)

[7] Shao C. H., Huang J. J. , Chen G.N., Yeh J.T. and Chen K.N. , *Polym. Degrad. Stab*. **65**, 359-371 (1999)

[8] Naughton F.C. , *J. Am. Oil Chem. Soc.* **51**,65 (1974)

[9] Patel S.R. and Patel R.G, . *High Performance Polymers.* **3**, 237 (1991)

[10] Patel P., Shah T. and Suthar B. , *J. Appl. Polym. Sci.* **40**, 1037-1047(1990)

[11] Vogel A.I. *Elemental Practical Organic Chemistry, Part-3, Quantitative Organic Analysis,* second edition Delhi, (CBS publishers & distributors) (1987)

Table 1
Analytical data of polyurethanes

	System	Intrinsic Viscosity (η)		Average Molecular Weight $\overline{Mn}$	Elemental Analysis (%)		
		dl/gm	Solvent		C	H	N
Monomer	BPMP			---	(74.17) 73.35	(6.18) 6.10	--- 0.26
PU-1	BPMP+TDI	0.75	DMF	3334	(74.50) 73.17	(5.93) 5.45	(2.51) 2.75
PU-2	BPMP+IPDI	0.70	DMF	3575	(72.50) 71.65	(6.46) 5.95	(2.34) 2.25
PU-3	BPMP+MDI	0.74	DMF	3416	(71.60) 72.30	(6.32) 6.25	(2.45) 2.70
PU-4	BPMP+HMDI	0.85	DMF	3662	(73.73) 72.50	(5.73) 5.35	(2.29) 2.80

(Calculated values are listed in Parenthesis)

Table 2
Thermal properties of polyurethanes

	Glass Transition Temperature (^{o}C)	% Weight Loss (^{o}C)			IPDT (^{o}C)	Char Yield (%)
		10%	30%	90%		
PU-1	190	230	290	549	380	7.03
PU-2	150	220	298	530	376	3.90
PU-3	160	225	258	515	341	2.34
PU-4	168	255	390	550	372	4.68

Table 3
Flame retardant, photo resistance and hardness properties of polyurethane films

System	Proportion	LOI %	λ_{max} nm	Hardness	
				Shore A	Shore D
COPU : PU-1	70:30	28	360	80	30
COPU : PU-2	70:30	26	362	90	70
COPU : PU-3	70:30	24	374	85	60
COPU : PU-4	70:30	30	363	90	70

Table 4
Chemical resistance properties of polyurethanes

System	Weight change data of polyurethane films (gm)				
	Methanol	Water	10% NaOH	20% NaOH	10% HCl Solution
PU-1	0.04	0.02	0.03	0.04	0.01
PU-2	0.03	0.0	0.02	0.02	0.03
PU-3	0.01	0.01	0.02	0.04	0.02
PU-4	0.01	0.0	0.01	0.02	0.02

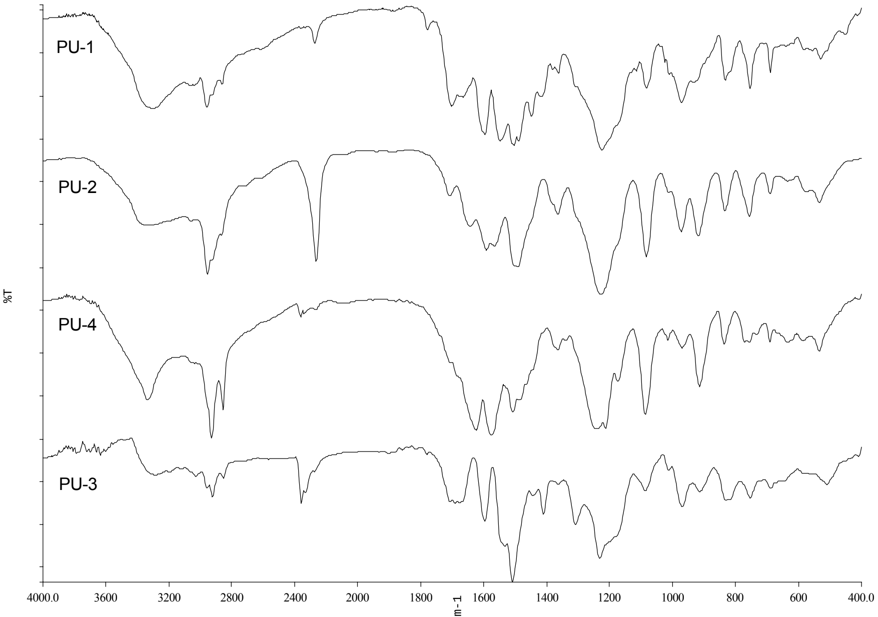

Fig. 1 FT-IR spectra of polyurethane samples PU-1 , PU-2, PU-3,PU-4

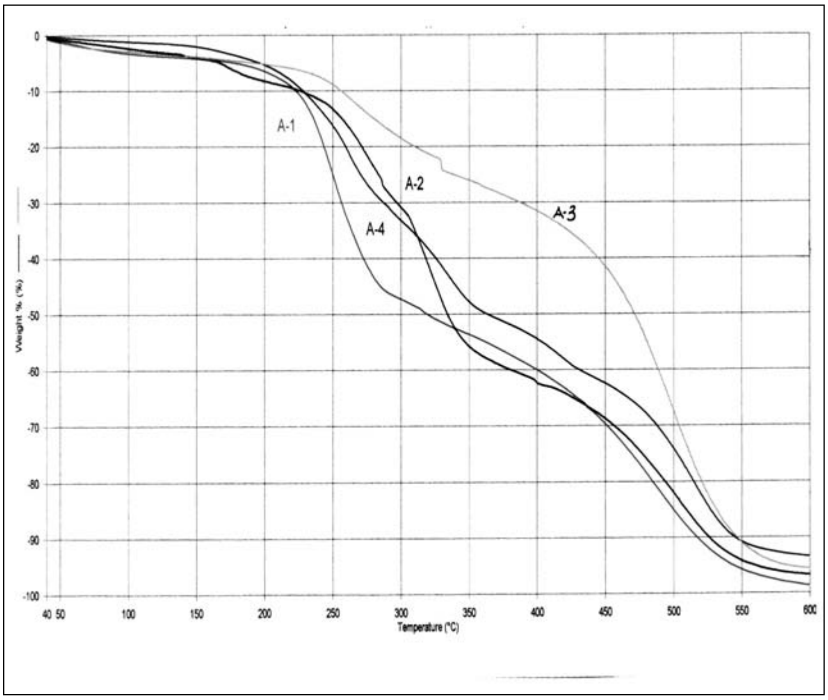

Fig. 2 TGA curves of polyurethane sample (A1) PU-2 , (A2) PU-3, (A3) PU-4, (A4) PU-1 in air at heating rate 10° C min^{-1}

'Prajna' - Jounal of Pure & Applied Sciences, 14 (2006) 79-93

GENERALIZED SEMICHARACTERS AND WEIGHTS ON SEMIGROUPS

H. V. Dedania and J. H. Shah
Department of Mathematics, Sardar Patel University, Vallabh Vidyanagar - 388 120
Department of Mathematics, R. G. Shah Science College, Vasana, Ahmedabad - 380 007

Abstract

Generalized semicharacters on a semigroup *S* are investigated. A large number of examples of weights and general methods to construct weights on *S* are exhibited. For an abelian semigroup *S*, the Gelfand space of the convolution algebra $C_C(S)$ with the inductive limit topology is identified with set of all generalized semicharacters on *S*. The semisimplicity, and the existence of identity in $C_C(S)$ are also characterized in term of *S*.

Keywords and Phrases

Semigroup, weight, commutative Topological algebra, Gelfand space, semisimplicity, radical, generalized semicharacter.

1 Introduction:

Let S be a semigroup with the binary operation being additive. A *weight* on S is a mapping $\omega : S \longrightarrow (0, \infty)$ such that $\omega(s+t) \leq \omega(s)\omega(t)$ $(s, t \in S)$. For a function $f : S \longrightarrow \mathbb{C}$, let supp$f$ denote the support of f with the topology on S being discrete; i.e., $\text{supp} f = \{s \in S : f(s) \neq 0\}$. Define

$$C_c(S) := \{f : S \longrightarrow \mathbb{C} : \text{supp} f \text{ is finite } \}$$

and

$$\ell^1(S, \omega) := \{f : S \longrightarrow \mathbb{C} : ||f||_\omega := \sum_{s \in S} |f(s)|\omega(s) < \infty\}.$$

It is clear that $C_c(S)$ is a dense subset of $\ell^1(S, \omega)$ for any weight ω on S. Then the normed linear space $(C_c(S), || \cdot ||_\omega)$ is a normed algebra and the Banach space $(\ell^1(S, \omega), || \cdot ||_\omega)$ is a Banach algebra with respect to the usual convolution product.

Weights on $\mathbb{N}$ and $\mathbb{Z}$ were considered first by Beurling [Be]. The ℓ^1-algebras on groups and semigropus with weights (so called Beurling algebras) are also recently studied in [BhDe1, BhDe3, De1]. In fact it is noted in [Da, p.536] that the golden age for the study of $\ell^1(\mathbb{Q}^+, \omega)$ (which is a special case of our object $\ell^1(S,\ \omega)$) lies in the future. The Banach algebra structure of $\ell^1(S,\ \omega)$ is very much influenced by the presence of the semigroup S and the weight ω; e.g., if S is an abelian group, then $\ell^1(S,\ \omega)$ is always semisimple [BhDe2]; whereas for a semigroup, $\ell^1(S,\ \omega)$ can be radical or semisimple depending on weight ω [De1, Theorem 2.1.5].

In this connection, Section-2 is devoted to introduce generalized semicharacters. In Section-3, we give a large number of examples of weights on S as well as general methods to construct weights. As an application, in the last section, the Gelfand space of the commutative convolution topological algebra $C_c(S)$ equipped with the inductive limit topology is identified with the set of all generalized semicharacters on S.

2 Generalized Semicharacters:

A mapping $\theta : S \longrightarrow \mathbb{C}$ is a *generalized semicharacter* on S if it is not identically zero and if $\theta(s+t) = \theta(s)\theta(t)$ $(s, t \in S)$. Let $H_{gs}(S)$ denote the set of all generalized semicharacters on S. A generalized semicharacter $\theta \in H_{gs}(S)$ is a *semicharacter* if $\theta(S) \subseteq \mathbb{T} \cup \{0\}$, where $\mathbb{T}$ is the unit circle in the complex plane. Let $H_s(S)$ denote the set of all semicharacters on S. A generalized semicharacter $\theta \in H_{gs}(S)$ is a *bounded semicharacter* if $|\theta(s)| \leq 1$ $(s \in S)$. Let $H_{bs}(S)$ denote the set of all bounded semicharacters on S. A generalized semicharacter $\theta \in H_{gs}(S)$ is a *generalized character* if $\theta(s) \neq 0$ for any $s \in S$. Let $H_g(S)$ denote the set of all generalized characters on S. A generalized character $\theta \in H_g(S)$ is a *character* if $|\theta(s)| = 1$ $(s \in S)$. Let $\widehat{S}$ denote the set of all characters on S. A generalized character $\theta \in H_g(S)$ is a *bounded character* if $|\theta(s)| \leq 1$ $(s \in S)$. Let $H_b(S)$ denote the set of all bounded characters on S.

Note that $H_s(S) \subseteq H_{bs}(S) \subseteq H_{gs}(S)$ and $\widehat{S} \subseteq H_b(S) \subseteq H_g(S)$, and each of them contains the constant map $1_S : S \longrightarrow \mathbb{C}$, where $1_S(s) = 1$ $(s \in S)$. Throughout, we take the discrete topology on S, the pointwise topology on $H_{gs}(S)$, and the subspace topology on each other subsets of $H_{gs}(S)$. It is clear that $H_{gs}(S)$ is a Hausdorff topological space.

For $\theta, \eta \in H_{gs}(S)$, define $(\theta \dot{+} \eta)(s) = \theta(s)\eta(s)$ $(s \in S)$. Then it is clear that $(\theta \dot{+} \eta)(s + t) = (\theta \dot{+} \eta)(s)(\theta \dot{+} \eta)(t)$ $(s, t \in S)$. However $\theta \dot{+} \eta$ may not be a generalized semicharacter; i.e., $H_{gs}(S)$ need not be closed under the binary operation $\dot{+}$. In fact the following example exhibits that none of the sets $H_s(S)$, $H_{bs}(S)$, and $H_{gs}(S)$ are closed. Take $S = (\mathbb{Z}^+ + \lambda\mathbb{Z}^+) \setminus \{0\}$ for some irrational positive real number λ. Define

$$\theta(m + \lambda n) = \begin{cases} 0 & \text{if } m \neq 0 \\ 1 & \text{if } m = 0 \end{cases}$$

and

$$\eta(m + \lambda n) = \begin{cases} 0 & \text{if } n \neq 0 \\ 1 & \text{if } n = 0 \end{cases}$$

Then it is routine to verify that $\theta \in H_s(S)$, $\eta \in H_s(S)$, and $\theta \dot{+} \eta \equiv 0$ on S. Hence $\theta \dot{+} \eta \notin H_s(S)$; in fact $\theta \dot{+} \eta \notin H_{gs}(S)$.

However, the next result says that, even if S is not a group, the sets $H_g(S)$ and $\widehat{S}$ are abelian groups with binary operation $\dot{+}$.

Theorem 2.1 *Let S be a semigroup. Then*

(i) $H_g(S)$ and $\widehat{S}$ are abelian groups;

(ii) $H_b(S)$ is a unital, cancellative, abelian semigroup.

Proof: *(i)* First we show that $H_g(S)$ is an abelian group. Let $\theta, \eta \in H_g(S)$. Then $\theta(s) \neq 0$ and $\eta(s) \neq 0$ for all $s \in S$. So $(\theta \dot{+} \eta)(s) = \theta(s)\eta(s) \neq 0$ for all $s \in S$. Hence $\theta \dot{+} \eta \in H_g(S)$. The constant map $1_S : S \longrightarrow \mathbb{C}$; $1_S(s) = 1$ $(s \in S)$ is the identity of $H_g(S)$. The associativity of $\dot{+}$ is clear. Finally, let $\theta \in H_g(S)$. Define $\theta^{-1}(s) = 1/\theta(s)$ $(s \in S)$. Then $\theta^{-1} \in H_g(S)$ and $\theta \dot{+} \theta^{-1} = \theta^{-1} \dot{+} \theta = 1_S$. Thus $H_g(S)$ is an abelian group.

Next we show that $\widehat{S}$ is an abelian group. Let $\theta, \eta \in \widehat{S}$. Then $|(\theta \dot{+} \eta)(s)| = |\theta(s)\eta(s)| = 1 \cdot 1 = 1$. Thus $\theta \dot{+} \eta \in \widehat{S}$. Let $\theta \in \widehat{S}$. Then $|\theta^{-1}(s)| = 1/|\theta(s)| = 1$ $(s \in S)$. So $\theta^{-1} \in \widehat{S}$. Hence $\widehat{S}$ is an abelian group.
(ii) Let $\theta, \eta \in H_b(S)$. Then $0 < |(\theta \dot{+} \eta)(s)| = |\theta(s)||\eta(s)| \leq 1$ $(s \in S)$. So $\theta \dot{+} \eta \in H_b(S)$. Thus $H_b(S)$ is an abelian semigroup. Now $1_S \in H_b(S)$, and so $H_b(S)$ is unital. Finally let $\theta_1, \theta_2, \eta \in H_b(S)$ such that $\theta_1 \dot{+} \eta = \theta_2 \dot{+} \eta$. Then $\theta_1(s)\eta(s) = (\theta_1 \dot{+} \eta)(s) = (\theta_2 \dot{+} \eta)(s) = \theta_2(s)\eta(s)$ $(s \in S)$. Since $\eta(s) \neq 0$ for each $s \in S$, we have $\theta_1(s) = \theta_2(s)$ $(s \in S)$. So $H_b(S)$ is cancellative. ☐

Corollary 2.2 *Let S be a group. Then every generalized semicharacter is a character. Hence $H_g(S) = H_{gs}(S)$, and $H_b(S) = H_{bs}(S) = \widehat{S}$.*

Proof: Clearly $H_g(S) \subseteq H_{gs}(S)$. Let $\theta \in H_{gs}(S)$. Suppose, if possible, there exists $t \in S$ such that $\theta(t) = 0$. Since S is a group, $\theta(s) = \theta(s - t + t) = \theta(s-t)\theta(t) = \theta(s-t) \cdot 0 = 0$ for each $s \in S$, which is a contradiction. Hence $\theta \in H_g(S)$. Thus $H_g(S) = H_{gs}(S)$. The other equalities can be proved by similar arguments. ☐

Remark 2.3 Even if S is not a group, it may happen that $H_{gs}(S) = H_g(S)$. e.g., $H_{gs}(\mathbb{N}) = H_g(\mathbb{N}) \cong H_g(\mathbb{Z}) \cong \mathbb{C}^\bullet (= \mathbb{C} \setminus \{0\})$. Indeed let $z \in \mathbb{C}^\bullet$. Define $\theta_z(n) = z^n$ $(n \in \mathbb{N})$. Then $\theta_z \in H_g(\mathbb{N})$. Conversely, let $\theta \in H_g(\mathbb{N})$. Set $z = \theta(1)$. Then $z \neq 0$. Now for any $n \in \mathbb{N}$, $\theta(n) = \theta(1)^n = z^n = \theta_z(n)$. This proves that $H_g(\mathbb{N}) \cong \mathbb{C}^\bullet$. Another example is $S = [1, \infty)$. Let $\theta \in H_{gs}(S)$. Suppose, if possible, there exists $t_0 \in S$ such that $\theta(t_0) = 0$. Then, for any $t \in [1+t_0, \infty)$, $\theta(t) = \theta(t-t_0+t_0) = \theta(t-t_0)\theta(t_0) = 0$. Now let $t \in [1, 1+t_0)$. Then there exists $n \in \mathbb{N}$ such that $nt > 1 + t_0$. Hence $\theta(t)^n = \theta(nt) = 0$, i.e., $\theta(t) = 0$. So $\theta \equiv 0$ on S; a contradiction. This proves that $H_{gs}(S) = H_g(S)$.

3 Weights on Semigroups:

The Banach algebra structure of the convolution algebra $\ell^1(S, \omega)$ is greatly influenced by the weight ω. In this section, our main objective is to develope some general methods which gaurantee a variety of weights on semigroups.

Recall that a *weight* on a semigroup S is a positive map $\omega : S \longrightarrow (0, \infty)$ such that $\omega(s+t) \leq \omega(s)\omega(t)$ $(s, t \in S)$. Let $\eta : S \longrightarrow \mathbb{R}$ be a function. Define $\omega(s) = e^{\eta(s)}$ $(s \in S)$. Then it is clear that ω is a weight on S if and only if the function η is subadditive, i.e., $\eta(s+t) \leq \eta(s) + \eta(t)$ $(s, t \in S)$. This simple observation will be proved very important to verify some functions to be weights.

Lemma 3.1 *Let $\lambda \in \mathbb{R}$, let S be a semigroup, and let $\theta \in H_g(S)$. Define $\omega(s) = \exp(\lambda \log |\theta(s)|)$ $(s \in S)$. Then ω is a weight on S.*

Proof: For $s, t \in S$, we have

$$\begin{aligned}
\omega(s+t) &= \exp(\lambda \log |\theta(s+t)|) = \exp(\lambda \log |\theta(s)\theta(t)|) \\
&= \exp(\lambda[\log |\theta(s)| + \log |\theta(t)|]) = \exp(\lambda \log |\theta(s)|) \exp(\lambda \log |\theta(t)|) \\
&= \omega(s)\omega(t).
\end{aligned}$$

Thus ω is a weight. $\square$

Lemma 3.2 *Let $\lambda > 0$, let S be a semigroup, and let $\eta : S \longrightarrow [0,\infty)$ be subaddititve. Define $\omega(s) = [1+\eta(s)]^{\lambda}$ $(s \in S)$. Then ω is a weight on S.*

Proof: For $s, t \in S$, we have

$$\begin{aligned} \log\omega(s+t) &= \lambda\log(1+\eta(s+t)) \le \lambda\log(1+\eta(s)+\eta(t)) \\ &\le \lambda\log([1+\eta(s)][1+\eta(t)]) = \lambda\log(1+\eta(s)) + \lambda\log(1+\eta(t)) \\ &= \log\omega(s) + \log\omega(t). \end{aligned}$$

Hence ω is a weight. $\square$

Lemma 3.3 *Let $0 < \lambda \le 1$, let S be a semigroup, and let $\eta : S \longrightarrow [0,\infty)$ be subaddititve. Define $\omega(s) = \exp(\eta(s)^{\lambda})$ $(s \in S)$. Then ω is a weight on S.*

Proof: For $s, t \in S$, we have

$$\begin{aligned} \log\omega(s+t) &= \eta(s+t)^{\lambda} \le [\eta(s)+\eta(t)]^{\lambda} \\ &\le \eta(s)^{\lambda} + \eta(t)^{\lambda} \ \text{(Because } 0 \le \lambda \le 1) \\ &= \log\omega(s) + \log\omega(t). \end{aligned}$$

Hence ω is a weight. $\square$

Remark 3.4 *Let $\omega : \mathbb{R} \longrightarrow [1,\infty)$ such that $\omega(-s) = \omega(s)$ $(s \in \mathbb{R})$ and ω being increasing on $\mathbb{R}^+$. If ω is a weight on $\mathbb{R}^+$, then ω is a weight on $\mathbb{R}$. Indeed, let $s, t \in \mathbb{R}$ such that $s > 0$, $t < 0$, and $s + t > 0$. Then $\omega(s+t) \le \omega(s) \le \omega(s)\omega(t)$. Other different cases of s and t can be verified in the similar way. So ω is a weight on $\mathbb{R}$.* $\square$

Lemma 3.5 *Let $\omega(s) = \exp(\frac{|s|}{1+\log(1+|s|)})$ $(s \in \mathbb{R})$. Then ω is a weight on $\mathbb{R}$.*

Proof: Note that $\omega(s) \ge 1$ $(s \in \mathbb{R})$, $\omega(-s) = \omega(s)$ $(s \in \mathbb{R})$, and ω is increasing on $\mathbb{R}^+$. So, by Remark above, it is enough to prove that ω is a weight on $\mathbb{R}^+$. Let $s, t \in \mathbb{R}^+$. Then

$$\begin{aligned}\log\omega(s+t) &= \frac{|s+t|}{1+\log(1+|s+t|)} = \frac{s+t}{1+\log(1+s+t)} \\ &= \frac{s}{1+\log(1+s+t)} + \frac{t}{1+\log(1+s+t)} \\ &\leq \frac{s}{1+\log(1+s)} + \frac{t}{1+\log(1+t)} \\ &= \log\omega(s) + \log\omega(t).\end{aligned}$$

Hence ω is a weight on $\mathbb{R}^+$; and hence on $\mathbb{R}$. □

Lemma 3.6 *Fix $a > 1$, let S be a semigroup, and let $\eta : S \longrightarrow (0, \infty)$ be subadditive. Define $\omega(s) = \frac{1+a\eta(s)}{1+\eta(s)}$ $(s \in S)$. Then ω is a weight on S.*

Proof: For $s, t \in S$, we have

$$\begin{aligned}\omega(s+t) &= \frac{1+a\eta(s+t)}{1+\eta(s+t)} = 1 + (a-1)\frac{\eta(s+t)}{1+\eta(s+t)} \\ &\leq 1 + (a-1)[\frac{\eta(s)}{1+\eta(s)} + \frac{\eta(t)}{1+\eta(t)}] \\ &\leq [1 + (a-1)\frac{\eta(s)}{1+\eta(s)}][1 + (a-1)\frac{\eta(t)}{1+\eta(t)}] \\ &= [\frac{1+a\eta(s)}{1+\eta(s)}][\frac{1+a\eta(t)}{1+\eta(t)}] = \omega(s)\omega(t).\end{aligned}$$

Hence ω is a weight. □

Lemma 3.7 *Let $\omega_1, \ldots, \omega_n$ be weights on a semigroup S. Let $\lambda_i > 0$ $(i = 1, \ldots, n)$, and let $0 < p, q < \infty$. For $s \in S$, define*

$$\begin{aligned}\omega_{p,q}(s) &= [\sum_{i=1}^{n} \omega_i(s)^p]^q; \\ \omega_g(s) &= \max\{\omega_1(s), \cdots, \omega_n(s)\}; \\ \omega_w(s) &= \omega_1(s)^{\lambda_1} \cdots \omega_n(s)^{\lambda_n};\end{aligned}$$

Then $\omega_{p,q}$, ω_g, and ω_w are weights on S.

Proof: For $s, t \in S$, we have

$$\begin{aligned}\omega_{p,q}(s+t) &= [\sum_{i=1}^{n} \omega_i(s+t)^p]^q \leq [\sum_{i=1}^{n} \omega_i(s)^p \omega_i(t)^p]^q \\ &\leq [\sum_{i=1}^{n} \omega_i(s)^p]^q [\max\{\omega_i(t)^p : i = 1, \cdots, n\}]^q \\ &\leq [\sum_{i=1}^{n} \omega_i(s)^p]^q [\sum_{i=1}^{n} \omega_i(t)^p]^q = \omega_{p,q}(s)\omega_{p,q}(t).\end{aligned}$$

Thus $\omega_{p,q}$ is a weight. It is clear that ω_g and ω_w are weights. □

Lemma 3.8 *Let ω_i be weights on S_i $(i = 1, \ldots, n)$. Let $S = S_1 \oplus \cdots \oplus S_n$. Let $\lambda_i > 0$ $(i = 1, \ldots, n)$ and $0 < p, q < \infty$. For $s = (s_1, \ldots, s_n) \in S$, define*

$$\begin{aligned}\widetilde{\omega}_{p,q}(s) &= [\sum_{i=1}^{n} \omega_i(s_i)^p]^q; \\ \widetilde{\omega}_g(s) &= \max\{\omega_1(s_1), \cdots, \omega_n(s_n)\}; \\ \widetilde{\omega}_w(s) &= \omega_1(s_1)^{\lambda_1} \cdots \omega_n(s_n)^{\lambda_n};\end{aligned}$$

Then $\widetilde{\omega}_{p,q}$, $\widetilde{\omega}_g$, and $\widetilde{\omega}_w$ are weights on S.

Proof: For $s, t \in S$, we have

$$\begin{aligned}\widetilde{\omega}_{p,q}(s+t) &= [\sum_{i=1}^{n} \omega_i(s_i+t_i)^p]^q \leq [\sum_{i=1}^{n} \omega_i(s_i)^p \omega_i(t_i)^p]^q \\ &\leq [\sum_{i=1}^{n} \omega_i(s_i)^p]^q [\max\{\omega_i(t_i)^p : i = 1, \cdots, n\}]^q \\ &\leq [\sum_{i=1}^{n} \omega_i(s_i)^p]^q [\sum_{i=1}^{n} \omega_i(t_i)^p]^q = \widetilde{\omega}_{p,q}(s)\widetilde{\omega}_{p,q}(t).\end{aligned}$$

Thus $\widetilde{\omega}_{p,q}$ is a weight. It is clear that $\widetilde{\omega}_g$ and $\widetilde{\omega}_w$ are weights. □

Lemma 3.9 *Let $\theta \in H_g(S)$. Define $\omega(s) = \max\{|\theta(s)|, |\theta(s)|^{-1}\}$ $(s \in S)$. Then ω is a weight on S.*

Proof: For $s, t \in S$, we have

$$\begin{aligned}\omega(s+t) &= \max\{|\theta(s+t)|, |\theta(s+t)|^{-1}\} = \max\{|\theta(s)||\theta(t)|, |\theta(s)|^{-1}|\theta(t)|^{-1}\} \\ &\leq \max\{|\theta(s)|, |\theta(s)|^{-1}\}\max\{|\theta(t)|, |\theta(t)|^{-1}\} = \omega(s)\omega(t).\end{aligned}$$

Thus ω is a weight. $\square$

Lemma 3.10 *Let S be a unital semigroup. Let d be an invariant metric on S, i.e., $d(s+u, t+u) = d(s,t)$ $(s, t, u \in S)$. Let $\omega(s) = \exp d(s, 0)$ $(s \in S)$. Then ω is a weight on S.*

Proof: For $s, t \in S$, $d(s+t, 0) \leq d(s+t, 0+t) + d(0+t, 0) = d(s, 0) + d(t, 0)$. Now it is clear that ω is a weight on S. $\square$

Theorem 3.11 *Let $S \subseteq \mathbb{R}$ be any non-empty set. For $s, t \in S$, define $s * t = \min\{s, t\}$. Then $(S, *)$ is a semigroup and a mapping $\omega : S \longrightarrow (0, \infty)$ is a weight on S if and only if $\omega(s) \geq 1$ $(s \in S)$.*

Proof: Clearly S is an (abelian) semigroup. Assume that ω is a weight on S. Let $s \in S$. Then $0 < \omega(s) = \omega(s * s) \leq \omega(s)\omega(s)$. Hence we must have $\omega(s) \geq 1$. Conversely, assume that $\omega(s) \geq 1$ $(s \in S)$. Let $s, t \in S$. Then $\omega(s * t) = \omega(s)$ or $\omega(t)$. By the assumption, $\omega(s * t) \leq \max\{\omega(s), \omega(t)\} \leq \omega(s)\omega(t)$. Hence ω is a weight on S. $\square$

Next two results are generalization of Lemma 4.1.2 and Lemma 4.1.3 in the first author's Ph.D. Thesis [De1].

Theorem 3.12 *Let $r \geq 1$. Let ω be a weight on a field F such that $\omega(0) = 1$. Let V be a vector space over F. Let $B = \{v_\alpha : \alpha \in \Lambda\}$ be a basis for V. For $v \in V \setminus \{0\}$, we have a unique expression $v = \lambda_1 v_{\alpha_1} + \cdots + \lambda_k v_{\alpha_k}$, where $\lambda_1, \ldots, \lambda_k \in F$ and $v_{\alpha_1}, \ldots, v_{\alpha_k} \in B$. Define*

$$\widetilde{\omega}_1(v) = \omega(\lambda_1)\cdots\omega(\lambda_k) \quad \textit{and} \quad \widetilde{\omega}_2(v) = r + \omega(\lambda_1) + \cdots + \omega(\lambda_k).$$

Set $\widetilde{\omega}_1(0) = \widetilde{\omega}_2(0) = 1$. *Then both* $\widetilde{\omega}_1$ *and* $\widetilde{\omega}_2$ *are weights on* V.

Proof: It is clear that both $\widetilde{\omega}_1$ and $\widetilde{\omega}_2$ are strictly positive functions on V. Now let $u = \delta_1 v_{\alpha_1} + \cdots + \delta_k v_{\alpha_k}$ and $v = \lambda_1 v_{\beta_1} + \cdots + \lambda_l v_{\beta_l}$ belong to V. We may assume that $k = l (= m$ say) and $\alpha_i = \beta_i (1 \leq i \leq m)$. Then

$$\begin{aligned}
\widetilde{\omega}_1(u+v) &= \widetilde{\omega}_1([\delta_1 v_{\alpha_1} + \cdots + \delta_k v_{\alpha_k}] + [\lambda_1 v_{\beta_1} + \cdots + \lambda_l v_{\beta_l}]) \\
&= \widetilde{\omega}_1((\delta_1 + \lambda_1) v_{\alpha_1} + \cdots + (\delta_m + \lambda_m) v_{\alpha_m}) \\
&= \omega(\delta_1 + \lambda_1) \cdots \omega(\delta_m + \lambda_m) \leq \omega(\delta_1)\omega(\lambda_1) \cdots \omega(\delta_m)\omega(\lambda_m) \\
&= [\omega(\delta_1) \cdots \omega(\delta_m)][\omega(\lambda_1) \cdots \omega(\lambda_m)] = \widetilde{\omega}_1(u)\widetilde{\omega}_1(v).
\end{aligned}$$

So $\widetilde{\omega}_1$ is a weight on V. Similarly,

$$\begin{aligned}
\widetilde{\omega}_2(u+v) &= \widetilde{\omega}_2([\delta_1 v_{\alpha_1} + \cdots + \delta_k v_{\alpha_k}] + [\lambda_1 v_{\beta_1} + \cdots + \lambda_l v_{\beta_l}]) \\
&= \widetilde{\omega}_2((\delta_1 + \lambda_1) v_{\alpha_1} + \cdots + (\delta_m + \lambda_m) v_{\alpha_m}) \\
&= r + \omega(\delta_1 + \lambda_1) + \cdots + \omega(\delta_m + \lambda_m) \\
&\leq r + \omega(\delta_1)\omega(\lambda_1) + \cdots + \omega(\delta_m)\omega(\lambda_m) \leq \widetilde{\omega}_2(u)\widetilde{\omega}_2(v).
\end{aligned}$$

Thus $\widetilde{\omega}_2$ is a weight on V. ☐

Theorem 3.13 *Let* $r > 1$. *Let* $\{r_1, r_2, \ldots\}$ *be a sequence in* $(0, \infty)$ *and let* $\{s_1, s_2, \ldots\}$ *be a sequence in* $[1, \infty)$. *Let* ω *be a weight on a field* F *such that* $\omega(0) = 1$. *Let* V *be a vector space over* F *with a countable basis* $B = \{v_1, v_2, \ldots\}$. *For* $v \in V \setminus \{0\}$, *we have a unique expression* $v = \lambda_1 v_1 + \cdots + \lambda_k v_k$, *where* $\lambda_1, \ldots, \lambda_k \in F$ *and* $v_{\alpha_1}, \ldots, v_{\alpha_k} \in B$. *For such* v, *define*

$$\widetilde{\omega}_1(v) = \omega(\lambda_1)^{r_1} \cdots \omega(\lambda_k)^{r_k} \quad \textit{and} \quad \widetilde{\omega}_2(v) = r + s_1\omega(\lambda_1) + \cdots + s_k\omega(\lambda_k).$$

Set $\widetilde{\omega}_1(0) = \widetilde{\omega}_2(0) = 1$. *Then both* $\widetilde{\omega}_1$ *and* $\widetilde{\omega}_2$ *are weights on* V.

Proof: It is clear that both $\widetilde{\omega}_1$ and $\widetilde{\omega}_2$ are strictly positive functions on V. Now let $u = \delta_1 v_{\alpha_1} + \cdots + \delta_k v_{\alpha_k}$ and $v = \lambda_1 v_{\beta_1} + \cdots + \lambda_l v_{\beta_l}$ belong to V. We may assume that $k = l (= m \text{ say})$ and $\alpha_i = \beta_i$ $(i = 1, \ldots, m)$. Then

$$\begin{aligned}
\widetilde{\omega}_1(u+v) &= \widetilde{\omega}_1([\delta_1 v_1 + \cdots + \delta_m v_m] + [\lambda_1 v_1 + \cdots + \lambda_m v_m]) \\
&= \widetilde{\omega}_1((\delta_1 + \lambda_1) v_{\alpha_1} + \cdots + (\delta_m + \lambda_m) v_{\alpha_m}) \\
&= \omega(\delta_1 + \lambda_1)^{r_1} \cdots \omega(\delta_m + \lambda_m)^{r_m} \\
&\leq \omega(\delta_1)^{r_1} \omega(\lambda_1)^{r_1} \cdots \omega(\delta_m)^{r_m} \omega(\lambda_m)^{r_m} \\
&= [\omega(\delta_1)^{r_1} \cdots \omega(\delta_m)^{r_m}][\omega(\lambda_1)^{r_m} \cdots \omega(\lambda_m)^{r_m}] = \widetilde{\omega}_1(u)\widetilde{\omega}_1(v).
\end{aligned}$$

So $\widetilde{\omega}_1$ is a weight on V. Now

$$\begin{aligned}
\widetilde{\omega}_2(u+v) &= \widetilde{\omega}_2([\delta_1 v_{\alpha_1} + \cdots + \delta_k v_{\alpha_k}] + [\lambda_1 v_{\beta_1} + \cdots + \lambda_l v_{\beta_l}]) \\
&= \widetilde{\omega}_2((\delta_1 + \lambda_1) v_{\alpha_1} + \cdots + (\delta_m + \lambda_m) v_{\alpha_m}) \\
&= r + s_1 \omega(\delta_1 + \lambda_1) + \cdots + s_m \omega(\delta_m + \lambda_m) \\
&\leq r + s_1 \omega(\delta_1)\omega(\lambda_1) + \cdots + s_m \omega(\delta_m)\omega(\lambda_m) \leq \widetilde{\omega}_2(u)\widetilde{\omega}_2(v).
\end{aligned}$$

So $\widetilde{\omega}_2$ is also a weight on V. ☐

Examples 3.14 We close this section by exhibiting some weights on classical semigroups, which can not be extended over arbitrary semigroups. Some of them are completely new constructions, while some were scattered in the literature; however we list them out for the sake of completeness.

1. Let $\gamma > 1$ and $\omega(s) = exp(-s^{\gamma})$ $(s > 0)$;
2. Let $\gamma > 0$ and $\omega(s) = \exp(-s(\log(1+s))^{\gamma})$ $(s > 0)$;
3. Let $\omega(s) = \exp \frac{1-s^3}{s}$ $(s > 0)$;

4. For $s = p/q \in \mathbb{Q}^\bullet$ with $(p, q) = 1$, let $\omega(s) = q$ and $\omega(0) = 1$.

5. For $s = p/q \in \mathbb{Q}^\bullet$ with $(p, q) = 1$, let $\omega(s) = |p| + q$ and $\omega(0) = 1$.

6. Let $k \geq 1$ and $r \in \mathbb{N}$. Define $\omega(n) = \frac{k}{(rn)!}$ $(n \in \mathbb{N})$.

7. Let ω be a weight on $\mathbb{R}$. Define $\overline{\omega}(x + iy) = \omega(x)$ $(x + iy \in \mathbb{C})$.

8. For $\lambda > 0$, let
$$\omega(s) = \begin{cases} 1 & \text{if } s \geq 0 \\ 1 - \lambda s & \text{if } s \leq 0 \end{cases}$$

9. For $\lambda \geq 0$, let
$$\omega(s) = \begin{cases} (1 + s)^\lambda & \text{if } s \geq 0 \\ 1 & \text{if } s \leq 0 \end{cases}$$

10. For $\gamma > 0$ and $\lambda > 0$, let
$$\omega(s) = \begin{cases} 1 + \gamma s & \text{if } s \geq 0 \\ 1 - \lambda s & \text{if } s \leq 0 \end{cases}$$

4 Commutative Convolution Algebra $C_c(S)$:

The linear space $C_c(S)$ is interesting on two counts. One is that it becomes a topological algebra with two different products (pointwise and convolution) and with different topologies in each product. Another reason is that it is a dense subalgebra of $\ell^1(S, \omega)$ and so it helps to prove some Banach algebra properties of $\ell^1(S, \omega)$. Here we study $C_c(S)$ with convolution product and the inductive limit topology. For standard terminologies and definitions we shall refer to [Da].

A semigroup S is *separating* if $s = t$ whenever $s, t \in S$ and $s + t = s + s = t + t$. Every cancellative semigroup is separating. The semigroup S admits a set of relative units if there exists a subset U of S such that, for each $s \in S$, there exists $u \in U$ satisfying $s+u = u+s = s$. If S has an identity, denoted by 0, then $\{0\}$ is a (finite) set of relative units for the semigroup S. Let τ be the inductive limit topology on $C_c(S)$. Then $(C_c(S), \tau)$ is a topological algebra with the convolution product due to [Ma, Lemma 2.1, p.114]. The semigroup S is abelian iff $C_c(S)$ is commutative. For a commutative topological algebra A, let $\Delta(A)$ denote the Gelfand space of A [Da].

Theorem 4.1 *Let S be an abelian semigroup. Then*

(i) S is separating iff $C_c(S)$ is semisimple.

(ii) $C_c(S)$ has an identity if S has a finite set of relative units.

(iii) $\Delta(C_c(S)) \cong H_{gs}(S)$.

Proof: *(i)* Assume that S is separating. Then, by [HeZu, Theorem 3.5], $\ell^1(S)$ is semisimple. Since $\ell^1(S)$ is a commutative Banach algbera, its subalgebra $C_c(S)$ is also semisimple.

Conversely, assume that S is not separating. Then there exists $s \neq t$ in S such that $s+t = s+s = t+t$. Let $f = \delta_s - \delta_t$, where δ_x denotes the point mass at x. Then $f \in C_c(S)$ and $f^2 = (\delta_s - \delta_t)^2 = \delta_s^2 - 2\delta_s\delta_t + \delta_t^2 = \delta_{s+s} - 2\delta_{s+t} + \delta_{t+t} = 0$. Since $C_c(S)$ is commutative, f belongs to the radical of $C_c(S)$ due to [Da, Proposition 1.5.6(iii)]. So $C_c(S)$ is not semisimple.

(ii) Assume that $C_c(S)$ has an identity. Since $C_c(S)$ is dense in $\ell^1(S)$, the algebra has also identity. By [HeZu, Theorem 7.5], S has a finite set of relative units. Conversely, assume that S has a finite set of relative units. Then, by [HeZu, Theorem 7.6], $\ell^1(S)$ has an identity, say e. In fact, $\operatorname{supp} e$ is finite, and so $e \in C_c(S)$. Thus $C_c(S)$ has an identity.

(iii) For $\theta \in H_{gs}(S)$, define $\varphi_\theta(f) = \sum_{s\in S} f(s)\theta(s)$ for all $f = \sum_{s\in S} f(s)\delta_s \in C_c(S)$. Then it is clear that $\varphi_\theta \in \Delta(C_c(S))$. Conversely, let $\varphi \in \Delta(C_c(S))$. Define $\theta(s) = \varphi(\delta_s)$ $(s \in S)$. Since φ is a complex homomorphism, it is not identically zero. So there exists $s \in S$ such that $\theta(s) = \varphi(\delta_s) \neq 0$. Hence $\theta \in H_{gs}(S)$. Define $T : H_{gs}(S) \longrightarrow \Delta(C_c(S))$ as $T(\theta) = \varphi_\theta$. Then it is easy to see that T is one-one, onto, continuous and its inverse T^{-1} is also continuous. Hence $H_{gs}(S) \cong \Delta(C_c(S))$. □

The following corollary follows easily from the Theorem above.

Corollary 4.2 *Let S be a cancellative, abelian semigroup. Then (i) $C_c(S)$ is semisimple; (ii) $C_c(S)$ has an identity iff S has an identity.* □

Acknowledgement: The authors are thankful to S. J. Bhatt for reading the manuscript and for some suggestions. The first author acknowledges financial support from UGC as a Major Research Project No. F.8-9/2004(SR).

References

[Be] A. Beurling, *Sure les intégrales de Fourier absolument convergentes et leur applications à une transformation functionelle*, Neuvième Congres des Math. Scand., Helsinki (1938).

[BhDe1] S. J. Bhatt and H. V. Dedania, *Beurling algebras and uniform norms*, Studia Math., 160(2)(2004)179-183.

[BhDe2] S. J. Bhatt and H. V. Dedania, *Beurling algebra is semisimple: an elementary proof*, Bull. Australian Math. Soc., 66(2002)93-95.

[BhDe3] S. J. Bhatt and H. V. Dedania, *Banach algebras with unique uniform norm II*, Studia Math., 147(3)(2001)211-235.

[Da] H. G. Dales, *Banach algebras and automatic continuity*, London Math. Soc. Monographs, Vol. 24, Clarendon Press, Oxford, 2000.

[De1] H. V. Dedania, *Weighted discrete semigroup algebras*, Ph. D. Thesis, University of Leeds, LEEDS (UK), 1997.

[De2] H. V. Dedania, *On the Gelfand space of Weighted discrete abelian semigroup algebras*, Mathematics Today, 19(2)(2001)15-24.

[HeZu] E. Hewitt and H. S. Zuckerman, *The ℓ^1-algebra of a commutative semigroup*, Tran. American Math. Soc., 83 (1956) 70-97.

[Ma] A. Mallios, *Topological Algebras; selected topics*, Elsevier Science Publishers B. V., New York, 1986.

'Prajna' - Jounal of Pure & Applied Sciences, 14 (2006) 94-98

THE ESTIMATION OF $D_3(x)$

H. B. Modi
Department of Mathematics, Bhavnagar University, Bhavnagar- 364 002
E-mail: hbm_bhav_uni@yahoo.com

Abstract

Let $d_3(n)$ denote the number of representation of n in the form $n = \alpha_1 \times \alpha_2 \times \alpha_3$, where α_1's are positive integers. We study the asymptotic formula of $D_3(x) = \sum_{n \le x} d_3(x)$.

Introduction and Preliminaries

We know the Dirichlet's Divisor Problem (D.D.P) is to estimate $\sum_{n \le x} d(n)$, where *d(n)* denote the number of divisors of *n* .We have the following result.

Theorem 1 : ([1], Theorem 3.3) $\sum_{n \le x} d(n) = x \log x + (2\gamma - 1)x + O(\sqrt{x})$, where γ is Euler's constant.

If we look at the definition of *d(n),* then we see that the number *d(n)* is actually the number of representations of *n* as a product of two integers viz, the number of representation *n = a x b*, where *a* and *b* are positive integers. e.g. the divisor of 12 are 1, 2, 3, 4, 6 and 12 the corresponding representations of 12 as a product of two integers are given by

12 = 1 x 12, 12 = 2 x 6, 12 = 3 x 4, 12 = 4 x 3, 12 = 6 x 2, 12 = 2 x 1.

Here we denote by $d_2(n)$, the number of representations of *n* as a product of two integers. Clearly $d_2(n) = d(n)$.

The generalization of D.D.P. was also considered by Dirichlet, which we call the Generalized Dirichlet's Divisor Problem (G.D.D.P.)

Generalized Dirichlet's Divisor Problem (G.D.D.P.) : Let *k* be any fixed integer ≥ 2. Then we define $d_k(n)$ to be the number of representations of *n* in the form $n = \alpha_1 \times \alpha_2 \times \ldots\ldots \times \alpha_\kappa$, where α_ι's are positive integers. Observe that when $k = 2$, it is the same as $d_2(n)$. Now if we write $D_k(x) = \sum_{n \le x} d_k(n)$, then the G.D.D.P. is to get an estimate for $D_k(x)$. Clearly we have

$$D_2(x) = x \log x + (2\gamma - 1)x + O(\sqrt{x}).$$

We have the following theorem.

Theorem 2 : ([2], Theorem 12.1.3) For a fixed integer k ≥ 2, we have

$$D_k(x) = xP_k(\log x) + \Delta_k(x)$$

Where P_k is a polynomial of degree k~1 and $\Delta_k(x) = \mathrm{O}(x^{1-\frac{1}{k}} \log^{k-2} x)\cdot$

In Theorem 2 we had a theoretical form for an estimate of $D_k(x)$ for every integer k ≥ 2. For $D_2(x)$, we have complete information, whereas for $D_3(x)$, at this stage we only know that

$$D_3(x) = x(a_2 \log^2 x + a_1 \log x + a_0) + \mathrm{O}(x^{\frac{2}{3}} \log x)$$

for some suitable constant a_i's. But we don't know the exact value or any other convenient form for this constants. Hence theoretically we have complete information for $D_3(x)$, but practically we don't know the exact estimation for $D_3(x)$. In this paper we find the actual formula for $D_3(x)$.

Main Theorem

$$D_3(x) = x(a_2 \log^2 x + a_1 \log x + a_0) + \mathrm{O}(x^{\frac{2}{3}} \log x)$$

where $a_2 = \frac{1}{2}$, $a_1 = 3\gamma - 1$, and $a_0 = 2\gamma^2 - 3\gamma - 5\gamma_1 + 1$ with γ_1 is the constant

$$\gamma_1 = \frac{1}{2}(1 - \log 2)\log 2 + \int_2^\infty \frac{(t - [t])(1 - \log t)}{t^2}\, dt.$$

We need the following results to prove the main Theorem.

Lemma 1: ([1], Theorem 3.1) (Euler's summation formula) If f has a continuous derivative f' on the interval $[y, x]$, where $0 < y < x$, then

$$\sum_{y<n\le x} f(n) = \int_y^x f(t)d(t) + \int_y^x (t - [t])f'(t)d(t) + f(x)([x] - x) - f(y)([y] - y).$$

Lemma 2: ([1], Theorem 3.2(a)) $\sum_{n \le x} \frac{1}{n} = \log x + \gamma + \mathrm{O}(x^{-1})$

Lemma 3: ([1], Theorem 3.2(b)) For $s > 0,\ s \ne 1$

$$\sum_{n \le x} \frac{1}{n^s} = \frac{x^{1-s}}{1 - s} + \zeta(s) + \mathrm{O}(x^{-s}) = \mathrm{O}(x^{1-s})$$

Lemma 4 : $\sum\limits_{n\le x} \dfrac{\log n}{n} = \dfrac{1}{2}\log^2 x + \gamma_1 + O(x^{-1}\log x)$

Proof : $\sum\limits_{n\le x} \dfrac{\log n}{n} = \dfrac{\log 2}{2} + \sum\limits_{2<n\le x} f(n)$ where $f(n) = \dfrac{\log n}{n}$ $(n \ge 2)$.

Using Lemma 1, we get

$$\sum_{n\le x} \frac{\log n}{n}$$

$$= \frac{\log 2}{2} + \int_2^x \frac{\log t}{t} + \int_2^x (t-[t])\left(\frac{t\,\frac{1}{t} - \log t}{t^2}\right)dt + \frac{\log x}{x}([x]-x) - f(2)([2]-2)$$

$$= \frac{1}{2}(1-\log 2)\log 2 + \frac{1}{2}\log^2 x + I_1 - I_2 + O(x^{-1}\log x)$$

where $I_1 = \int_2^\infty \dfrac{(t-[t])(1-\log t)}{t^2}\,dt$ and $I_2 = \int_x^\infty \dfrac{(t-[t])(1-\log t)}{t^2}\,dt$

Using $\log t = O(t^{\epsilon})$ for every $\epsilon > 0$, we get the integral I_1 is convergent and

$I_2 = O(\int_x^\infty f'(t)dt) = O(f(x)) = O(x^{-1}\log x)$

Hence

$$\sum_{n\le x} \frac{\log n}{n} = \frac{1}{2}\log^2 x + \gamma_1 + O(x^{-1}\log x)$$

Lemma 5:

$$\sum_{n\le x} \frac{d_2(n)}{n} = \frac{1}{2}\log^2 x + 2\gamma\log x - 4\gamma_1 + O(x^{-\frac{1}{2}}\log x)$$

Proof : We have

$$\sum_{n\le x} \frac{d_2(n)}{n} = \sum_{n\le x}\frac{1}{n}\left(\sum_{\substack{d,\delta\\ d\delta=n}} 1\right) = \sum_{\substack{d,\delta\\ d\delta\le x}} \frac{1}{d\delta} = 2\sum_{\substack{d,\delta\\ d\delta\le x\\ d\le\delta}} \frac{1}{d\delta} - \sum_{d\le\sqrt{x}} \frac{1}{d^2}$$

$$= 2 \sum_{d \leq \sqrt{x}} \frac{1}{d} \sum_{d \leq \delta \leq \frac{x}{d}} \frac{1}{\delta} - \sum_{d \leq \sqrt{x}} \frac{1}{d^2}$$

$$= 2 \sum_{d \leq \sqrt{x}} \frac{1}{d} \{ \sum_{\delta \leq \sqrt{x}} \frac{1}{\delta} - \sum_{\delta \leq d-1} \frac{1}{\delta} \} - \sum_{d \leq \sqrt{x}} \frac{1}{d^2}$$

Using Lemma 2 and Lemma 3, we obtain

$$\sum_{n \leq x} \frac{d_2(n)}{n} = 2 \log x \sum_{d \leq \sqrt{x}} \frac{1}{d} - 4 \sum_{d \leq \sqrt{x}} \frac{\log d}{d} + O(x^{-\frac{1}{2}})$$

Using Lemma 2 and Lemma 4, we get

$$\sum_{n \leq x} \frac{d_2(n)}{n} = \frac{1}{2} \log^2 x + 2\gamma \log x - 4\gamma_1 + O(x^{-\frac{1}{2}} \log x).$$

This proves the result.

Proof of the Main Theorem

We consider

$$D_3(x) = \sum_{\substack{\alpha_1, \alpha_2, \alpha_3 \\ \alpha_1 \alpha_2 \alpha_3 \leq x}} 1 = \sum_{\substack{m, n \\ mn \leq x}} d_2(n) = \sum_{m \leq x} \sum_{n \leq \frac{x}{m}} d_2(n)$$

$$\text{f} = \sum_{m \leq x^{\frac{1}{3}}} \sum_{n \leq \frac{x}{m}} d_2(n) + \sum_{x^{\frac{1}{3}} < m \leq x} \sum_{n \leq \frac{x}{m}} d_2(n)$$

$$= \sum_{m \leq x^{\frac{1}{3}}} \sum_{n \leq \frac{x}{m}} d_2(n) + \sum_{n \leq x^{1-\frac{1}{3}}} d_2(n) \sum_{x^{\frac{1}{3}} < m \leq \frac{x}{n}} 1$$

$$= \sum_{m \leq x^{\frac{1}{3}}} D_2\left(\frac{x}{m}\right) + \sum_{n \leq x^{\frac{2}{3}}} d_2(n) \{ \frac{x}{n} - x^{\frac{1}{3}} + O(1) \}$$

$$= \sum_{m \leq x^{\frac{1}{3}}} D_2\left(\frac{x}{m}\right) + x \sum_{n \leq x^{\frac{2}{3}}} \frac{d_2(n)}{n} - x^{\frac{1}{3}} D_2(x^{\frac{2}{3}}) + O(D_2(x^{\frac{2}{3}}))$$

Hence

$$(1)\ldots\ D_3(x) = \sum_{m \le x^{\frac{1}{3}}} D_2\left(\frac{x}{m}\right) + x \sum_{n \le x^{\frac{2}{3}}} \frac{d_2(n)}{n} - x^{\frac{1}{3}} D_2(x^{\frac{2}{3}}) + O(x^{\frac{2}{3}} \log x).$$

We consider

$$\sum_{m \le x^{\frac{1}{3}}} D_2\left(\frac{x}{m}\right)$$

$$= \sum_{m \le x^{\frac{1}{3}}} \left\{ \frac{x}{m} \log \frac{x}{m} + (2\gamma - 1) \frac{x}{m} + O\left(\sqrt{\frac{x}{m}}\right) \right\}$$

$$= x \log x \sum_{m \le x^{\frac{1}{3}}} \frac{1}{m} - x \sum_{m \le x^{\frac{1}{3}}} \frac{\log m}{m} + (2\gamma - 1)x \sum_{m \le x^{\frac{1}{3}}} \frac{1}{m} + O\left(\sqrt{x} \sum_{m \le x^{\frac{1}{3}}} \frac{1}{m^{\frac{1}{2}}}\right)$$

Using Lemma 2, Lemma 3 and Lemma 4 we get

$$(2)\ldots \sum_{m \le x^{\frac{1}{3}}} D_2\left(\frac{x}{m}\right) = \frac{5}{18} x \log^2 x + \frac{(5\gamma - 1)}{3} x \log x + (2\gamma^2 - \gamma - \gamma_1)x + O(x^{\frac{2}{3}} \log x)$$

Using Lemma 5, we obtain

$$(3)\ldots\ x \sum_{n \le x^{\frac{2}{3}}} \frac{d_2(n)}{n} = \frac{2}{9} x \log^2 x + \frac{4\gamma}{3} x \log x - 4\gamma_1 x + O(x^{\frac{2}{3}} \log x).$$

Finally,

$$(4)\ldots\ x^{\frac{1}{3}} D_2(x^{\frac{2}{3}}) = \frac{2}{3} x \log x + (2\gamma - 1)x + O(x^{\frac{2}{3}}).$$

Using (2), (3) and (4) in (1), we obtain the result.

References

[1] Apostol Tom M., *Introduction to Analytic Number Theory*, Springer-Verlag, New-York, Heidelberg, Berlin, 1976.

[2] Titchmarsh E.C. ,*The Theory of Riemann Zeta Function*, Oxford University Press, 951 (Reprint 1976).

'Prajna' - Jounal of Pure & Applied Sciences, 14 (2006) 99-103

REGULAR AEROBIC EXERCISE : A SIMPLE , EASY & AN AFFORDABLE TOOL FOR A HEALTHY HEART

Wasim A. Shaikh
Dept. of Physiology , Pramukhswami Medical College,
HM Patel Centre for Medical Care & Education , Karamsad – 388325.

Abstract

Exercise is one of the non-pharmacological methods prescribed in the management and prevention of Coronary Artery Disease (CAD) along with dietary modifications. The role of exercise in the control of CAD has been investigated by many researchers and they have found various beneficial effects of exercise.This review article aims to highlight the major beneficial effects of regular aerobic exercise on the cardiovascular system which help in preventing and managing CAD .

Introduction

The World Health Organisation has reported a tremendous rise in the prevalence of Cardiovascular Diseases mainly Coronary Artery Diseases (CAD) all over the world and especially in developing nations like India. In the year 2002 , 16.7 million deaths across the world were due to Cardiovascular diseases mainly CAD which was more than 50 % of the total deaths (32 million) during the year. An alarming fact which has come up is the early age of onset of CAD in India and that when it is diagnosed it is in the advanced stages due to delay in presentation by the patients [1] .

Coronary Artery Disease is a disease where there is a decreased oxygenation to the Heart due to Ischaemia.(decrease in blood supply). It occurs due to narrowing of the lumen of the Coronary arteries (arteries supplying blood to the heart) mainly because of deposition of lipids (fats) on the inner wall of arteries surrounding the lumen of artery thereby decreasing the blood flow and oxygenation to the part supplied by the artery. Patients of CAD suffer from either Angina (Chest Pain of Cardiac Ischaemia) or Myocardial Infarction (Heart Attack, death of a part or whole of heart tissue) or Heart Failure.The major causes of CAD are Tobacco use (Smoking) ,Physical Inactivity and Inappropriate Diet (Increase Consumption of Saturated Fats) [2] .

This article intends to highlight the role of Regular Aerobic exercise for prevention and control of CAD and associated risk factors like Hypertension , Obesity and Diabetes Mellitus .

Aerobic Exercise and Its Recommended Requirement

A physical exercise in which most of the energy comes from the breakdown of energy sources (i.e., fat and glycogen) in the presence of oxygen is called an Aerobic Exercise.

These are the exercises which involve isotonic form of muscle contractions (movement occurs at a joint) for a duration of atleast 20 minutes continiously like Walking , Running , Jogging , Swimming and Cycling [3] . To make an aerobic exercise fruitful for the heart , it should be performed regularly at moderate intensity. It is recommended by the American Heart Association and American College of Sports Medicine to do aerobic exercise involving large group of muscles like Brisk Walking , Swimming or cycling for atleast 30 minutes per session per day with atleast 3 to 6 such sessions in a week. The exercise should be performed at moderate intensity of 60 % to 75 % of Maximum Heart Rate (MHR) for age as predicted by the formula, MHR = 220 – Age in years . It is also recommended to start slowly and gradually increase the duration ,frequency and intensity of exercise so that the body can adapt to the exercise stress and this would also help the individual to incorporate exercise as a routine habit by making the exercise session comfortable [4,5] .

Brisk Walking at 60 % to 75 % MHR is a simple , easy and affordable means of Aerobic exercise as it does not require any specific instruments , place or training . Brisk walking involves to and fro movements of upper limbs at the shoulder joint along with the movements of lower limbs . It is an exercise which only requires fresh air and an even surface which are not very difficult to find . This exercise has minimal risks involved in terms of injury as compared to other common forms of aerobic exercise like Jogging , Cycling and Swimming.

Beneficial Effects of Regular Aerobic Exercise on the Cardiovascular System

A Large amount of research has been done in the western part of the world to know the effects of regular aerobic exercise on the cardiovascular system and the major effects have been discussed below .

1. Aerobic exercise when performed regularly increases the maximum oxygen utilizing capacity (Aerobic Capacity, VO2max) of the cardiac as well as skeletal muscles by causing muscular hypertrophy . This increases the ability of a person to perform aerobic work for a longer duration and at higher intensity without increasing the load on the cardiovascular system . The aerobic capacity increases due to Angiogenesis (an increase in the capillary density) and increase in the number of mitochondrias , oxidative enzymes and glycogen stores in the muscles. [6,7,8] .

2. Aerobic exercise decreases the blood pressure with an average fall of 10mmHg and about 7.5 mmHg in systolic blood pressure and diastolic blood pressure respectively.The fall in blood pressure remains for 8 to 12 hours after the exercise session and thereby decreases the risk of developing CAD [9] .

3. Studies have shown that regular aerobic exercise improves the Dyslipidaemia ,a major risk factor associated with CAD . It has been observed that aerobic exercise increases the blood level of High Density Lipoproteins (HDL, Heart Friendly) by 5 % and reduces the blood level of Total Cholesterol by 6.3 % , Low Density Lipoproteins (LDL, Heart Enemy) by 10.1 % and TC/ HDL ratio by 13.4 %[10].
4. Aerobic exercise also improves the Insulin Sensitivity and thereby improves the utilization of glucose at rest and shifts the lipid profile towards a healthy side [11].
5. Studies have demonstrated a decrease in the Fibrinogen level and Plasminogen Activator Inhibitor level in blood with an increase in action of Tissue Plasminogen Activator thus decreasing the risk of development of intravascular thrombus , arterial occlusion and ischaemia [7, 12] .
6. Regular aerobic exercise has also shown to decrease the sympathetic tone on the heart and level of catecholamines in the blood with a consequent decrease risk of Arrythmias (Irregular Heart beat Rhythm) [8, 13].
7. The endothelial function of the coronaries also improves with release of vasodilatory substances like Nitric Oxide (NO) which decreases the risk of cardiac ischaemia [14,15] .
8. Regular aerobic exercise controls and prevents the development of Obesity and related disorders thereby preventing CAD [16] .

Conclusion

It is indicated by the results of various studies that regular aerobic exercise has many beneficial effects in the prevention and management of Coronary Artery Disease and therefore people should be encouraged to incorporate aerobic exercise as a part of their lifestyle to prevent CAD.

Acknowledgement

I would like to acknowledge my teacher Dr.SK Singh , Professor and Head of Physiology Department at Pramukhswami Medical College, Karamsad who has been the motivating force for me and who guided me in writing this review article.

I am also grateful to Pramukhswami Medical College , HM Patel Centre for Medical Care & Education at Karamsad which gave me the opportunity to write this review article by providing research facilities ,library services and 24 hour internet services.

References

[1] WHO REPORT 2003.Chapter 6: Neglected Global Epidemics: three growing threats.

[2] Magnus P, Beaglehole R. The real contribution of the major risk factors to the coronary epidemics: time to end the "Only-50%" myth. *Archives of Internal Medicine*, 2001, 161:2657—2660;

[3] Guyton AC , Hall JE . Textbook of Medical Physiology. 9th edition.Bangalore: Prism; 1996.

[4] American College of Sports Medicine Position Stand: the recommended quantity and quality of exercise for developing and maintaining cardiorespiratory and muscular fitness, and flexibility in healthy adults. *Med Sci Sports Exerc.* . 1998; 30: 975–991.

[5] Fletcher G F et al . Exercise Standards for Testing and Training . A Statement for Healthcare Professionals From the American Heart Association. *Circulation.* 2001;104:1694

[6] Leon AS, Richardson M. Exercise, health, and disease. In: Roberts SO, Robergs RA, Hanson P, eds. Clinical Exercise Testing and Prescription: Theory and Application. Boca Raton, Fla: CRC Press; 1997: 281–302.

[7] Squires RW. Mechanisms by which exercise training may improve the clinical status of cardiac patients. In: Pollock ML, Schmidt DH, eds. Heart Disease and Rehabilitation, 3rd ed. Champaign, Ill: Human Kinetics; 1995: 147–160.

[8] Haskell WL. Sedentary lifestyle as a risk factor for coronary heart disease. In: Pearson TA, ed. Primer in Preventive Cardiology. Dallas, Tex: American Heart Association; 1994: 173–187.

[9] Blair SN, Goodyear NN, Gibbons LW, et al. Physical fitness and incidence of hypertension in healthy normotensive men and women. *JAMA.* . 1984; 252: 487–490.

[10] Tran ZV, Weltman A. Differential effects of exercise on serum lipid and lipoprotein levels seen with changes in body weight: a meta-analysis. *JAMA.* . 1985; 254: 919–924.

[11] Wasserman DH, Zinman B. Fuel homeostasis. In: Ruderman N, Devlin JT, eds. The Health Professional's Guide to Diabetes and Exercise. Alexandria, Va: American Diabetes Association; 1995; 29–47.

[12] Stratton JR, Chandler WL, Schwartz RS, et al. Effects of physical conditioning on

fibrinolytic variables and fibrinogen in young and old healthy adults. *Circulation.* . 1991; 83: 1692–1697.

[13] Leon AS, Connett J, Jacobs DR, Jr et al. Leisure-time physical activity levels and risk of coronary heart disease and death: the Multiple Risk Factor Intervention Trial. *JAMA.* . 1987; 258: 2388–2395.

[14] Miller VM, Vanhoutte PM. Enhanced release of endothelium-derived factor(s) by chronic increases in blood flow. *Am J Physiol.* . 1988; 255: H446–H451.

[15] Hambrecht R, Wolf A, Gielen S, et al. Effect of exercise on coronary endothelial function in patients with coronary artery disease. *N Engl J Med.* . 2000; 342: 454–460.

[16] Blair SN. Evidence for success of exercise in weight loss and control. *Ann Intern Med.* . 1993; 119: 702–706.

'Prajna' - Jounal of Pure & Applied Sciences, 14 (2006) 104-107

PERFORMANCE EVALUATION OF MoSe$_2$ PEC SOLAR CELLS

Deepa Makhija[1], **R. J. Pathak**[*], **K. D. Patel, V. M. Pathak and R. Srivastava**
Department of Physics, Sardar Patel University, Vallabh Vidyanagar – 388120. Gujarat
[*]R.R. Mehta College of Science,Palanpur-385001(Gujarat)
[1]E-mail: makhija_deepu@yahoo.com

Abstract

MoSe$_2$, a member of group VI transition metal chalcogenides possesses energy gap close to the maxima of incident solar radiation and it is highly stable against photocorrosion and photodecomposition due to d→d transition of the carriers. The present paper contains the findings based on the studies of variation of the short circuit current and open circuit voltage of MoSe$_2$/I$_2$/ I$^-$/Pt PEC solar cells with incident intensity of polychromatic light and the results have been discussed.

Introduction

Recent years have seen a spurt in the activities on layered transition metal dichalcogenides (TMDCs) because the electrical and other physical properties of these compounds exhibit a vast range of variation. MoSe$_2$ is one of a member of these compounds, which form a layered structure. The basic structure of loosely coupled Se-Mo-Se sheets makes these compounds extremely interesting. Within a layer, the bonds are strong while adjacent layers they are extremely weak and this leads to an anisotropic nature [1]. MoSe$_2$ has a considerable attention because of its attractive thermoelectrical and antifriction characteristics [2]. Since Tributsch [3,4] reported 1% efficiency of MoSe$_2$ /Fe^{2+}/Fe^{3+}/Pt PEC solar cell in 1977, a lot of work has been carried out on PEC solar cells. In the present investigations, the variation of the short circuit current and the open circuit voltage of MoSe$_2$ based PEC solar cells obtained at different intensities.

Experimental

A glass rod having external diameter around 0.5 cm and around 10 cm in length having fine bore has been used to prepare the semiconductor electrode of a PEC solar cell. One end of the glass rod was flattened and used as the base for mounting the crystals of MoSe$_2$ grown by vapour transport method. The connecting copper wire (27 SWG) was passed through the narrow bore and flattened at one end for providing larger area of the ohmic contact obtained using conducting silver paste between the wire and the crystal. The edges of the crystals were covered with an insulating epoxy to avoid any kind of contact between the back contact and the electrolyte. The so prepared electrode was used as photoelectrode along with Iodine/Iodide electrolyte (0.025MI$_2$+2M NaI + 0.5M Na$_2$So$_4$ + 0.5M H$_2$So$_4$) and platinum counter electrode to form the PEC solar cell. The intensity of incident illumination was measured using optical power meter (Graseby, model no. 371, USA). The photovoltage and photocurrent of such cell have been measured using a digital multimeter (Protek, model no. 506, India) and the electrometer (Keithley, model no. 614, USA) respectively with the respective accuracies of 0.1mV and 0.01µA. The series combination of various variable resistances of different values has been used to vary the photovoltage and photocurrent in the external circuit.

Results and Discussion

The performance of photovoltaic or PEC solar cells can be characterized by the parameters like fill factor, flat band potential, open circuit voltage, short circuit current etc. The photoconversion characteristics of $MoSe_2/I_2/I^-$/Pt PEC solar cells have been investigated under polychromatic illumination of different intensities, which show low photoconversion efficiencies. The variation of the short circuit current and the open circuit voltage of $MoSe_2$ based PEC solar cells as obtained at different intensities have been shown in figure 1 and 2. From these figures, it is quite clear that the short circuit current linearly increases with increase in the input intensity. The increase in the short circuit current is linear upto around 90mW/cm^2. Above this the non-linear behaviour is observed.

The absorption of photons by the semiconducting material leads to the generation of electron-hole pairs in the semiconductor. In n-type semiconductor, the holes being the minority carriers take part in the oxidation process at the semiconductor- electrolyte interface. The linear nature of the $I_{sc} \rightarrow I_L$ in figure 1 upto I_L= 90mW/cm^2 clearly indicate the fact that almost all the photogenerated holes take part in the oxidation process at the $MoSe_2/I_2/I^-$ electrode. Above 90mW/cm^2 intensity of incident polychromatic illumination, the rate of oxidation decreases with increasing intensity, which results into the non-linear increase in the value of short circuit current with increasing intensity. The photocurrent depends on two basic process occurring within a PEC solar cell. (1) the photogeneration of carriers and their efficient transport within the semiconducting material and (2) the electrochemical kinetics, which include the oxidation/reduction process occurring at the two electrodes.

The variation of photocurrent with intensity of light shows a linear or a non-linear behaviour depending upon the rates of these two reactions. If the oxidation/reduction process is faster and more efficient than the photogeneration of carriers within the semiconductor, all the photogenerated carriers reaching the interface take part in the oxidation/reduction process with the ionic species. This indicates that all the photogenerated carriers are being absorbed by the ionic species, which results into a linear increase in the photocurrent as the intensity of illumination increases. But, if the oxidation /reduction process does not respond to the number of photogenerated carriers, the photocurrent in the output circuit shows a non-linear dependence on the intensity of incident illumination.

In the present investigation, the short circuit current starts saturating above I_L = 90mW/cm^2, which is an indication of the fact that the electrochemical kinetics at the semiconductor - electrolyte interface start dominating the overall charge transport process across the interface. According to Kline et.al [5] and Bicelli et al. [6], the observed deviation from linearity can also be attributed to the presence of recombination centers within the semiconducting materials. The recombination centers associated with the semiconducting material having surface steps result in a low quantum yield [7,8,9,] at low densities and limit the photocurrent at higher intensities of light. Also, the bulk and space charge layer recombination are the mechanisms, which accounts for the deviations from linearity at higher intensities [9]. Thus, it can be inferred that linear region of these characteristics is preferable for better photoconversion characteristics of such cells.

Similar results have been obtained when the variation of open circuit voltage with the intensity of incident illumination is investigated. Here also, it can be seen that above around 70mW/cm^2 intensity of incident illumination, the open circuit voltage starts deviating from the normal linear behaviour. These results re-affirm the domination of electrochemical kinetics in the photoconversion characteristics in present case at higher intensities.

References

1. Wilson J.A. and Yoffe A.D., Adv.Phys. **18**,193 (1969)
2. Kalikhman, V.L., Kasiyan,Mikhailyak I.M: Sov.Powder Metall. And Met. Veram. (USA) **12,** 922 (1973)
3. Tributsch H., Z. Naturforch, **A32,** 972 (1977),
4. Tributsch H., Ber. Bunsenger. *Phys. Chem.*, **81,** 361 (1977)
5. Kline G., Kam K.K.and Zeigler R., Solar Energy Mater., **6,** 337 (1982)
6. Bicelli L.P., Pederferri P.and Razzni G., Hydrogen Energy Process, **5,** 1055 (1980)
7. Tributsch H., Solar Energy Mater., **1,** 257 (1979)
8. Lewerenz H.J, Heller A. and Disalvo F.J., J.Amer. Chem. Soc., **102,** 1877 (1980)
9. Frautak T.E, Canceled D.and Parkinson B.A., J.Appl. Phys. **51,** 6018 (1980)

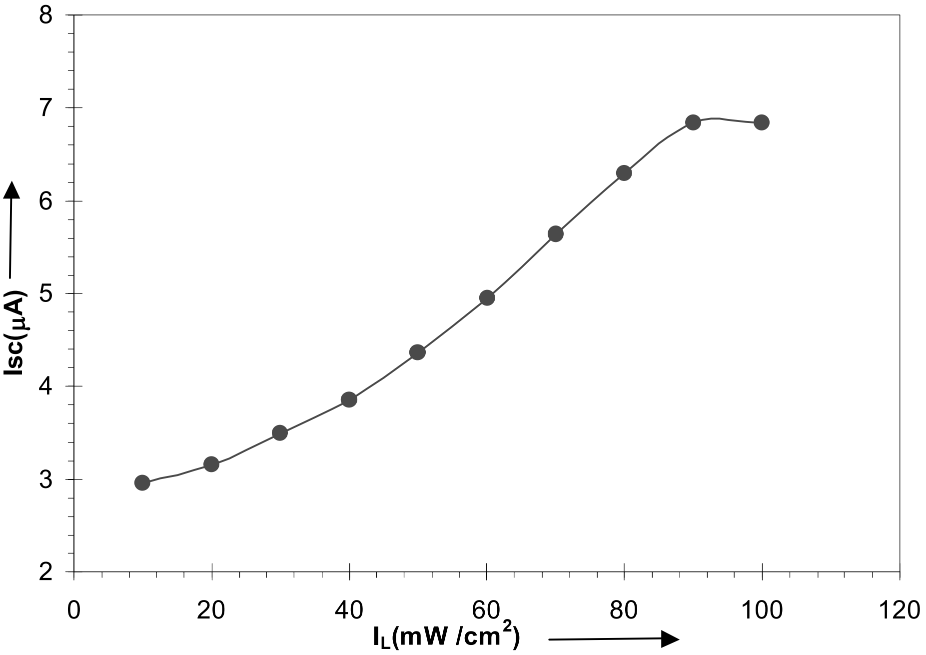

Fig.1: Variation of short circuit current (Isc) with intensity of illumination I_L

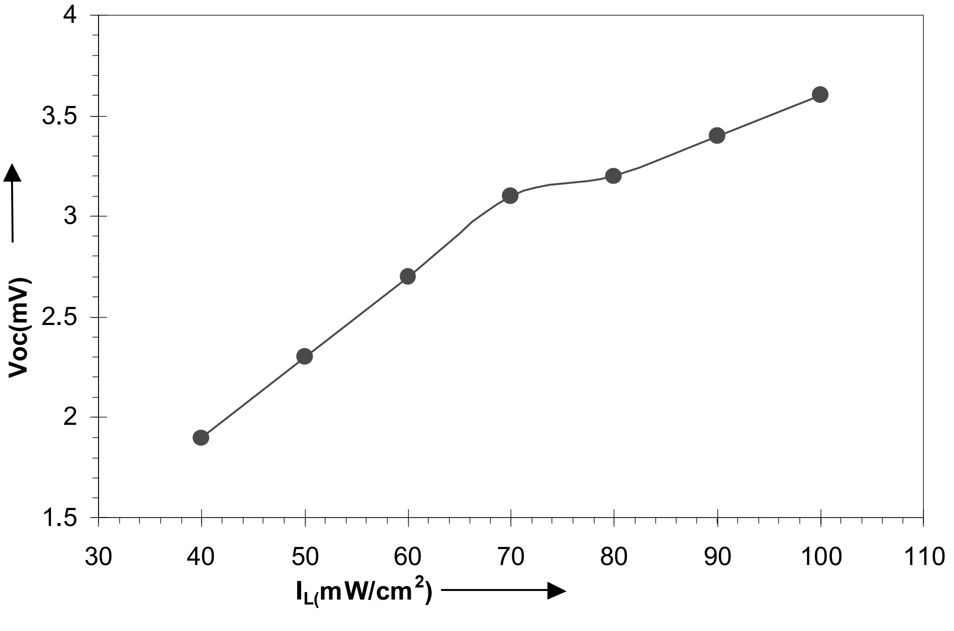

Fig. 2 : Variation of open circuit voltage with the intensity of illumination in case of $MoSe_2$ / I_2 / I^- / Pt PEC solar cells

'Prajna' - Jounal of Pure & Applied Sciences, 14 (2006) 108-116

VARIABLE PHASE CALCULATIONS ON e-H_2 AND e-CO SCATTERING PROCESSES

Sumona Gangopadhyay, P. C. Vinodkumar and K. N. Joshipura
Department of Physics, Sardar Patel University, Vallabh Vidyanagar-388 120, Gujarat
E-mail: knjoshipura@yahoo.com

Abstract

Various scattering cross sections have been calculated for the impact of electrons on H_2 and CO molecules in the energy range 20-2000 eV. We have considered two theoretical approaches viz., the asymptotic phase shift method and the variable phase method and both the results are found to be consistent. The well-known complex potential formalism is employed to these systems to determine total elastic (Q_{el}) and total cumulative electronically inelastic (Q_{inel}) cross sections. From the total inelastic cross section, the ionization cross section has been extracted using the complex scattering potential – ionization contribution (CSP-ic) method. Adequate comparisons have been made with other experimental and theoretical data.

Introduction

There are several fields of physics (astrophysics, plasma physics, ionospheric physics) and technological fields, which require the accurate knowledge of the electron–atom (and molecule) total cross sections (TCS). The e-H_2 scattering is particularly interesting because it deals with the simplest electron-molecule system. H_2 and CO being the most abundant astrophysical molecules, play a vital role in various outer space environments and hence have been chosen for the present study. The intermediate and high energy electron impact calculations on the total cross sections for H_2 and CO molecules have been done by Jain and Baluja [1], who have employed a simple approach based on the spherical-complex-optical potential (SCOP) of the given electron-target system. Some semi-empirical calculations were carried out on the TCS e-H_2 scattering at 20-2000 eV by other workers as mentioned by Zecca *et al.* [2] in their review paper. Measurements of TCS have been done for e-CO scattering by Kwan *et al* [3] and for e- H_2 by Hoffman *et al.* [4] at low and intermediate energies.

In this work we have calculated basically the electron impact TCS Q_T, total inelastic cross sections Q_{inel} and the total elastic cross sections Q_{el} for the above molecules at the incident energies (E_i) from ionization threshold (~10 eV) to 2000 eV. We have employed the Variable Phase Approach (VPA) of Calogero as discussed in [5], this has been used previously by [1] but our present calculations differ from [1] in three major aspects. Firstly, we calculate the relevant quantities not only in VPA but also in the asymptotic phase shift method. Secondly, our model of the absorption potential is an improved version of the one used earlier [1]. And finally we have extended the calculations to obtain total ionization cross sections Q_{ion}, and this is a new feature of the present approach. In the SCOP formulation the total (complete) cross section of electron-molecule scattering is made up of two terms as follows.

$$Q_T(E_i) = Q_{el}(E_i) + Q_{inel}(E_i) \tag{1}$$

Here Q_{el} is the total elastic cross section and Q_{inel} is the total inelastic cross section. We note two important points here. First of all Q_{inel} cannot be measured directly and secondly since our potentials are spherical the cross section Q_T does not include the effects of rotational-vibrational excitations due to non-spherical potentials. In the present case of H_2 and CO these effects are relatively small and they can be included in a simple way by defining the grand total cross section as under,

$$Q_{TOT}(E_i) = Q_T(E_i) + Q_{NS}(E_i) \tag{2}$$

where Q_{NS} stands for the TCS of the non-spherical interactions.

In recent years, we [6,7] have developed and successfully employed a semi-empirical approach called 'complex scattering potential-ionization contribution' (CSP-ic) method for determining the total ionization cross section Q_{ion} from Q_{inel}. Presently we have followed this approach and deduced the total ionization cross sections for H_2 and CO molecules. Adequate comparisons of our results have been made in this paper.

Theoretical Models And Calculations

Our calculations of all these TCSs are based on a complex scattering potential, generated from spherically averaged charge densities of the target molecules. For H_2 the molecular charge density is obtained by starting with the atomic orbital of the form $e^{-ër}/r$ with ë =2*Z and the variational parameter Z=1.2005. For CO molecule, the single center molecular charge density is obtained by a linear combination of constituent atomic charge densities, renormalized to account for covalent molecular bonding. This molecular charge density is employed to construct a complex (optical) potential, namely,

$$V_{opt}(r) = V_R(r) + iV_{abs}(r) \tag{3}$$

Where the real part is the sum of three terms namely the static, exchange and the polarization potentials i.e.,

$$V_R(r) = V_{st}(r) + V_{ex}(r) + V_{pol}(r) \tag{4}$$

The absorption potential accounts for the total loss of scattered flux into all allowed channels of electronic excitation and ionization. A currently popular model form of V_{abs} is that of [8], who proposed quasi-free, Pauli-blocking, dynamic absorption potential given in au, as

$$V_{abs}(r,E_i) = -\tfrac{1}{2}\rho(r)v_{loc}\sigma_{ee}$$

$$= \rho(r)(\tfrac{T_{loc}}{2})^{1/2}\cdot(\tfrac{8\pi}{10k_F^3E_i})\cdot\theta(p^2-k_F^2-2\Delta)\cdot(A_1+A_2+A_3) \quad (5)$$

In these expressions, ν_{loc} is the local speed of the external electron, and σ_{ee} denotes the average total cross section of the binary collision of the external electron with a target electron. The local kinetic energy of the incident electron is obtained from

$$T_{loc} = E_i - V_R = E_i - (V_{st} + V_{ex} + V_{pol}) \quad (6)$$

For a given energy, the dominant term in equation (6) is V_{st}. Further $p^2 = 2E_i$ in au, $k_F = [3\pi^2\rho(r)]^{1/3}$ is the Fermi wave vector and Δ is an energy parameter. In equation (5), $\theta(x)$ is the Heaviside unit step function, such that $\theta(x) = 1$ for $x>0$, and is zero otherwise. The dynamic functions A_1, A_2 and A_3 defined in [8] depend differently on the molecular properties ρ, Δ and E_i. Full details of the V_{abs} potential in the present context of molecules are discussed in [6,7].

After generating the full complex potential equation (3) of a given electron-molecule system, we treat it exactly in a partial wave analysis by solving the following set of first order differential equations for the real (δ_R) and imaginary (δ_I) parts of the complex phase shift function under the (VPA) as explained in [5].

$$\delta'_R(kr) = -\tfrac{2}{k}[V_R(r)\cdot(X^2-Y^2) + 2V_{abs}(r)\cdot XY] \quad (7)$$

$$\delta'_I(kr) = -\tfrac{2}{k}[-2V_R(r)\cdot XY + V_{abs}(r)\cdot(X^2-Y^2)] \quad (8)$$

where

$$\begin{aligned} X &= \cosh\delta_I(kr)[\cos\delta_R(kr)\cdot j_l(kr) - \sin\delta_R(kr)\cdot\eta_l(kr)] \\ Y &= \sinh\delta_I(kr)[\sin\delta_R(kr)\cdot j_l(kr) + \cos\delta_R(kr)\cdot\eta_l(kr)] \end{aligned} \quad (9)$$

and $j_l(kr)$ and $\eta_l(kr)$ are the usual Riccati-Bessel functions [5]. The above equations are integrated up to a sufficiently large r depending on *l* and k values. Thus the final S- matrix is written as

$$S_l(k) = \exp(-2\delta_I)\exp(i2\delta_R) \tag{10}$$

The integrated elastic (Q_{el}), inelastic (Q_{inel}) and total (Q_T) cross sections are described in terms of the S- matrix as follows:

$$Q_{el} = \tfrac{\pi}{k^2}\sum_{l=0}^{l_{\max}}(2l+1)\,|\,1 - S_l(k)\,|^2 \tag{11}$$

$$Q_{inel} = \tfrac{\pi}{k^2}\sum_{l=0}^{l_{\max}}(2l+1)[1-|\,S_l\,(k)\,|^2\,] \tag{12}$$

$$Q_T = \tfrac{2\pi}{k^2}\sum_{l=0}^{l_{\max}}(2l+1)[1 - \mathrm{Re}\,S_l(k)] \tag{13}$$

In order to solve coupled differential equations (7) and (8), we need a large number of partial waves in the present intermediate and high-energy regions. The value of $l_{\max}$ was varied from 20 to 300, depending upon the impact energy.

Now in order to deduce total ionization cross-section from total inelastic cross section the above results must be extended suitably. Therefore in the CSP-ic method we introduce the following ratio function.

$$R(E_i) = \frac{Q_{ion}(E_i)}{Q_{inel}(E_i)} \tag{14}$$

Such that, $0 \leq R\,(Ei) \lesssim$ _ This ratio is expressed as a continuous function of energy and the required Q_{ion} are obtained as discussed in our recent papers [6, 7].

Results Discussion And Conclusions

In this paper, we have calculated total inelastic cross sections (Q_{inel}), total elastic cross sections (Q_{el}) and the total cross sections (Q_T) from our models for the molecular potentials. The coupled differential equations (7) and (8) were solved by the standard fourth order RK-method, and asymptotic phase shifts were also determined by solving the radial Shroedinger equation under appropriate boundary condition, with the help of the Numerov method. We have then extracted the ionization cross sections (Q_{ion}) from the total inelastic cross sections (Q_{inel}), as in [6,7]. Our results are exhibited comprehensively in figures 1 to 4. Let us note that the contributions of rotational-vibrational excitations are included here at low energies below 20 eV [2], so that the total cross sections are actually Q_{TOT} as per our equation (2).

In figure 1, we have plotted total scattering cross sections versus E_i from 10 to 2000 eV for H_2 molecule. The previous data by [1] and [4] are in good agreement with our presently calculated Q_{el} and Q_T. For e-H_2 collisions, experimental ionization cross- section data are available from Straub *et al.* [9] and Rapp and Englander [10]. For H_2 molecule the ratio R is about 0.75 in the peak region and about 1.0 above 1000 eV. And we see that our presently calculated ionization cross sections Q_{ion} are in good agreement with the experimental data and also with the previous theoretical obtained data (Kim *et al.* [11]). The lower curves describe how Q_{inel} approaches Q_{ion} at large energies.

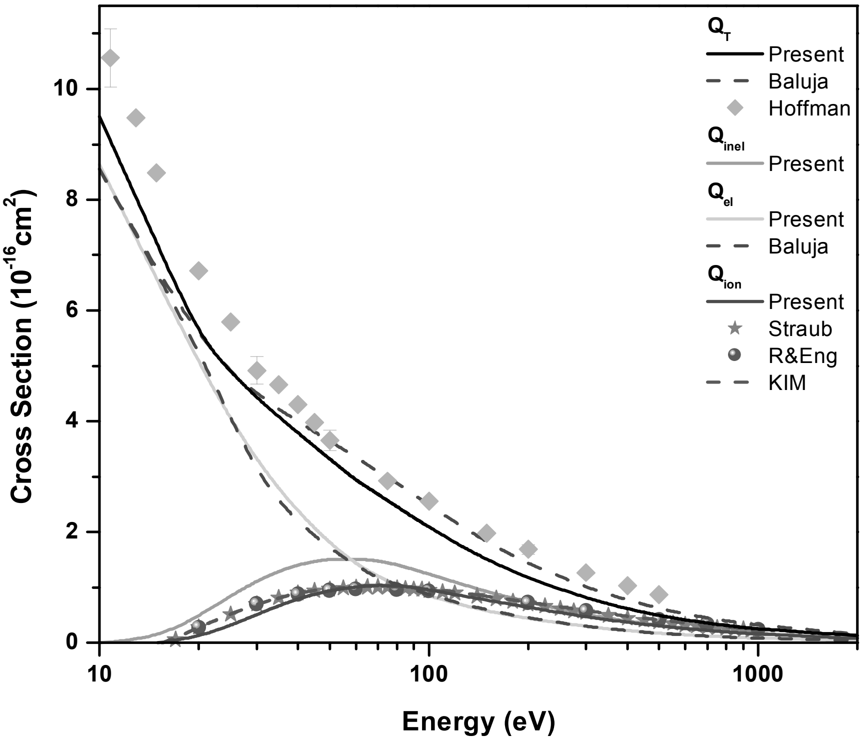

Figure 1 Total Cross sections for e-H_2 at various energies.

We find from the present calculations that the SCOP along with CSP-ic method is a useful theoretical tool to determine all the major total cross sections within the framework of a common general formulation. This is evident from our figure 2, which shows the relative contribution of different scattering processes.

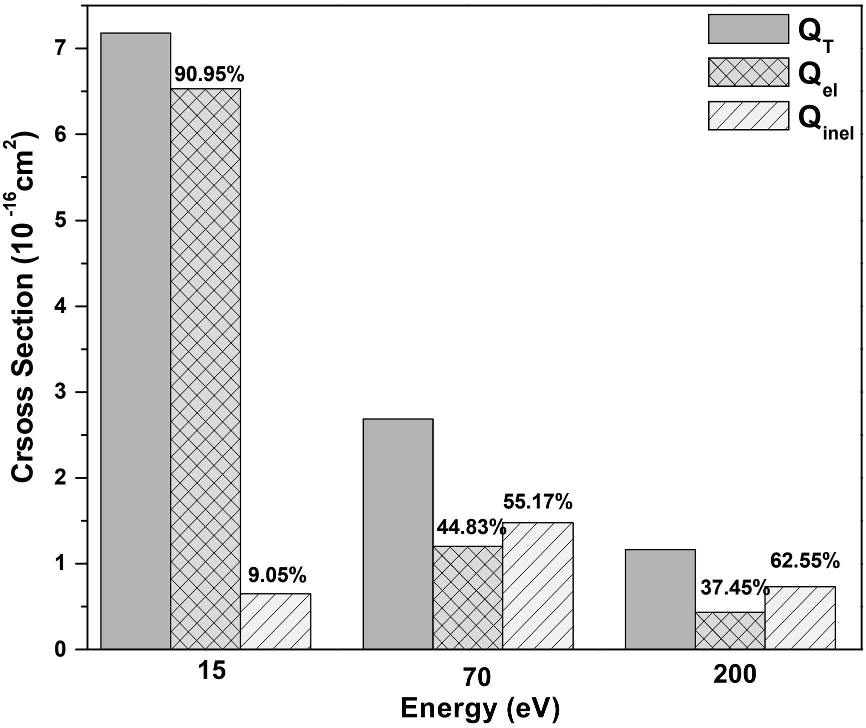

Figure 2 Relative contributions in e-H_2 scattering

A bar chart showing the relative importance of different scattering channels in H_2 molecule at different incident energies is given in figure 2. The cross section of vibrational and rotational excitations is very small beyond 15 eV. Here the energies have been chosen to be at the ionization threshold (15 eV), at the peak of the ionization cross-section (70 eV) and at far away from the peak (2000 eV).

In figure 3, we have plotted Q_T, Q_{el}, Q_{inel} and Q_{ion}, versus incident energy from 10 eV to 2000 eV for CO molecule. The present Q_T in CO shows a peak in the lower energy region. Qualitatively it is a good result, but the lack in accuracy is because of the model potentials, which are not good at lower energies.

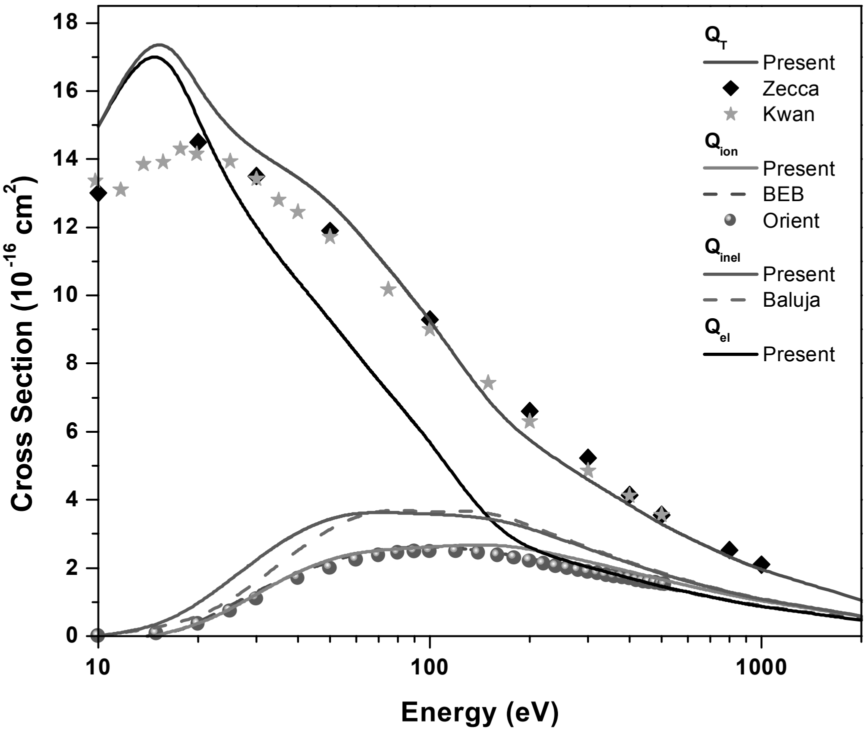

Figure 3 Total Cross sections for e-CO at various energies.

For e-CO collisions, experimental ionization data are available from Orient *et al.* [12] and Rapp and Englander [10]. The ratio R is about 0.75 at the peak region and nearly 1.0 above 1000 eV. And we see that our presently calculated ionization cross sections are in very good agreement with the experimental data [10, 12] and theoretical data of Kim *et al.* [13]. Further, a bar chart showing the relative importance of different scattering channels in CO molecule at different incident energies is given in figure 4. We find that in both the targets Q_{el} and Q_{inel} are almost equal near ionization peak.

In conclusion the present paper investigates an almost complete picture of various scattering and energy loss processes exhibited by H_2 and CO molecules bombarded with electrons of intermediate to high energies. The analysis presented through the bar-charts i.e. figures 2 and 4 have not been carried out so far in any of the earlier investigations, chiefly because the different TCS were earlier determined either through different measurements or through different theoretical methods. The present approach has the advantage of yielding several different TCSs under the same theoretical umbrella. It will be useful and interesting to extend this analysis to other important atomic and molecular targets.

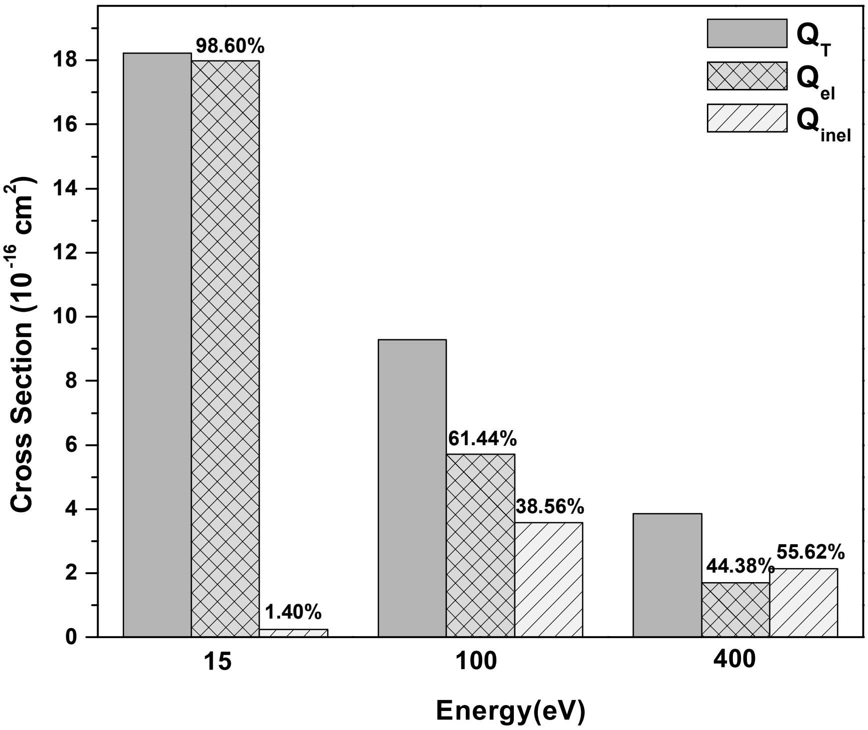

Figure 4 Relative contributions in e-CO scattering

Aknowledgement

The authors acknowledge with thanks the financial support from Indian Space Research Organization (ISRO, Bangalore), through a major research project under the *Respond* program.

References

[1] Jain A. and Baluja K. L., Phys. Rev. **A 45** (1992) 202

[2] Zecca A., Karwasz G. P. and Brusa R. S., *La Rivista Del Nuovo Cimento*, **19,** (1996) 1

[3] Kwan Ch. K., Hsieh Y-F. , Kauppila E., Smith S. J., Stein T. S. and Uddin M. N., Phys. Rev. **A 27** (1983) 1328

[4] Hoffman K. R., Dabaneh M. S., Hsieh Y-F. , Kauppila W. E., Pol V., Smart J. H. and Stein T.S., Phys. Rev. **A 25** (1982) 1393

[5] Calogero F., *Variable Phase Approach to Potential Scattering* (Academic, New York, 1974)

[6] Joshipura K. N., Vinodkumar Minaxi, Limbachiya C.G. and Antony B. K., Phys. Rev. **A 69** (2004) 022705

[7] Vinodkumar M., Joshipura K. N., Limbachiya C.G. and Antony B.K., Eur. Phys. J. **D 37** (2006) 67

[8] Staszewska G., Schwenke D. M. and Truhlar D. G., J. Chem. Phys. **81** (1984) 3078.

[9] Straub H. C., Penaull P., Lindsay B. G., Smith K. A. and Stebbing R. F., Phys. Rev. **A 54** (1996) 2146

[10] Rapp D. and Englander-Golden P., J. Chem. Phys. **43** (1965) 1464

[11] Kim Y-K. and Rudd M. E., Phys. Rev. **A 50** (1994) 3954

[12] Orient O. J. and Srivastava S. K., J Phys. **B 20** (1987) 3923

[13] Hwang W., Kim Y-K. and Rudd M. E., J. Chem. Phys. **104** (1996) 2956

'Prajna' - Jounal of Pure & Applied Sciences, 14 (2006) 117-128

INFRARED SPECTROSCOPY OF THE IODINE INCLUSION COMPOUNDS OF THREE (α, β and γ) – CYCLODEXTRINS

Mukesh Patel, Mehul Dave, K. R. Patel, S. G. Patel and A.T. Oza

Department of Physics, Sardar Patel University, Vallabh Vidyanagar – 388 120 Gujarat, India

Abstract

Study of infrared spectra of α-cyclodextrin, β-cyclodextrin, and γ-cyclodextrin with KI-I_2 (i.e. I_3^- ions) reveals changes in the spectra of three cyclodextrins in the range 400-1800 cm^{-1}. New bands in the C-O-C stretching range are caused by charge transfer interaction of iodine with oxygen atoms. Other changes in the spectra are ascribed to hydrogen bonding between water molecules and cyclodextrins, water of crystallization, structural effects and the interaction of iodine atoms with the hydrocarbon linings of cyclodextrin molecules.

Introduction

The physical (mainly structural, electrical and optical) properties of the inclusion compounds of iodine are subject of recent interest [1-2]. Earlier work has been summarized and referred elsewhere [3-15]. Long ago the infrared absorption spectra of amylose, poly (vinyl alcohol) and their iodine complexes were reported [16-18]. The properties of three cyclodextrins (α,β, and γ) are summarized in table 1 [19-21]. I_2 molecules or rather KI-I_2 (i.e. I_3^- ions) form inclusion compounds in these cyclic matrices. Here a systematic study of the infrared spectra of KI-I_2 complexes of these three cyclodextrins is carried out to get information on how interactions vary as the channel diameter changes and what is the effect of variation of channel diameter on electrical properties, particularly the band gap along iodine chains.

Materials and Methods

α-cyclodextrin-KI-I_2-xH_2O, β-cyclodextrin-KI-I_2-yH_2O and γ-cyclodextrin-KI-I_2-zH_2O complexes were prepared by mixing the three cyclodextrins one by one with KI-I_2 mixture in 1:1 molecular proportions in a mortar. All the three inclusion compounds were blue or blue-violet materials.

The KBr mull infrared absorption spectra of the three complexes were obtained using a Nicolet 400 D Spectrophotometer after preparing pellets of the complexes with dry KBr powder by compressing in a die. The spectra were recorded in the full infrared range 400 - 4000 cm^{-1}. Primary structure, various conformations and secondary (cyclic) structure of cyclodextrins are well-known.

Results

The six infrared spectra obtained in this work are shown in figures 1, 2 and 3. There are several changes in the spectra in 400-1800 cm^{-1} range. Apart from the relative broadening and intensity changes of some bands, there are new bands and qualitative changes in the structure of a few bands of these cyclodextrins.

Since potassium iodide and molecular iodine are infrared inactive, the vibration spectra of the complexes indicate changes in the vibration bands of the host matrices due to interaction with $KI-I_2$. However, water included in the complexes is infrared active. The O-H stretching vibration of water lies in the 3000-3300 cm^{-1} range. Very broad band around 3300 cm^{-1} in α-cyclodextrin-$KI-I_2$ xH_2O, still broader band around 3400 cm^{-1} in β-cyclodextrin-$KI-I_2$ – yH_2O, and a broad band in 3350 cm^{-1} in γ-cyclodextrin-$KI-I_2$, zH_2O can be ascribed to this vibration (table I, II AND III). Another band due to water near 1642 cm^{-1} in α-cyclodextrin complex, 1635.8 cm^{-1} in β-cyclodextrin complex and 1642.5 cm^{-1} in γ-cyclodextrin complex is sharp but intense. If the water is present as lattice water, there are additional bands between 300 and 600 cm^{-1} and these bands are also seen in the spectra of three complexes. Noise is found between 400 cm^{-1} and 500 cm^{-1} because of thermal motion of hydrogen atoms of free lattice water molecules. Similar thermal noise is also observed in the range between 3500 and 4000 cm^{-1} where O-H stretching band is located.

A shoulder develops in the spectra of $KI-I_2$ complex at 425 cm^{-1} which is absent in the spectra of cyclodextrins. A new band at 756 cm^{-1} in the spectra of iodine complexes is absent in the spectra of cyclodextrins. New bands observed in $KI-I_2$ complexes near 1092 cm^{-1} and 1159 cm^{-1} are absent in the spectra of cyclodextrins. A ladder structure (series of shoulders) in the low frequency tail of the 1414 cm^{-1} band is observed which is absent in the spectra of only cyclodextrins.

Discussion

New peaks observed in an earlier study of the infrared spectrum of dried formation. Since these peaks lie in the C-O-C stretching range, these bands are also found in ether-iodine complex. There is charge transfer interaction of iodine with glucosidic oxygen atoms in the C-O-C groups as suggested by Murakami in 1964. Similarly, the infrared spectrum of polyvinyl alcohol-iodine complex exhibited new bands at 770 cm^{-1} and 1020 cm^{-1} and the broadening of the bands in the range 900-1000 cm^{-1}. Other changes like broadening of bands in the range 1000-1150 cm^{-1} were considered to be associated with crystallinity. This broadening is also found in the 950-1200 cm^{-1} range in the spectra of cyclodextrin-iodine complexes in the present work.

Bands at 1031 cm^{-1} and 1092 cm^{-1} in the spectrum of α-cyclodextrin- $KI-I_2$, $4H_2O$ observed in the present work can be assigned to the changes in the C-O-C stretching vibrations due to the iodine-oxygen charge transfer contacts. The broad and intense band around 3300 cm^{-1} is associated with stretching vibrations of OH groups of cyclodextrins hydrogen bonded with water. There is a possibility of interaction of iodine with the organic matrix through O-H----I hydrogen bonds.

I_3^- and I_2 mixed species are likely to exist in the complexes of three cyclodextrins. The configuration, local cyclic conformation and molecular packing (the unit cell and its contents) are important in crystalline polymers and hydrogen-bonded oligomers must be the same in all the three-cyclodextrain complexes. The crystal structure of α-cyclodextrin-KI-I_2 complex is known to be hexagonal [22]. Therefore, the site symmetry of I_3^- ions is likely to be the same and crystal structure would not be responsible for new bands in the spectra.

The broadening and intensity changes at 800-1200 cm^{-1} are due to crystallinity or solid state effects and include the stabilization of iodine chains due to exciton coupling, internal salvation, dispersive forces and interaction of iodine with the lattice, i.e. chain formation [23].

The bands at 709 cm^{-1} and 756 cm^{-1} are enhanced in the spectra of iodine complexes and are ascribed to low frequency C-H deformation modes or π_{C-H} modes. In these three cyclodextrins, this corresponds to the interaction of iodine with hydrocarbons lining (a network of CH and CH_2 groups) as suggested by Freudenberg [24].

It is found that an empty cyclic host molecule has a strained conformational state. There is a transition to a relaxed state during complex formation with a proper guest molecule. In the relaxed state the 12 hydroxy groups of 6 glucose molecules of the toroidal α-cyclodextrin molecule bend towards iodine in the channel, which increases the possibility of some O-H----I hydrogen bonding contacts. Similar situation takes place in β and γ cyclodextrins studied here. A low-frequency vibration like C-O-H group rocking will be allowed in the relaxed state. The band at 425 cm^{-1} region in the iodine complexes is ascribed to C-O-H group rocking governed by O-H----I interaction.

There is broadening in the bands due to increase in channel diameter in the range 1250 - 1550 cm^{-1}. β-cyclodextrin-KI-I_2 spectrum contains broader bands in the ranges 800-1200 cm^{-1} and 1250-1550 cm^{-1} as compared to that of α-cyclodextrin-KI-I_2. This shows the polyiodine chains are more stable in β-cyclodextrin than in α-cyclodextrin. However, the analysis of featureless absorption in the range 1800-2600 cm^{-1} clearly shows the transition from the valence band to conduction band changes from allowed direct to forbidden direct as channel diameter increases in figure. Band gap (forbidden energy gap) increases as the channel diameter increases from 6 Å to 8 Å (0.225 eV in α-cyclodextrin and 0.24 eV in β-cyclodextrin) in α and β cyclodextrins. Actually band should still increase in γ cyclodextrin along with broadening in the lower ranges. However, this is not found in figure 4. Band gap again decreases as channel diameter increases up to 10 Å in γ cyclodextrin (Table IV).

In the region lower than E_g there is a sharp fall in transmission showing an exponential band edge. There is large number of absorption bands within this exponential band edge. This shows that there are large numbers of localized states near the band edge. Localization near the band edge and related white noise are discussed earlier [17,18].

Conclusion

Here a comparative study of the infrared absorption and transmission spectroscopy of the iodine inclusion compounds of α, β and γ-cyclodextrin has been carried out. The band gap along the polyiodine chain increases as the channel diameter increases. Highly conducting polyiodine chain with lesser band gap can be stabilized only in inclusion compounds of smaller cavity diameter.

Acknowledgment

The authors are thankful to the University Grants Commission, New Delhi for DRS/SAP funding.

References

[1] Oza A.T. and Vinodkumar P.C., Ind. J. Phys., **72A**, 171 (1998).

[2] Oza A.T., High Pressure Research, **17**, 47 (2000).

[3] Hsu C, Ph.D. thesis, Temple University, Pennsylvania, USA, International Microfilms Publishing (1978).

[4] Kao H. I., Ph.D. thesis, Temple University, Pennsylvania, USA, International Microfilms Publishing (1978)

[5] Saenger W., in Proc. 8th Jerusalem Symp. On Environmental effect on molecular structure and properties, Ed. By B. Pullman, Riedel Pub. Co., Boston, p. 265 (1975).

[6] Marks T.J., J. Amer. Chem. Soc., 100, 3215 (1978).

[7] Mulazzi E., Pollini I, Piseri L, and Tubino R, Phys, Rev. B. **24,** 3555 (1981).

[8] Wu C., Kim B., Kao H.I., Griffin C.W., Jones M. and Labes M.M., Mol. Cryst. Liq. Cryst., **88**, 317 (1982).

[9] Leung P, Boshme R.F. and Coppens P., Mol. Cryst. Liq. Cryst., **78**, 319 (1981).

[10] Oza A. T., Ph.D. thesis, I.I.Sc., Bengalore (1980).

[11] Oza A.T., Physica Status Solidi (b), **114**, K 171 (1982).

[12] Oza A.T., Physica Status Solidi (a). **80,** 573 (1982).

[13] Cramer F, Naturwissenschaften, **38**, 188 (1955).

[14] Cramer F, Rev. Pure. Appl. Chem., **5**, 143 (1955).

[15] Hollo J. and Szeitli J., In strach and its derivatives, 4th Edition, Ed. J.A. Radley, Chapman and Hall, London p.226 (1968).

[16] Greenwood C.T., and Rosetti H, J. Poly. Sci., **27,** 481 (1958).

[17] Rossotti H, J. Poly. Sci., **36,** 557 (1959).

[18] Ferguson Loyod N., The Modern structural theory of Organic Chemistry, Prentice –Hall of India, New Delhi p.163 (1974).

[19] Schlenk H, and Sand D.M., J. Amer. Chem. Soc., **83**, 2312 (1961).

[20] Drago Russel, Physical Methods in Inorganic Chemistry, East-West Press, New Delhi p.218 (1974).

[21] Murakami H, J. Chem. Phys., **22**, 367 (1964).

[22] Dietrich H. V. and Cramer F, Chem. Ber., 87, 806 (1954).

[23] Reddy J. M., Knox K and Robin M.B., J. Chem. Phys., **40**, 1082 (1964).

[24] Freudenberg K, and Cramer F, Chem. Ber., **83**, 296 (1950).

Captions of the figures

Figure 1 : Infrared spectra of α-cyclodextrin and α-cyclodextrin-KI-I_2. xH_2O

Figure 2 : Infrared spectra of β-cyclodextrin and β-cyclodextrin-KI-I_2. yH_2O

Figure 3 : Infrared spectra of γ-cyclodextrin and γ-cyclodextrin-KI-I_2. zH_2O

Figure 4 : (a) A^2 vs hv showing A $A_o(hv- E_g)^{1/2}$ for α-cyclodextrin-KI-I_2. xH_2O

(b) A^2 vs hv showing A $A_o(hv- E_g)^{3/2}$ for β-cyclodextrin-KI-I_2. yH_2O

(c) A^2 vs hv showing A $A_o(hv- E_g)^{3/2}$ for γ-cyclodextrin-KI-I_2. zH_2O

Table I Band assignments in α-cyclodextrin and its KI-I_2 complex

α-cyclodextrin (Hydrated)		α-cyclodextrin-KI-I_2. $4H_2O$	
Wave number (cm^{-1})	Band assignment	Wave number (cm^{-1})	Band assignment
3416	water	3288	water
2939	ν_{C-H}	2925	ν_{C-H}
1656	Water	2858	ν_{O-H}
1407	δ_{C-H}	1643	water
1367	δ_{O-H}	1575	New Band
1159	ν_{C-C}	1414	δ_{C-H}
1031	ν_{C-O}	1150	ν_{C-C}
850	π_{C-H}	1091	ν_{C-O}
716	π_{C-H}	1031	New Band
575	water	957	New Band
		876	π_{C-H}
		756	π_{C-H}
		708	π_{C-H}
		581	water
		494	Group Vibrations

Table II Band assignments in β-cyclodextrin and its KI-I_2 complex

β-cyclodextrin (Hydrated)		β-cyclodextrin-KI-I_2. xH_2O	
Wave number (cm^{-1})	Band assignment	Wave number (cm^{-1})	Band assignment
3469	water	3402	water
2925	ν_{C-H}	2925	ν_{C-H}
1649	water	1635	water
1414	δ_{C-H}	1414	δ_{C-H}
1327	δ_{O-H}	1381	δ_{O-H}
1172	ν_{C-C}	1340	δ_{O-H}
1045	ν_{C-O}	1246	New Band
944	ν_{C-C}	1158	ν_{C-C}
850	π_{C-H}	1045	ν_{C-O}
763	π_{C-H}	950	ν_{C-C}
582	water	870	π_{C-H}
		762	π_{C-H}
		709	π_{C-H}
		602	water
		512	water

Table III Band assignments in γ-cyclodextrin and its KI-I_2 complex

γ-cyclodextrin (Hydrated)		γ—cyclodextrin-KI-I_2. xH_2O	
Wave number (cm^{-1})	Band assignment	Wave number (cm^{-1})	Band assignment
3167	water	3382	water
2952	ν_{C-H}	2932	ν_{C-H}
1676	water	1643	water
1649	ν_{O-H}	1444	δ_{C-H}
1454	δ_{C-H}	1240	ν_{C-C}
1374	δ_{O-H}	1172	ν_{C-C}
1173	ν_{C-C}	1085	New Band
857	π_{C-H}	1038	New Band
763	π_{C-H}	957	π_{C-H}
581	π_{C-H}	803	π_{C-H}
554	water	769	π_{C-H}
434	water	708	π_{C-H}
		584	water
		534	water

Table – IV Channel Diameter Vs Band gap

Cyclodextrin-KI-I_2 complex	Channel Diameter	Band gap (eV)
α	6	0.225
β	8	0.24
γ	10	0.23

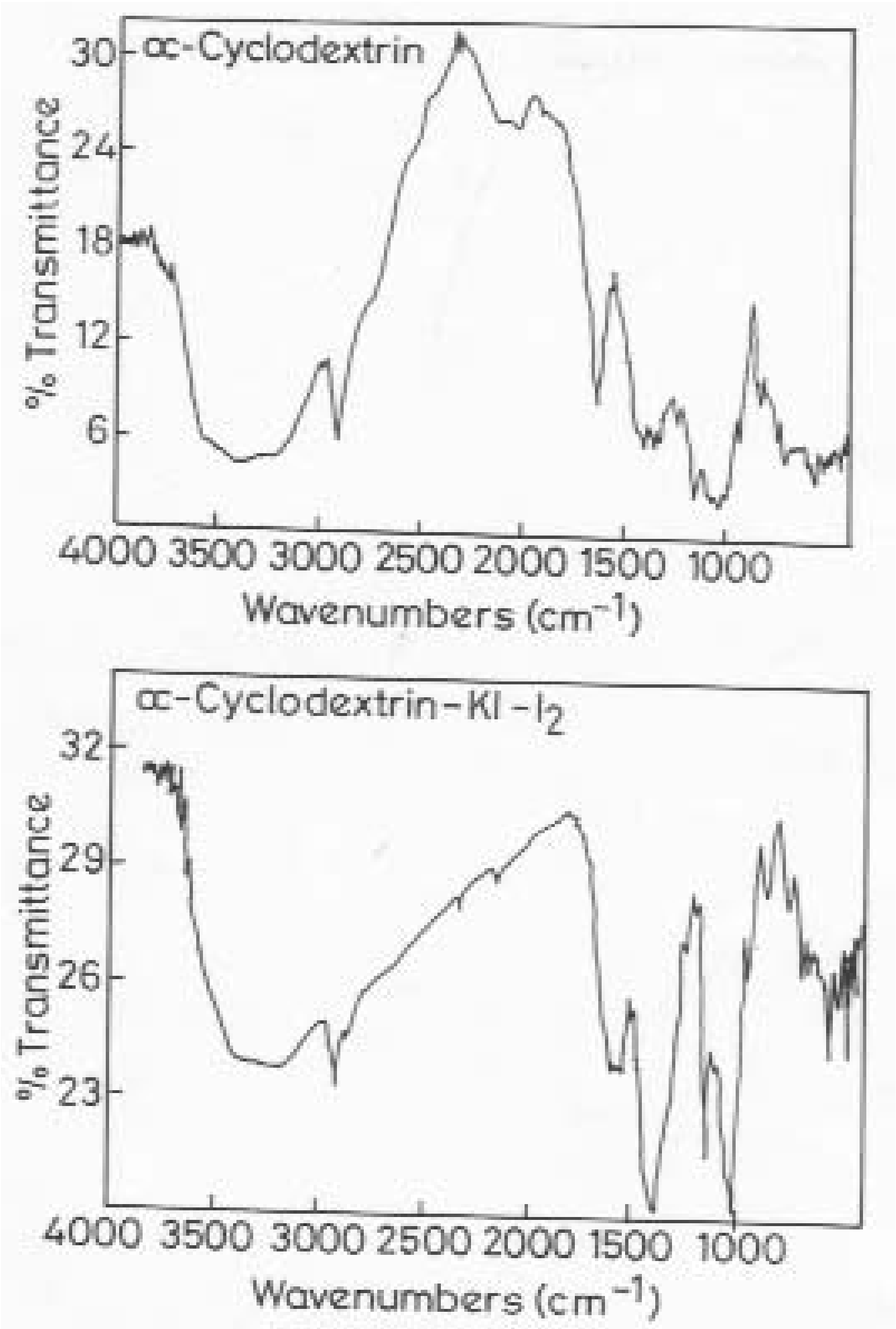

Figure1: Infrared spectra of α-cyclodextrin and α-cyclodextrin-KI-I_2. xH_2O

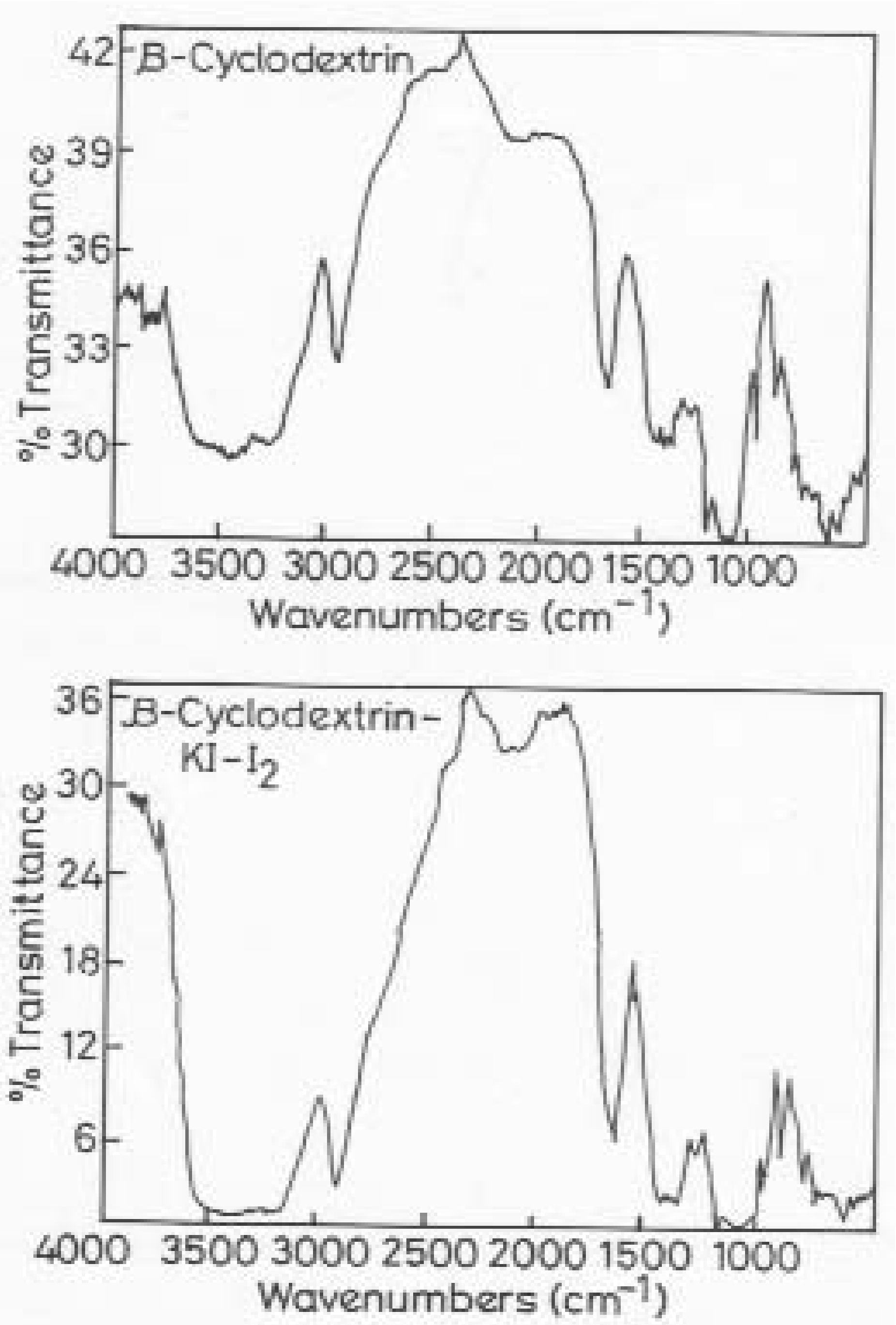

Figure 2: Infrared spectra of β-cyclodextrin and β-cyclodextrin-KI-I_2. yH_2O

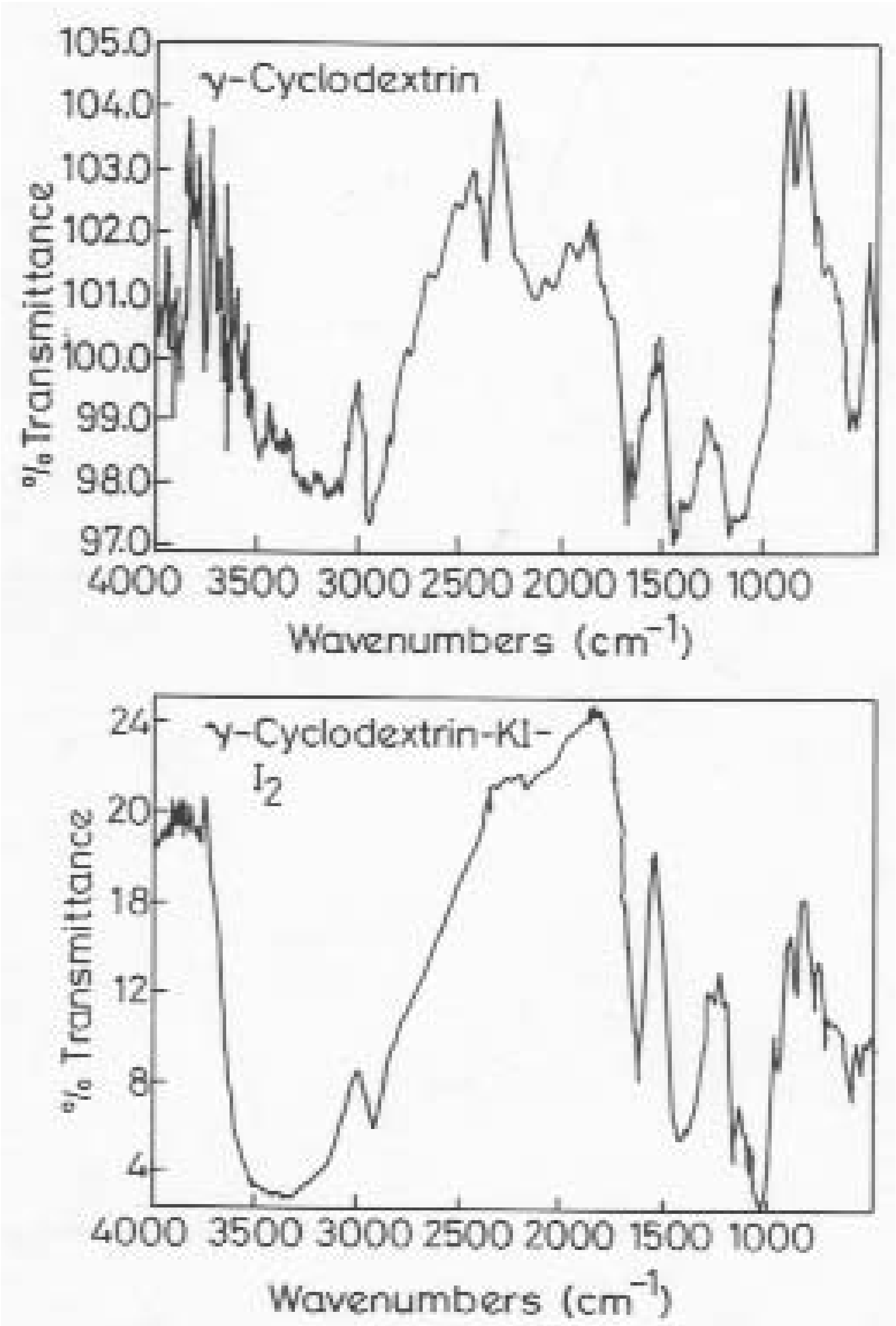

Figure 3 : Infrared spectra of γ-cyclodextrin and γ-cyclodextrin-KI-I_2. zH_2O

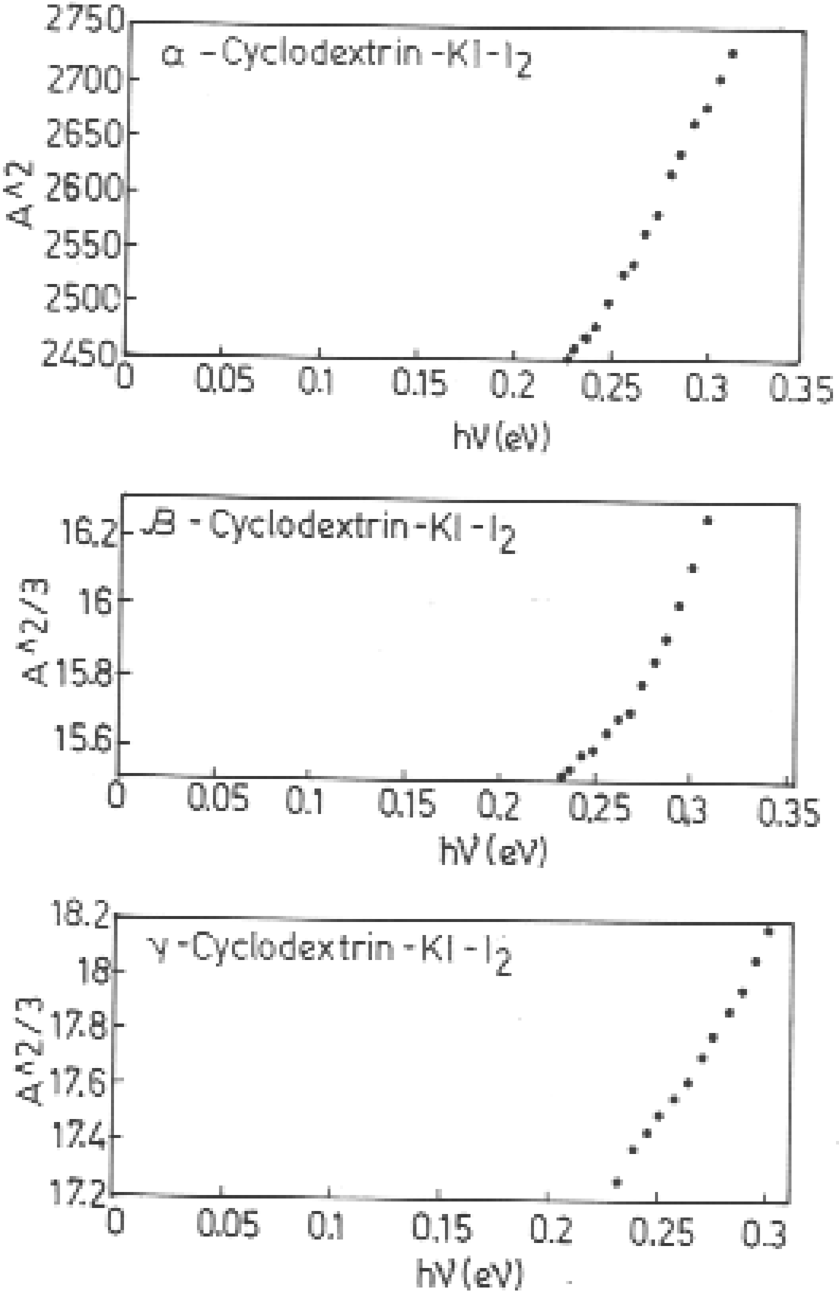

Figure 4: (a) A^2 vs hv showing A $A_o(hv- E_g)^{1/2}$ for α-cyclodextrin-KI-I_2. xH_2O
(b) A^2 vs hv showing A $A_o(hv- E_g)^{3/2}$ for β-cyclodextrin-KI-I_2. yH_2O
(c) A^2 vs hv showing A $A_o(hv- E_g)^{3/2}$ for γ-cyclodextrin-KI-I_2. zH_2O

'Prajna' - Jounal of Pure & Applied Sciences, 14 (2006) 129-139

INTERACTION OF ELECTROMAGNETIC WAVE WITH HUMAN HEAD AT DIFFERENT TELECOMMUNICATION FREQUENCIES

Bhavin Patel and P. C.Vinodkumar

Department of Physics, Sardar Patel University, Vallabh Vidyanagar- 388 120

Abstract

Interaction of the electromagnetic plane waves of commonly used telecommunication frequencies with the multilayer model of human head is investigated. Exact analytical expressions are derived for the plane wave complex reflection and transmission coefficients as a function of frequency at the interfaces of the stratified structure of human head. The induced electric field, power dissipation and SAR (Specific Absorption Rate) at different layers of human head are computed at frequencies 900, 1800 and 3000 MHz. The results are represented graphically.

Introduction

Today, we are living through an era in which electromagnetic wave energy utilization particularly in the telecommunications sector is playing an unavoidable influence in our daily life. The number of devices that operates at different frequencies of the electromagnetic spectrum is very common and has become essential communications in our routine life. Also the use of cellular telephones has increased rapidly during late 1990s. The number of cellular phone users world-wide is estimated to reach 900 million by the year 2006. The mobile phone and wireless technologies operate at different frequencies with different input power. Generally the hand held and the mobile cellular telephones operate at frequencies between 835 MHz and 900 MHz. While digital personal communications systems (PCS) operate in the 1850-1990 MHz band. Portable transceivers used for two-way communications typically operate near 30,150 and 450 MHz. Cordless telephone units typically operate near 50, 915, 2450 and 3000 MHz [1]. So, as typical cases, we report the effect on human head tissues by telecommunications systems at frequencies 900 MHz, 1800 MHz and 3000 MHz.

Mobile telephones are RF transmitting devices that are normally operated at the user's ear. There have been reports on the effects of electromagnetic (EM) radiation on the human head [2]-[7]. To understand the effects of electromagnetic radiation on biological tissues, the magnitude of the induced field needs to be determined within various tissues that are exposed. Also the human head is not a unique object. It may have vast variety of forms and sizes. We consider here a simple stratified human head model for the present study. Although MRI scan based anatomical head models are available but they require large computational recourses for field simulations [2]. In this stratified model of human head, we compute the induced electric field, power density and specific absorption rate (SAR) for each layer.

Theory And Calculation

In the multilayer model of human head [2],we consider 11 layers represented by the characteristic impedance of the medium (η_i, i = 1 to 11) and 12 interfaces (d_i, i = 1 to 12) that constitute the human head as a whole from left to right with a typical size of 18 cm. A schematic representation of the model across the head is shown in Figure-1 below. Different layers of human head from skin to brain and its numerical values listed in the Figure-1 represent typical thickness of each layer of a realistic human head.

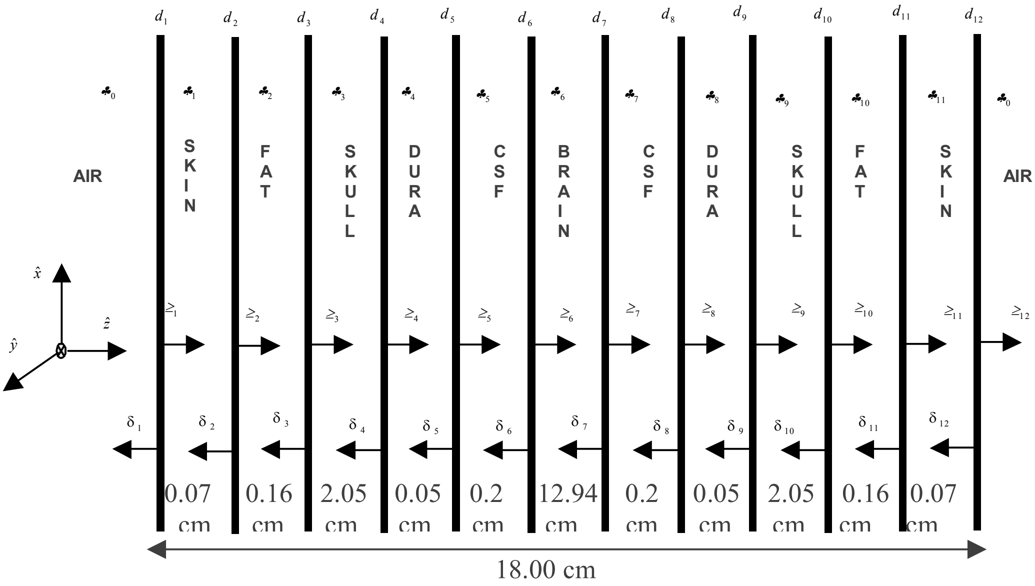

Figure-1: Stratified model of human head.

As shown in Figure-1 a plane wave propagating along the z-direction is incident on the multilayer lossy media representing human head from left. The Electric field (E_i) and Magnetic field (H_i) at the i^th^ layer can be written as,

$$\vec{E}_i = (a_i e^{-jk_i z} + b_i e^{jk_i z})\hat{x} \tag{1}$$

$$\vec{H}_i = \frac{(a_i e^{-jk_i z} - b_i e^{jk_i z})\hat{y}}{\eta_i} \tag{2}$$

Where i = 0, 1…N+1 represent the layers including the air and N^{th} total number of layers of the head. The constant a_i is the amplitude and the phase of incident wave in the i^{th} layer and b_i is the amplitude and the phase of reflected wave at the i^{th} layer. The amplitude of the incident electric field is represented by $|a_0|$ and can be obtained from the power of the incident wave, which is an input for the computations of other properties. For the present study we have considered N=11 such that our medium under study contain the air-head-air combinations with 13 distinct layers (including air) according to Figure-1.The magnitudes of the fields (E_i) and (H_i) are expressed in units of V/m and A/m respectively, k_i and η_i denote the propagation constant and characteristic impedance of i^{th} layer respectively. From the wave equation for lossy medium, we get

$$k_i^2 = \omega^2 \mu_i \varepsilon_i - j\omega\mu_i\sigma_i \tag{3}$$

$$\eta_i = \sqrt{\frac{\mu_i}{\varepsilon_i - j(\sigma_i / \omega)}} \tag{4}$$

Here ω represents the angular frequency of the electromagnetic wave, μ_i, ε_i and σ_i represent the permittivity, dielectric constant and conductivity of the medium correspond to the i^{th} layer. We consider the permeability μ_i in a vacuum. The dielectric properties of the different human head tissues, computed using the 4-Cole Cole formula and value of conductivity for different layers are available in literature [8]. There parameters at the selected frequencies of the present study and the mass density of different layers are given in Table-1. Further, since the thickness of 12th layer in this case is infinity, we can choose

$$b_{12} = 0. \tag{5}$$

The input impedance of i^{th} layer denoted by Z_i and is located at z = d_i, is given by

$$Z_i = \frac{E_i(z)}{H_i(z)} = \eta_i \frac{(a_i e^{-jk_i d_i} + b_i e^{jk_i d_i})}{(a_i e^{-jk_i d_i} - b_i e^{jk_i d_i})} \tag{6}$$

Accordingly, at the interface $z = d_i$, the reflection coefficient Γ_i and the transmission coefficient τ_i are defined as

$$\Gamma_i = \frac{b_{i-1}}{a_{i-1}} \tag{7}$$

$$\tau_i = \frac{a_i}{a_{i-1}} \tag{8}$$

Dividing equation (6) by $a_i e^{-jk_i d_i}$ and using equation (7), we get

$$Z_i = \eta_i \frac{(1+\Gamma_{i+1} e^{2jk_i d_i})}{(1-\Gamma_{i+1} e^{2jk_i d_i})} \tag{9}$$

The unknown incident/reflected constants field strengths a_i's and b_i's can be found by applying boundary conditions at the interfaces. Thus due to continuity of E_i and H_i across the interface $z = d_i$ the incident / reflected complex constants at the left of interface d_i are related to those at the right of the interface d_i by

$$a_{i-1} e^{-jk_{i-1} d_i} + b_{i-1} e^{jk_{i-1} d_i} = a_i e^{-jk_i d_i} + b_i e^{jk_i d_i} \tag{10}$$

$$\frac{a_{i-1} e^{-jk_{i-1} d_i} - b_{i-1} e^{jk_{i-1} d_i}}{\eta_{i-1}} = \frac{a_i e^{-jk_i d_i} - b_i e^{jk_i d_i}}{\eta_i} \tag{11}$$

Equation (6), can be rewritten as

$$\frac{a_i e^{-jk_i d_i} - b_i e^{jk_i d_i}}{\eta_i} = \frac{a_i e^{-jk_i d_i} + b_i e^{jk_i d_i}}{Z_i} \tag{12}$$

Comparing equation (11) and (12), we write

$$\frac{a_{i-1} e^{-jk_{i-1} d_i} - b_{i-1} e^{jk_{i-1} d_i}}{\eta_{i-1}} = \frac{a_i e^{-jk_i d_i} + b_i e^{jk_i d_i}}{Z_i} \tag{13}$$

Now using equation (10), the R.H.S. of equation (13) becomes

$$\frac{a_{i-1} e^{-jk_{i-1} d_i} - b_{i-1} e^{jk_{i-1} d_i}}{\eta_{i-1}} = \frac{a_{i-1} e^{-jk_{i-1} d_i} + b_{i-1} e^{jk_{i-1} d_i}}{Z_i} \tag{14}$$

Solving equation (14) and using equation (7) we get

$$\Gamma_i = \frac{(Z_i - \eta_{i-1})}{(Z_i + \eta_{i-1})} e^{-2jk_{i-1} d_i} \tag{15}$$

Similarly, using equation (10) and equation (8) the transmission coefficient at the i^{th} layer is obtained as

$$\tau_i = \left[\frac{(1+\Gamma_i e^{2jk_{i-1} d_i})}{(1+\Gamma_{i+1} e^{2jk_i d_i})} \right] e^{j(k_i - k_{i-1}) d_i} \tag{16}$$

Rewriting equation (15) as

$$\Gamma_i e^{2jk_{i-1}d_i} = \left(\frac{Z_i - \eta_{i-1}}{Z_i + \eta_{i-1}} \right) \tag{17}$$

And substituting equation (17) in equation (16) yields

$$\tau_i = \left[\frac{2Z_i}{Z_i + \eta_{i-1}} \right] \frac{e^{j(k_i - k_{i-1})d_i}}{(1 + \Gamma_{i+1} e^{2jk_i d_i})} \tag{18}$$

Now using the expressions derived above the relevant quantities such as reflection coefficient (Γ_i), transmission coefficient (τ_i), input impedance of medium (Z_i) and the corresponding field amplitudes a_i and b_i of each layer of human head tissues can be computed. We set the amplitude and phase of the reflected wave at the 12th layer (for the present case of N = 11, stratified head model) to be zero. That corresponds $b_{N+1} = 0$ in present case $b_{12} = 0$). So that corresponding equation (7), gives $\Gamma_{N+2} = \Gamma_{13} = 0$. Now from equation (9), Z_{N+1} (*i.e.* Z_{12}) and from equation (18), τ_{N+1} (*i.e.* τ_{12}) can be computed in terms of the characteristic impedance (η_i) and the propagation constant (k_i) of the respective layers. By using equation (15), the corresponding Γ_{N+1} (*i.e.* Γ_{12}) can be obtained. Recursively by using equations (9), (15) and (18) Z_i, τ_i and Γ_i can be computed from the 12th interface to the 1st interface of the multilayer model of head.

From the computed values of Γ_i, τ_i and using equation (7) and (8) b_i and a_i can also be obtained. The initial values of $a_i{}'s$ and $b_i{}'s$ are given by $a_1 = a_0\tau_1$ and $b_0 = a_0\Gamma_1$ where $a_0 = \sqrt{2\eta_0 P_{inc}}$ and η_0 is the characteristic impedance in free space ($\eta_0 = 377\Omega$), P_{inc} is the input power density of the electromagnetic plane wave in W/m^2.

Once we know the induced electric field in particular layer the dissipated power density can be obtained. The primary dosimetric parameter for the evaluation of the exposure hazard in the radiofrequency and microwave ranges is the specific absorption rate (SAR) [8], [9]. SAR is defined as the power absorbed by the unit mass of the biological tissue (Watts/Kilogram), and is given by

$$SAR = \frac{\sigma_i |E_i|^2}{2\rho_i} \tag{19}$$

Where σ_i is the conductivity of the tissue in (S/m), $|E_i|$ is induced electric field (V/m) and ρ_i is density of the tissue in (kg/m^3). The dissipated power density (W/m^3) absorbed in the layer having conductivity σ_i and induced electric field E_i is given by

$$P_i = \frac{|E_i|^2 \sigma_i}{2} \tag{20}$$

Using equation (1) and using the corresponding σ_i values as given in Table-1, electric field strength $|E_i|$ and the dissipated power density P_i are computed. Then the computed electric field strength and the dissipated power density are plotted in Figure-2 to Figure-4 across the dimension of the multilayer structure of human head at different frequencies.

Using equation (19) the SAR across the layers of human head is computed and is plotted in Figure-5 for the three chosen frequencies. The computed SAR is normalized to the input power of 1.0W/m^2 of the incident electromagnetic plane wave. If $|E_{io}|$ represents the electric field strength at the interface of the i^{th} layer at a distance d_i and the area of the cross-section A_i (here, we have considered cubical shape of the human head), the total electromagnetic power dissipated P_{Li} within the volume of the i^{th} layer of the human head can be obtained by integrating the power density given by equation (20) over the volume of the respective layer. For the layer having thickness t_i, conductivity σ_i and the skin depth which is the inverse of α_i, the integrated power in Watt is given by

$$P_{Li} = \frac{1}{2}\sigma_i |E_{oi}|^2 e^{-2\alpha_i d_i} \left[\frac{1 - e^{-2\alpha_i t_i}}{2\alpha_i}\right] A_i \tag{21}$$

Then the integrated SAR for each layer is computed as

$$(SAR)_{Li} = \frac{P_{Li}}{\rho_i t_i A_i} \tag{22}$$

The computed SAR values for each layer are listed in Table-2 for three frequencies. The integrated SAR across the head is also given.

No.	Human head tissue	Conductivity (σ) (S/m)			Relative Permittivity (ε_r)			Density Kg/m^3
		900 MHz	1800 MHz	3000 MHz	900 MHz	1800 MHz	3000 MHz	
1	Skin	0.86	1.21	1.84	43.75	41.36	39.78	1100
2	Fat	0.05	0.08	0.13	5.462	5.349	5.224	1100
3	Skull	0.34	1.32	1.01	20.79	42.89	17.94	1850
4	Dura	0.96	0.59	2.02	44.43	19.34	41.34	1030
5	CSF	2.41	2.92	4.01	68.64	67.2	65.39	1030
6	Brain	0.77	1.15	2.02	45.81	43.55	41.8	1030

Table-1 : The dielectric parameter and the conductivity for different human head tissues at 900 MHz, 1800 MHz and 3000 MHz [10].

No.	Tissue	SAR (Watt/kg)		
		900 MHz	1800 MHz	3000 MHz
1	Skin	9.0E-03	9.0E-03	1.7E-02
2	Fat	5.4E-04	5.6E-04	1.2E-03
3	Skull	2.2E-03	1.8E-03	2.2E-03
4	Dura	1.6E-03	1.8E-04	3.9E-04
5	CSF	8.7E-04	8.0E-05	1.1E-04
6	Brain	1.1E-04	1.2E-06	1.4E-05
Integrated SAR over the head		1.4E-02	1.2E-02	2.1E-02

Table-2 : Integrated SAR of different human head tissue at 900 MHz, 1800 MHz and 3000 MHz frequencies normalized to 1W/m^2 input power of telecommunication devices.

Results And Discussion

The computed values of induced electric field and power dissipation inside the stratified model of human head model at frequencies 900, 1800 and 3000 MHz with input peak power 1.0 watt/m^2 are shown in Figure-2 to Figure-4. It can be seen that there is a sharp fall at the skin layer with a further increased up to 1.0 cm inside the head, where both the electric field and the absorbed power density is more. In a 900 MHz plot the induced electric field strength is more in comparison of 1800 MHz at skin-fat interface. Also the same quantity in a brain is reduced at 1800 MHz. But in 3000 MHz which is generally used in cordless phone have more electric field strength in comparison of 1800 MHz. As the frequencies increases from 900 MHz to 1800 MHz the dissipated power density show peaking below 2 cm with considerable reduction in the power that reaches the interior layers up to the brain. However at 3000 MHz which is used for cordless phone services, a broad power distribution reaching beyond 4.0 cm from the skin layer with a peak around the fat-skull interface can be from Figure-4. Though most of the powers dissipated are absorbed at the skin-fat layers considerable amount of power is being dissipated within the interior layers reaching up to the brain. At frequencies, 900 MHz and 3000 MHz energy dissipated are noticeably large up to 2.5 cm inside the head corresponding to the skin, fat, skull, and cerebrospinal fluid (CSF) layers.

Similar variations in the local SAR (Watt/kg) across half portion of the human head are shown in Figure-5. The value of SAR obtained here are well within the limit of 2.0 W/kg, averaged over 10gm of contiguous tissue with a 6 minutes periods of exposure specified by the International Commission on Non-Ionizing Radiation Protection (ICNIRP) [9].

It is evident from the present study that the induced electric fields, the dissipated power density and SAR values vary significantly with respect to the operating frequency of the telecommunication devices. We can also conclude that the devices operating around 1800 MHz are safer devices as the absorbed power density becomes almost zero beyond the skull layer of the human head compared to other devices operating at 900 MHz and 3000 MHz.

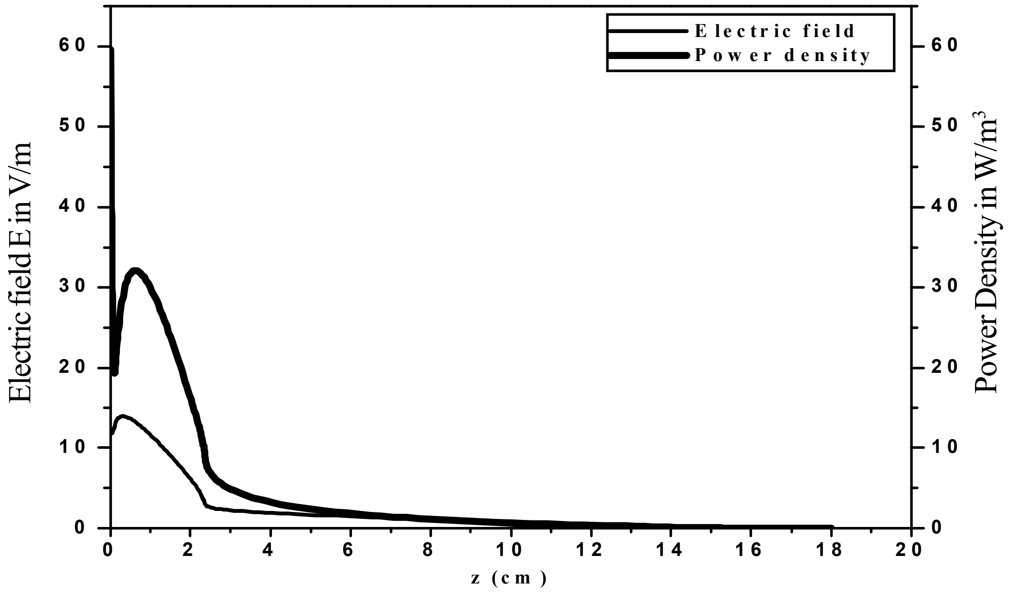

Figure -2 : Electric field and power dissipation in the head model at 900 MHz from 0 to 18 cm normalized to $P_{int} = 1.0$ W/m^2.

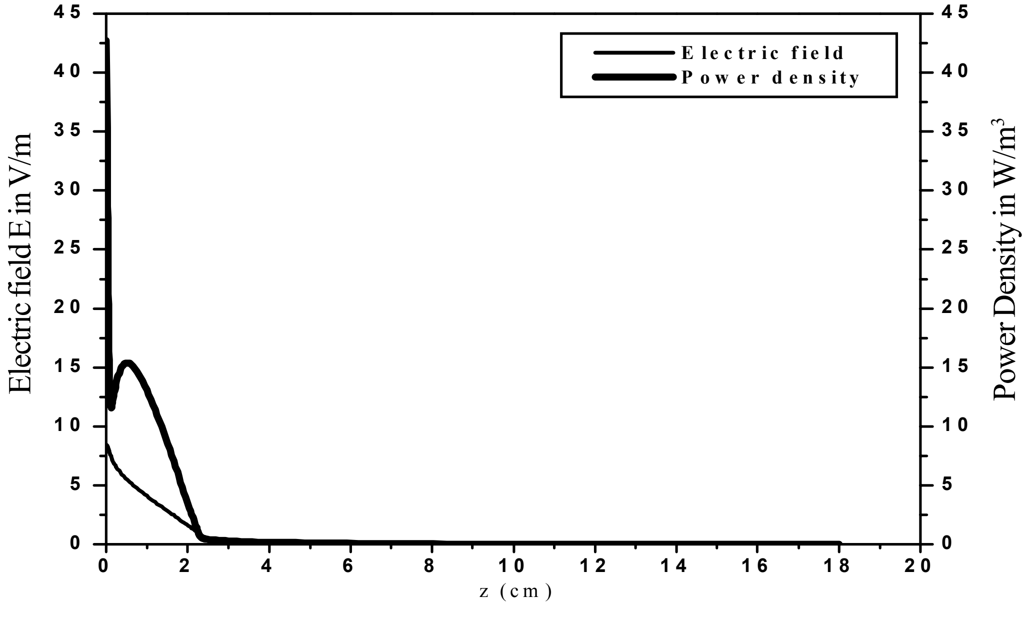

Figure -3 : Electric field and power dissipation in the head model at 1800 MHz from 0 to 18 cm normalized to $P_{int} = 1.0$ W/m^2.

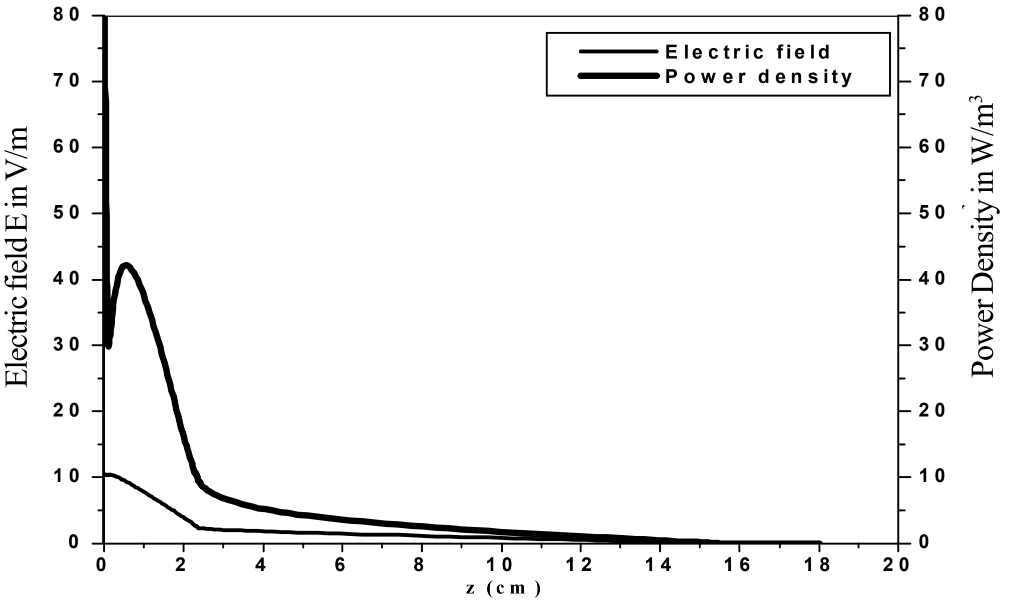

Figure -4 : Electric field and power dissipation in the head model at 3000 MHz from 0 to 18 cm normalized to $P_{int} = 1.0$ W/m^2.

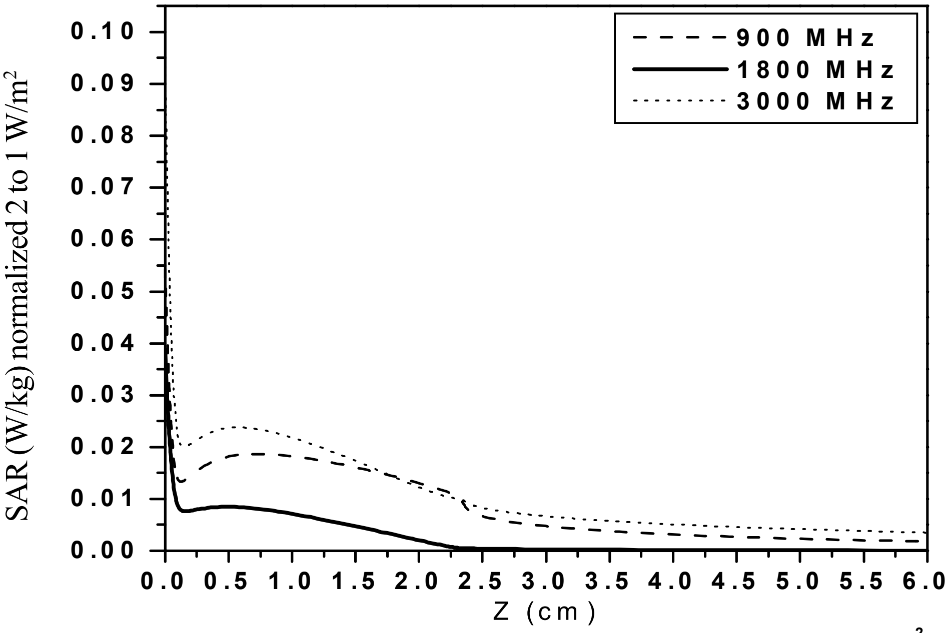

Figure -5 : SAR in W/kg Normalized to 1 W/m^2 at freqencies 900, 1800 and 3000 MHz.

References

[1] "Human exposure to radio frequency and microwave radiation from portable and mobile telephones and other wireless communication devices", IEEE committee on Man and Radiation, September 2000.

[2] Akram Abdulla, Andrew Teoh (2005) "A Multi-Layered Model of Human Head Irradiated by Electromagnetic Plane Wave of 100 MHz -300 GHz , Int. J. Sci. Res. Vol. **15**

[3] P. Dimbylow and O. Gandhi, (1991), Phys. Med. Biol., **36:**1075

[4] O. Gandhi (1982), IEEE Trans. Microwave Theor. Tech., **30:** 1831

[5] Livesay and K. Chen, (1974), IEEE S-MTT Int. Microwave Symp. Dig, 35

[6] Shapiro, R. Lutomirski and H. Yura (1971), IEEE Trans. Microwave Theor. Tech., **19**, 187

[7] Drossos, V. Santomaa and N. Kuster, (2000), IEEE Trans. Microwave Theor. Tech., **48**:1988

[8] IEEE C95.1 (1991,1992), IEEE standards for safety levels with respect to human exposure to radio frequency electromagnetic fields, 3 KHz to 300 GHz, Institute of Electrical & Electronics Engineers, and Inc. New York

[9] International Commission on Non-Ionizing Radiation Protection (ICNIRP) (1998), "Guidelines for Limiting Exposure to Time-varying Electric, Magnetic, and Electromagnetic Fields (Up to 300 GHz)," Health Physics **74**: 494-520

[10] C.Gabrial (2000), "Parametric model of the dielectric properties of body tissues", (http://niremf.ifac.cnr.it/cgi-bin/tissprop/htmldie/uniquery)

'Prajna' - Jounal of Pure & Applied Sciences, 14 (2006) 140-145

ELECTRIC AND MAGNETIC FIELD DUE TO GIVEN CURRENT IN A CONDUCTOR

V. H. Gandhi
Department of Physics, Gujarat University, Anmedabad-9

Abstract

For a linearly time dependent current flowing in a conductor, electric and magnetic field at any point has been derived.

Introduction

As shown in the figure an infinite straight wire carries the linearly time dependent current (David J Griffith (1991))

$$I(t) = 0 \quad \text{for} \quad t \le 0$$

$$I(t) = \alpha t \quad \text{for} \quad t > 0$$

Where α is constant

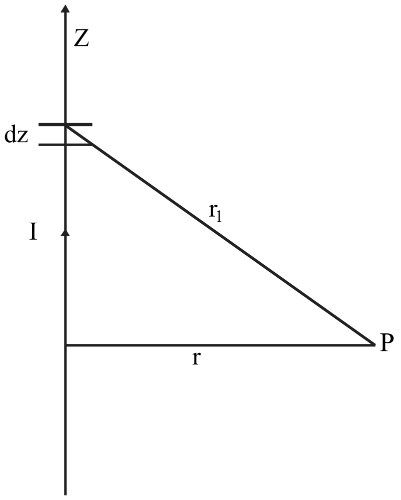

Find Scalar And Vector Potential

The Scalar Potential V of the system is zero because the wire is electrically neutral. The wire lies along the Z axis. The retarded Vector Potential at point P is given by

$$\vec{A}\left(\vec{r},t\right) = \hat{k}\frac{\mu_0}{4\pi}\int_{-\infty}^{\infty}\frac{I(t_r)}{r_1}dz \qquad \text{------------ (1)}$$

In general

$$t_r = t - \frac{r}{c}$$

t_r = retarded time

t = time at which the message is reaching at point P.

for t < r/c the message has not yet reached P and the potential is zero for t > r/c only point out to Contribute (beyond this t_r retarded time is negative, so $I(t_r)=0$)

$$Z = \pm\sqrt{r_1^2 - r^2}$$

$$Z = \pm\sqrt{(ct)^2 - r^2} \qquad \text{------------ (2)}$$

Here r_1 = ct

Where c is the velocity of light

Now from the diagram

$$r_1 = \sqrt{r^2 + z^2}$$

$$\vec{A}\left(\vec{r},t\right) = \hat{k}\frac{\mu_0}{4\pi}\int_{-\sqrt{(ct)^2-r^2}}^{\sqrt{(ct)^2-r^2}} \frac{\alpha t_r}{\sqrt{r^2+z^2}}\,dz \qquad \text{------------ (3)}$$

$$\vec{A}\left(\vec{r},t\right) = \hat{k}(2)\frac{\mu_0}{4\pi}\int_{0}^{\sqrt{(ct)^2-r^2}} \frac{\alpha t_r}{\sqrt{r^2+z^2}}\,dz$$

Now following the diagram

$$t_r = t - \frac{r_1}{c}$$

$$\vec{A}\left(\vec{r},t\right) = \hat{k}\frac{\mu_0\alpha}{2\pi}\int_{0}^{\sqrt{(ct)^2-r^2}} \frac{\left(t - {r_1}/{c}\right)}{\sqrt{r^2+z^2}}\,dz$$

$$\vec{A}\left(\vec{r},t\right) = \hat{k}\frac{\mu_0\alpha}{2\pi}\int_0^{\sqrt{(ct)^2-r^2}} \frac{\left(t-\frac{\sqrt{r^2+z^2}}{c}\right)}{\sqrt{r^2+z^2}}\,dz$$

$$\vec{A}\left(\vec{r},t\right) = \hat{k}\frac{\mu_0\alpha}{2\pi}\left[t\,ln\left\{z+\sqrt{r^2+z^2}\right\}-\frac{z}{c}\right]_0^{\sqrt{(ct)^2-r^2}}$$

$$\vec{A}\left(\vec{r},t\right) = \hat{k}\frac{\mu_0\alpha}{2\pi}\left[t\,ln\left\{\frac{\sqrt{(ct)^2-r^2}+ct}{r}\right\}-\frac{1}{c}\sqrt{(ct)^2-r^2}\right] \qquad \text{------------ (4)}$$

Equation (4) gives required Vector Potential at point P because of a given linearly time dependent current distribution.

Obtain Electric and Magnetic Field

Electric field $\vec{E}$ and magnetic field $\vec{\mathrm{B}}$ can be calculated by using following expressions

$$\left.\begin{aligned}\vec{E} &= -\nabla V-\frac{\partial\vec{A}}{\partial t}\\ \vec{B} &= \nabla\times\vec{A}\end{aligned}\right\} \qquad \text{------------ (5)}$$

Here current is flowing through the conductor so the cylindrical co-ordinate system is used.

$$\vec{E} = \hat{k}\frac{\mu_0\alpha}{2\pi}\left[\ln\left(\frac{\sqrt{(ct)^2-r^2}+ct}{r}\right)+t\left(\frac{r}{\sqrt{(ct)^2-r^2}+ct}\right)\frac{1}{r}\left(\frac{2c^2t}{2\sqrt{(ct)^2-r^2}}+c\right)\right.$$

$$\left.-\frac{1}{c}\frac{2c^2t}{2\sqrt{(ct)^2-r^2}}\right]$$

$$=\hat{k}\,\frac{\mu_0\alpha}{2\pi}\left[\ln\left(\frac{\sqrt{(ct)^2-r^2}+ct}{r}\right)+\frac{ct}{\sqrt{(ct)^2-r^2}}-\frac{ct}{\sqrt{(ct)^2-r^2}}\right]$$

$$=\hat{k}\,\frac{\mu_0\alpha}{2\pi}\left[ln\left(\frac{\sqrt{(ct)^2-r^2}+ct}{r}\right)\right]$$

First find $\vec{E}$

Now V = 0,

$$\therefore\ \vec{E}=-\frac{\partial\vec{A}}{\partial t}$$

$$\vec{E}=-\hat{k}\,\frac{\mu_0\alpha}{2\pi}\,\frac{\partial}{\partial t}\left[t\ln\left(\frac{\sqrt{(ct)^2-r^2}+ct}{r}\right)-\frac{1}{c}\sqrt{(ct)^2-r^2}\right] \qquad \text{------------ (6)}$$

From equation (6), $\vec{E}$ can be calculated as

$$\vec{E}=-\hat{k}\,\frac{\mu_0\alpha}{2\pi}\left[\ln\left(\frac{\sqrt{(ct)^2-r^2}+ct}{r}\right)\right] \qquad \text{------------ (7)}$$

Now to find $\vec{B}$

$$\vec{B}=\nabla\times\vec{A}$$

Using Cylindrical co-ordinates in our Vector Potential

$\vec{A}=Az\,\hat{k}$ it means Ar = 0 and Aφ = 0, Az is independent of φ.

$$\vec{B}=-\,\hat{\varphi}\frac{\partial Az}{\partial r}$$

$$.\vec{B} = -\hat{\varphi}\frac{\partial}{\partial r}\left[\frac{\mu_0\alpha}{2\pi}\left\{t\,ln\left(\frac{\sqrt{(ct)^2-r^2}+ct}{r}\right)-\frac{1}{c}\sqrt{(ct)^2-r^2}\right\}\right] \text{------------ (8)}$$

$$\vec{B} = -\hat{\varphi}\,\frac{\mu_0\alpha}{2\pi}\left[t\left(\frac{r}{\sqrt{(ct)^2-r^2}+ct}\right)\right.$$

$$\left(\frac{r\frac{(-2r)}{2\sqrt{(ct)^2-r^2}}-\left(\sqrt{(ct)^2-r^2}+ct\right)}{r^2}\right)$$

$$\left.-\frac{1}{c}\,\frac{(-2r)}{2\sqrt{(ct)^2-r^2}}\right]$$

$$=-\hat{\varphi}\frac{\mu_0\alpha}{2\pi}\left[t\left(\frac{r}{\sqrt{(ct)^2-r^2}+ct}\right).\right.$$

$$\left.\left(\frac{-r^2-(ct)^2+r^2-(ct)\sqrt{(ct)^2-r^2}}{r^2\sqrt{(ct)^2-r^2}}\right)+\frac{r}{c\sqrt{(ct)^2-r^2}}\right]$$

$$=-\hat{\varphi}\frac{\mu_0\alpha}{2\pi}\left[\frac{-ct^2}{r\sqrt{(ct)^2-r^2}}+\frac{r}{c\sqrt{(ct)^2-r^2}}\right]$$

$$=-\hat{\varphi}\frac{\mu_0\alpha}{2\pi}\left[\frac{-\left((ct)^2-r^2\right)}{rc\sqrt{(ct)^2-r^2}}\right]$$

$$= \hat{\varphi}\frac{\mu_0\alpha}{2\pi c}\frac{\sqrt{(ct)^2 - r^2}}{r}$$

From equation (8), $\vec{B}$ can be obtained as

$$\vec{B} = \hat{\varphi}\frac{\mu_0\alpha}{2\pi c}\frac{\sqrt{(ct)^2 - r^2}}{r} \qquad \text{------------ (9)}$$

Equation (7) and (9) gives the required expression for $\vec{E}$ and $\vec{B}$.

Conclusion

$\vec{E}$ and $\vec{B}$ both are perpendicular to each other. $\vec{E}$ and $\vec{B}$ depends on the position of point P.

Reference

David J Griffith (1991) Second edition, Introduction to electrodynamics

'Prajna' - Jounal of Pure & Applied Sciences, 14 (2006) 146-153

EFFECT OF STRETCHING ON PHYSICAL PROPERTIES AND CONSEQUENTLY ON CRYSTALLINITY OF NYLON-6 CORD

D. Patel, G. Bhavin, S. Patel, J. Neetha*, K.A. Job and A. Chandra****

* Plastics Technology, Institute of Science & Technology for Advanced Studies & Research (ISTAR), Vallabh Vidyanagar, Gujarat 388120., E.mail: neethajob@yahoo.co.in

** R & D Center, Apollo Tyres Ltd, Wagodia, Baroda

Key Words: Nylon cord, Tyre Cord, Crystallinity, Stretching etc.

Abstract

The influence of the different dipping parameters has great importance on the properties of the cord and also on the final performance of the tyres in service. The performance of the tyres in service is also influenced by the crystallinity of the nylon tire cord. In this work an attempt to study the above variations and the variations between the different suppliers of fabric was conducted.

Introduction

A tyre is an annular toroidal shaped inflated envelop made of elastic material reinforced with textile material which is a composite material. Tyre is an integral part of the vehicle and intermediately between the vehicle and on the road, of which the tread is the main part that come in contact with the road surface.

The main load bearing component of the tire is the carcass, which comprises of textile cords coated with rubber. Generally Nylon is used as cord material in carcass for the bias truck tyres, whereas for radial the cord is of polyester fabric type.

As cords are the main load bearing component of the tyre their physical properties , adhesion with the rubber and dimensional stability are most important.

The greige fabric doesn't have good adhesion property with the rubber and therefore a dipping process is required where on the greige fabric is dipped in a solution called "Dip solution" comprising Resorcinol , formaldehyde and latex. Generally Nylon-6 is used in bias tyre carcass reinforcement.

The manufacture of Nylon –6 is a continuous process, although batch reactors are also used. Caprolactum, which is solid at ambient temperature, melted in steam jacketed vessels, and in molten caprolactum is passed through a series of filters to remove impurities. Which is mixed with stabilisers, and additives and pumped into reactors which are stainless steel vessels heated by Dow thermvapour in various sections upto 550 ^{0}K. Polymerisation is carried out and 85% conversion obtained. The polymer chips are remelted in electrically heated extruders and forced through spinneret. The filament emerging from the spinneret are air cooled in a spinning duct and yarn is then wound on metal tubes or cones. In fabric dipping unit the fabric is passed through a series of zones , first a dip zone, then drying zone heat treatment zone, normalizing zone, and finally cooling zone. The wound fabric is covered with a polyethylene sheet and black PP film to protect from moisture, UV radiation and sunlight.

In calendaring operation dipped fabrics are coated with rubber compounds for further processing. It is then sent to bias cutting and tyre building.

Experimental

Nylon –6 Cord of 1680/2 denier was used.

Testing

1) Tensile testing: Tensile testing of the dipped cords were done on Zwick UTM. Breaking strength, % elongation and part load elongation were measured. A cord of appropriate length is clamped in pneumatically operated clamps. Force is applied according to the denier of the cord.

2) Shrinkage: Shrinkage force tester (Testrite MKV) was utilized for this purpose. Suitable length of cord is taken and it is tied up with at one end. On the other end calculated amount of load was placed. Now this assembly is placed between two heated plates maintained at 177^{0}C for 2min. and percentage shrinkage was automatically measured.

3) Dip Pick up %: This was measured by dissolving the Nylon –6 component in Formic acid and thereafter calculating the residue left over.

4) H- Adhesion: This test was carried out to determine the adhesion between rubber and the dipped fabric. Rubber compound of suitable gauge was used and dipped fabric was placed and molding was done. The molded sample was tested in Instron Tensile Machine.

5) Twist Tester: The twist tester in the cord was determined by using twist tester machine. The twisted cord was untwisted and the number of turns were determined.

6) X-Ray diffraction studies: X-ray diffraction studies was conducted on Philips X-pert-MPD model. The Nylon tyre cord was cut into small pieces of 1cm length and cord

was untwisted and filament bunch was taken out. The specimen was placed in sample holder and X-ray were allowed to bombard on it. The angle of bombardment was varied from 0-99 0, and at a particular angle peak with maximum intensity was obtained. The scanning was continued till 99^0 for detection of other stay peaks. X-ray diffraction spectrograph consists of a plot of X-ray counts received by detector vs the scattering angle of the detector.

Results and Discussion

Nylon –6 tyre cord 1680/2 denier from two different sources was dipped at different stretches. Two rolls were dipped from each sources. Source A was dipped at stretches of 5% , 6%, 7% and 8 % where as source B was dipped at 5.5 % , 6.5%, 7.5 % and 8.5 % stretches.

1. It was observed that there is no appreciable increase in breaking strength as the stretching is increased. This is observed for the samples from both the suppliers and after calendaring also. In the case of elongation at break there is decrease in value for both sources after dipping and calendaring. This may be due to the better orientation of the polymer chains in the direction of stretching. This is further confirmed by the decrease in the part Load Elongation (PLE) values of both the suppliers after dipping and calendaring.

Table 1 Source A (dipped)

Properties	**Greige**	**Dipped with stretching**			
		5%	6%	7%	8%
Breaking strength (Kg)	29.7	29.34	29.34	29.29	29.34
Elongation at break (%)	32.36	24.64	23.93	23.25	23.32
PLE @ 9.07Kg	13.38	10.17	9.7	9.28	9.13

Table 2 Source B (dipped)

Properties	**Greige**	**Dipped with stretching**			
	5.5%	6.5%	7.5%	8.5%	
Breaking strength (Kg)	30.29	29.46	29.56	29.87	28.86
Elongation at break (%)	33.47	23.31	23.78	22.37	20.83
PLE @ 9.07Kg	14.03	9.38	9.25	8.0	7.97

Table 3 Source A (Calendared)

Properties	Greige	Calendared with stretching at dipping			
		5%	6%	7%	8%
Breaking strength (Kg)	29.7	29.46	29.56	29.87	28.86
Elongation at break (%)	32.36	23.31	23.78	22.37	20.83
PLE @ 9.07Kg	13.38	9.38	9.25	8.0	7.97

Table 4 (Calendared) Source B

Properties	Greige	Calendared with stretching during dipping			
		5.5%	6.5%	7.5%	8.5%
Breaking strength (Kg)	30.29	30.76	31.01	30.46	30.44
Elongation at break (%)	33.47	23.03	22.67	22.05	22.38
PLE @ 9.07Kg	14.03	9.08	8.6	8.64	8.76

2. The uncoiling of chains and orientation of molecules in the direction of stretching is also reflected in the testrite shrinkage values. There is an increase in shrinkage values. This also observed in calendared samples.

Table 5 Testrite Shrinkage (%) Dipping

Properties	Greige	Dipped with stretching			
		5%	6%	7%	8%
Testrite shrinkage (%)(Source A)	7.28	6.45	6.93	7.56	8.1
		5.5%	6.5%	7.5%	8.5%
Testrite shrinkage (%) (Source B)	8.08	7.06	7.53	8.0	8.75

Table 6 Testrite Shrinkage (%) Calendaring

Properties	Greige	Calendared with stretching during dipping			
		5%	6%	7%	8%
Testrite shrinkage (%)(Source A)	7.28	6.56	6.67	8.32	8.4
		5.5%	6.5%	7.5%	8.5%
Testrite shrinkage (%) (Source B)	8.08	6.76	7.36	8.0	7.67

3. There is an increase in single cord stiffness also showing that the cord stiffness increases on increase in stretching. As stretching increases DPU is also showing decreasing trend which is given in the following table.

Table 7 Source A (Dipping)

Properties	Greige	Calendared with stretching during dipping			
		5%	6%	7%	8%
Single cord stiffness		72.48	75.32	77.8	62.8
DPU %		6.5	5.6	4.7	3.9

Table 8 (Source B) (Dipping)

Properties	Greige	Calendared with stretching during dipping			
		5.5%	6.5%	7.5%	8.5%
Single cord stiffness		44.52	52.28	64.89	66.69
DPU %		6.33	4.71	4.5	3.56

4) It is observed that H-adhesion initially increases as stretching increases, and decreases afterwards. This shows that there is an optimum level of stretching to be given and dip pick up required for maximum adhesion with the rubber compound. This is also reflected in the case of strip adhesion which are given in following tables.

Table 9 Source A

Properties	Greige	Calendared with stretching during dipping			
		5. %	6. %	7. %	8. %
H-adhesion (Kg)		19.19	18.45	18.67	20.55
Strip adhesion (Kg)		20.43	21.76	20.18	20.5

Table 10 Source B

Properties	Greige	Calendared with stretching during dipping			
		5.5%	6.5%	7.5%	8.5%
H-adhesion (Kg)		19.9	18.45	18.67	20.55
Strip adhesion (Kg)		20.43	21.76	20.18	20.5

5. Absolute crystallinity of the fabric samples were not determined. However the full width at Half Maximum (FWHM) values of the samples were compared. Full width at half maximum of the peak is as indication of % crystallinity of the material. Since, as the peak height increases, crystallinity increases so, as FWHM values decreases with peak height crystyallinity. In this study we have observed that in all the cases from greige to dipped fabric crystallinity increases with increases in stretching. This is because chain gets uncoiled and will be more oriented in the direction of stretching. An X ray diffraction graph of sample from source A (5% stretching) is shown in Figure 1 and the FWHM calculation is illustrated in Figure 2.

Conclusion

When a polymer sample is stretched above its Tg, molecular deformation is caused by uncoiling, which is frozen into structure when the sample is cooled. Another rheological component is unrecoverable viscous flow caused by the molecules as they slide over each other. Unrecoverable viscous flow increases as stretching temperature increases. Therefore shrinkage obtained on the molecules and unrecoverable viscous flow that occur during stretching . Thus increase in stretching increase crystallinity of fabric as supported by FWHM values of XRD.

References

1. S.N. Chakravarty, Rubber Asia, , March 1999.
2. Charles. B. Freeman, Rubber & Plastics New, 4, 1990.
3. Wilson. M.W., Textile Research Journal, 21, 47, 1951
4. Warson. H. Polymer Emulsion adhesives, 1993.
5. Gazeley, K.F., NR Technology, 12, 85, 1981.
6. Gazeley, K.F, Proceedings of Adhesives , Sealents conference, 85, 1985.

Figure 1 An X-Ray diffraction graph of source A sample with 5% stretching

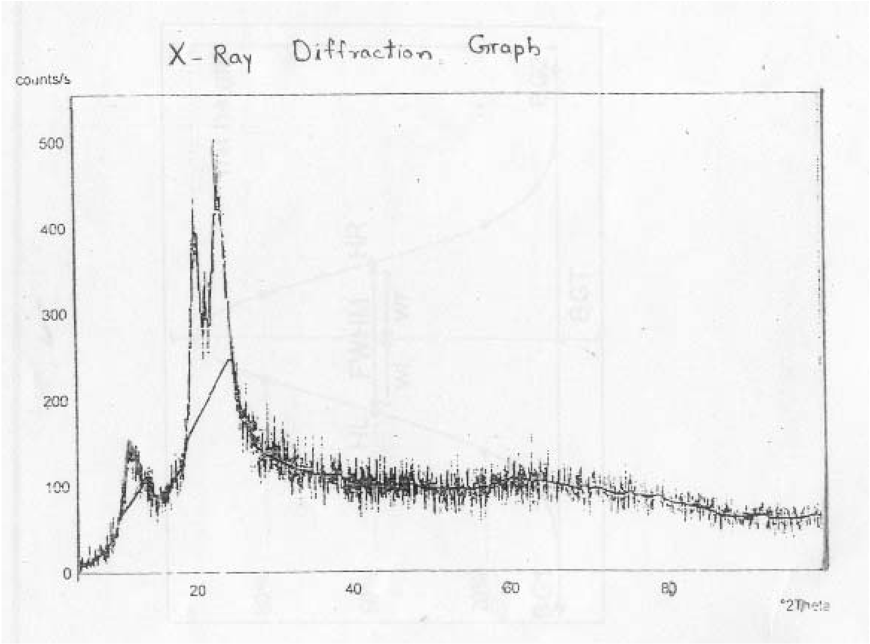

Figure 2 Illustration of FWHM calculation